Untangling the Connections Between Fruit Ripening and Susceptibility to Fungal Pathogens

By

Christian James Silva

Dissertation

Submitted in partial satisfaction of the requirements for the degree of

Doctor of Philosophy

in

Plant Biology

in the

Office of Graduate Studies

of the

University of California

Davis

Approved:

Barbara Blanco-Ulate, Chair

Diane Beckles

Cai-Zhong Jiang

Committee in Charge

2021

For Bill and Jose, who led the way

Contents

List of Figures

List of Tables

Abstract

Untangling the Connections Between Fruit Ripening and Susceptibility to Fungal Pathogens

Fruit infections by fungal pathogens significantly impact the quality, marketability, and safety of produce in preharvest and postharvest scenarios. Fruit ripening, which transforms the fruit into an attractive, nutritious, and delicious food for consumers, also dramatically increases susceptibility to fungal disease. Ripening is an exceptionally complex collection of physiological and biochemical changes produced by large-scale transcriptional reprogramming in a relatively short period time, and identifying individual components of ripening that impact susceptibility is a major challenge. Furthermore, the infection strategies of necrotrophic pathogens are diverse and adapted to the ripening stage of the host.

The major objective of this Ph.D. dissertation has been to isolate specific elements of fruit ripening and fruit-pathogen interactions that have a disproportionate impact on disease outcome and which may serve as targets for breeding or postharvest control. I hypothesized that ripening-associated susceptibility is driven by accumulation of susceptibility factors (such as cell wall-degrading enzymes), and that pathogens can respond to and even manipulate these features during infection. Given the complexity of ripening and fruit-pathogen interactions, I have employed a systems-level approach, leveraging multiple multiple techniques including disease development assays, physiological assessments of ripening, measurement of phytohormones, mutant studies, cell wall glycomics, and various functional transcriptomic methods. The bulk of this research has been conducted using infections of tomato (*Solanum lycopersicum*) by the model necrotroph *Botrytis cinerea*, or gray mold (Chapters 1, 2, and 3). However, I have also used the principles and techniques developed in the tomato-*B. cinerea* pathosystem to expand our knowledge of fruit-pathogen interactions to other systems, specifically infections of tomato by two other necrotrophic pathogens, *Rhizopus stolonifer* and *Fusarium acuminatum* (Chapters 1 and 2), and the agriculturally important pathosystem of nectarine and *Monilinia laxa*,

or brown rot (Chapter 4). Through this research, I have detailed infection strategies and virulence factors (Chapters 1, 3, and 4), characterized fruit responses at different developmental stages (Chapters 2, 3, and 4), and identified susceptibility factors that increase during ripening in tomato (Chapter 3).

A major emerging theme of this research has been the importance of pectin integrity and degradation in the fruit cell wall to the infection success. Both host and pathogen catabolism of pectin influence susceptibility to disease. Expression of fungal pectin-degrading enzymes is emphasized on unripe fruit, where the cell wall is more intact than it is in ripe fruit (Chapter 1). The massive upregulation of the tomato gene pectate lyase during ripening, which facilitates fruit softening, substantially increases susceptibility to *B. cinerea*, as demonstrated by CRISPR mutants (Chapter 2). Moreover, *B. cinerea* can induce the expression of multiple host pectin-degrading enzymes during infections of unripe fruit, effectively recruiting these enzymes to accelerate softening and increase susceptibility (Chapter 3). This induction appears to be dependent on the *B. cinerea* pectin-degrading enzymes *BcPG1* and *BcPG2*, which may be required for the initial establishment of infection on unripe fruit (Chapter 3).

The role of the phytohormone ethylene in fruit-pathogen interactions has also obtained additional clarity through this research. Ethylene has contradictory functions in fruit-pathogen interactions, as it both promotes ripening and participates in plant defense signaling. High levels of ethylene in ripe tomato fruit and the inoculated unripe fruit of a hypersusceptible tomato mutant likely result in a net increase susceptibility, regardless of any defense signaling gained, though low, well-regulated levels of ethylene may still be useful during defense of unripe fruit up to 3 days post inoculation (Chapter 2). The eventual accumulation of increasing amounts of ethylene in response to *B. cinerea* after 4 days post-inoculation may be the trigger for induction of host cell wall degradation and other susceptibility-promoting ripening processes (Chapter 3). Comparable findings from gene expression analyses and ethylene measurements in the nectarine-*M. laxa* pathosystem indicate that this dual functionality of ethylene is similar elsewhere (Chapter 4).

Untangling increased susceptibility from fruit ripening is of tremendous importance in

the ongoing battle against postharvest food losses. My research has progressed our understanding of how specific aspects of pathogen strategy, host response, and transcriptional and physiological changes during fruit ripening impact fungal disease. Additionally, the systems-level approaches I have deployed in the tomato-*B. cinerea* may serve as guidance for research in non-model pathosystems, as demonstrated in the study of the nectarine-*M. laxa* pathosystem. Ultimately, this research will assist in the management of postharvest diseases in fruit crops and facilitate breeding efforts for increased resistance to fungal pathogens in ripe fruit.

Acknowledgments

My Ph.D. would not have been possible without the tremendous mentorship of Barbara Blanco-Ulate. I cannot imagine surviving the challenges of graduate school without her guidance, encouragement, intellect, and compassion. Our weekly meetings always elevated me above the trappings of analysis paralysis and my perfectionist tendencies. In times of emotional stress (and there were many), she perfectly balanced empathy and patience with the push I needed to move forward. She has gifted me many valuable lessons, including making peace with uncertainty, the courage to try unfamiliar things, and the confidence to solve problems as they appear. I am indebted to her for both my academic journey and my own personal growth.

The companionship of my labmates has been a true blessing these past five years. They have been a bountiful source of support, feedback, joy, and laughter, and have spent countless hours assisting me with experiments. Thank you, Jaclyn Adaskaveg, Isabel Ortega-Salazar, Saskia Mesquida-Pesci, and Stefan Petrasch.

I've had the pleasure of receiving excellent mentorship and advice from several professors during my academic career. I would like to thank Cai-Zhong Jiang and Diane Beckles for their support and for challenging and improving my ideas as members of both my Qualifying Exam Committee and my Dissertation Committee. Amanda Larracuente gave me my first substantial lab experience, taught me programming, and gave me the confidence to apply to graduate school. Katherine Schaefer transformed my scientific writing. Daven Presgraves engaged my intellect and helped me develop my scientific thinking. Michael Clark inspired me to think critically about science and science education. I am incredibly grateful for them.

My friends and colleagues in Lleida, particularly Marta Balsells-Llauradó and Charo Torres, provided me with incredibly gracious hospitality during my visit to Spain. It has been a real pleasure to collaborate them on a project that has broadened my horizons, both scientifically and culturally.

My friends and family have done enormous amount to help me maintain my motivation, happiness, and sanity these past few years. I owe everything to the love of my

parents, John and Angela Silva, my sister, Carissa Silva, and my grandmothers, Mary Ann and Esther. I am cannot express enough love and appreciation for the friendships of Sophia Pröschel, Dominic Maniaci, Veronica Thompson, Aedric Lim, Rongkui Han, Laney Casella, and Katie Lincoln.

Lastly, my life has been immeasurably enriched by beautiful dog, Ziggy. He brings warmth and light into my life every single day.

Chapter 1

Infection Strategies Deployed by *Botrytis cinerea*, *Fusarium acuminatum*, and *Rhizopus stolonifer* as a Function of Tomato Fruit Ripening Stage

1.1 Publication Statement

The content of this chapter was peer-reviewed and published as follows:

Petrasch, S., Silva, C. J., Mesquida-Pesci, S. D., Gallegos, K., van den Abeele, C., Papin, V., Fernandez-Acero, F. J., Knapp, S. J., and Blanco-Ulate, B. (2019). Infection Strategies Deployed by *Botrytis cinerea*, *Fusarium acuminatum*, and *Rhizopus stolonifer* as a Function of Tomato Fruit Ripening Stage. *Frontiers in Plant Science*, 10:223.

For this publication, I wrote the paper and shared first authorship with S. Petrasch. Additionally, I prepared the RNA-Seq libraries, constructed and assessed the *R. stolonifer* and *F. acuminatum* transcriptomes performed the bioinformatics and statistical analyses.

1.2 Abstract

Worldwide, 20–25% of all harvested fruit and vegetables are lost annually in the field and throughout the postharvest supply chain due to rotting by fungal pathogens. Most postharvest pathogens exhibit necrotrophic or saprotrophic lifestyles, resulting in decomposition of the host tissues and loss of marketable commodities. Necrotrophic fungi can readily infect ripe fruit leading to the rapid establishment of disease symptoms. However, these pathogens generally fail to infect unripe fruit or remain quiescent until host conditions stimulate a successful infection. Previous research on infections of fruit has

mainly been focused on the host's genetic and physicochemical factors that inhibit or promote disease. Here, we investigated if fruit pathogens can modify their own infection strategies in response to the ripening stage of the host. To test this hypothesis, we profiled global gene expression of three fungal pathogens that display necrotrophic behavior — *Botrytis cinerea*, *Fusarium acuminatum*, and *Rhizopus stolonifer* — during interactions with unripe and ripe tomato fruit. We assembled and functionally annotated the transcriptomes of *F. acuminatum* and *R. stolonifer* as no genomic resources were available. Then, we conducted differential gene expression analysis to compare each pathogen during inoculations versus in vitro conditions. Through characterizing patterns of overrepresented pathogenicity and virulence functions (e.g., phytotoxin production, cell wall degradation, and proteolysis) among the differentially expressed genes, we were able to determine shared strategies among the three fungi during infections of compatible (ripe) and incompatible (unripe) fruit tissues. Though each pathogen's strategy differed in the details, interactions with unripe fruit were commonly characterized by an emphasis on the degradation of cell wall components, particularly pectin, while colonization of ripe fruit featured more heavily redox processes, proteolysis, metabolism of simple sugars, and chitin biosynthesis. Furthermore, we determined that the three fungi were unable to infect fruit from the *non-ripening* (*nor*) tomato mutant, confirming that to cause disease, these pathogens require the host tissues to undergo specific ripening processes. By enabling a better understanding of fungal necrotrophic infection strategies, we move closer to generating accurate models of fruit diseases and the development of early detection tools and effective management strategies.

1.3 Introduction

Fungi are important plant pathogens that cause large economic losses due to their ability to inflict diseases such as rot, rust, and wilt in various plant organs both preharvest and postharvest (Dean et al., 2012; Nabi et al., 2017). Biotrophic fungi feed on living cells and suppress the host immune system by secreting effector proteins (Glazebrook, 2005; Oliver and Ipcho, 2004). In contrast, necrotrophic fungi feed on dead host cells

and cause necrosis by secreting toxins and cell wall-degrading enzymes (CWDEs), among other virulence factors (van Kan, 2006). Due to their ability to feed on dead host tissue, necrotrophic fungi are also sometimes grouped into the less defined group of saprotrophic fungi, which includes many fungi that do not actively kill host cells (Dyakov, 2007). Additionally, hemibiotrophs are pathogens that start their infection cycle as biotrophs and end as necrotrophs (Perfect and Green, 2001). Biotrophic infection mechanisms are well-studied, whereas those of necrotrophic fungi are less understood. The lower scientific interest in necrotrophic infection mechanisms may be due to their perceived lack of specificity. The brute force strategy of secreting toxins and CWDEs as well as the broad host range of many necrotrophic fungi is often interpreted as indiscriminate killing of host cells without the requirement for host-pathogen compatibility (van Kan, 2006). However, the reality of necrotrophic infections is multifaceted, as they involve several features initially believed to be unique to biotrophs, e.g., the suppression of the host immune system or symptomless endophytic growth (Van Kan et al., 2014; Veloso and van Kan, 2018). The relevance of host-pathogen compatibility in necrotrophic infections is also highlighted by the fact that necrotrophic fungi can readily infect ripe fruit but fail to infect unripe fruit or remain quiescent until host and environmental conditions stimulate a successful infection (Alkan and Fortes, 2015; Blanco-Ulate et al., 2016a,b; Prusky and Lichter, 2007).

To develop a better understanding of how fungi attempt to establish infections in fruit, we studied three impactful pathogens with broad host range: *Botrytis cinerea*, *Fusarium acuminatum*, and *Rhizopus stolonifer*. *B. cinerea* is the causal agent of gray mold, an economically devastating disease, and serves as a model species for plant-necrotroph interactions (Fillinger and Elad, 2016). In compatible hosts, such as ripe fruit, *B. cinerea* produces toxins, CWDEs, reactive oxygen species (ROS), and other virulence factors to induce rapid death and decay of the plant tissues (Blanco-Ulate et al., 2016a; Nakajima and Akutsu, 2014). In incompatible hosts, such as unripe fruit, *B. cinerea* establishes quiescent infections while suppressing the host immune system and promoting susceptibility in the host (Prusky et al., 2013; Weiberg et al., 2013). *B. cinerea* has been shown to

activate fruit ripening processes, including changes in plant hormone biosynthesis and signaling and induction of host CWDEs involved in fruit softening, all of which seem to favor fungal growth and colonization (Blanco-Ulate et al., 2013; Cantu et al., 2009; Swartzberg et al., 2008). Even though *B. cinerea* infection strategies have been studied in various pathosystems (Cantu et al., 2009; Ferrari et al., 2007; Rossi et al., 2017), it is mostly unknown whether *F. acuminatum* and *R. stolonifer*, two understudied fungal pathogens, implement similar mechanisms when interacting with compatible and incompatible hosts. *F. acuminatum* has been reported to infect roots and fruit (Jimenez et al., 1993; Logrieco et al., 1992; Marín et al., 2012; Visconti et al., 1989). Within the *Fusarium* genus, *F. acuminatum* is among the most toxic species as it produces strong mycotoxins, such as trichothecene and fumonisins, to kill host cells and induce tissue necrosis (Altomare et al., 1997; Visconti et al., 1989). *R. stolonifer* causes rotting of fruit and other fresh products, mainly by secreting CWDEs, and is considered to be one of the most destructive postharvest pathogens due to its extremely fast growth rate (Bautista-Baños et al., 2014, 2008).

We leveraged the fact that tomato fruit display an increase in susceptibility to necrotrophic fungal infection as a result of ripening to develop a system for studying compatible and incompatible host-pathogen interactions. The transition from unripe to ripe fruit results in a markedly different physicochemical environment for colonization. In comparison to unripe fruit, ripe fruit have higher levels of total soluble solids, greater titratable acidity (TA), lower firmness, and a different composition of secondary metabolites and volatiles (Blanco-Ulate et al., 2016b). In light of this, we anticipated that these pathogens would exhibit specific patterns of gene expression based on the fruit ripening stage and that the functions of these genes would reflect important strategies for interaction with the different host environments. First, we evaluated the incidence and progression of fungal infections caused by *B. cinerea*, *F. acuminatum*, and *R. stolonifer* when inoculated in tomato fruit. Then, to determine if the pathogens adapted their infection strategies as a function of the host developmental stage, we analyzed the transcriptomes of each fungus at two points post-inoculation in unripe and ripe tomato fruit and compared these against

their transcriptomes when grown under in vitro conditions. This approach allowed us to identify specific pathogenicity and virulence factors, e.g., CWDEs and toxin biosynthetic genes, that are differentially or commonly deployed by the pathogens in each host tissue. As necrotrophic infection strategies may be evolutionarily conserved as well as highly specific, we used the transcriptomic data to examine virulence functions among the three fungi and identified similarities in the adaptations of the pathogens to the different environments of ripe and unripe fruit. Finally, to further validate necrotrophic strategies dependent on the ripening stage of the fruit host, we evaluated the pathogenicity of the three fungal pathogens in fruit in a non-ripening tomato mutant. Overall, the approach followed in this study provides an initial platform to perform comparative transcriptomics among three fungi that cause economically relevant fruit diseases and sheds light into how pathogens with necrotrophic lifestyles adapt their infection mechanisms during compatible and incompatible interactions.

1.4 Materials and Methods

1.4.1 Plant and fungal material

Tomato fruit (*Solanum lycopersicum*) from the cultivar Ailsa Craig (AC) and the isogenic mutant *non-ripening* (*nor*) were used in this study. Plants were grown under field conditions in Davis, California, United States, during the 2017 season. Mature green (MG) fruit were harvested 31 days post-anthesis (dpa) and red ripe (RR, or equivalent for *nor*) fruit at 42 dpa. The fungal pathogens studied were *Botrytis cinerea* strain B05.10, an isolate of *Rhizopus stolonifer*, and an isolate of *Fusarium acuminatum*. Both isolates were obtained from postharvest infections of fresh produce and identified using morphological and sequencing methods. All fungi were grown on 1% potato dextrose agar (PDA) plates at room temperature (RT) until sporulation. Spore suspensions were prepared in 0.01% Tween® 20 (Sigma-Aldrich, USA). Fungi from axenic in vitro cultures were grown on 1% PDA plates at RT, and mycelium for RNA extraction was harvested before the fungi reached the sporulation stage.

1.4.2 Fruit inoculations

Tomato fruit from AC and *nor* were collected at MG and RR or RR-like stage. Selected AC MG fruit were green, firm, and had soluble solids content (SSC) of 5.24 ±0.44 g sucrose/100 g solution and TA of 5.20 ±1.24%. AC RR fruit were bright red, pliable when squeezed, and had SSC of 6.27 ±0.42 g sucrose/100 g solution and a TA of 3.47 ±0.26%. *nor* MG fruit were similar to AC MG fruit, and *nor* RR-like fruit were selected that were green in color slightly soft at the blossom end. Fruit were sterilized in 0.6% sodium hypochlorite, wounded four to six times on the blossom end with a sterile pipette tip (width: 1 mm, depth: 2 mm) and inoculated with 10 µl per wound using a 500 spores/µl suspension for *B. cinerea*, a 30 spores/µl suspension of *R. stolonifer*, and a 1,000 spores/µl suspension of *F. acuminatum*. The differences in fungal spore concentration were adjusted to ensure uniform and comparable development of lesions in tomato fruit. In the case of *R. stolonifer* inoculations of MG fruit, we also tested a concentration of 1,000 spores/µl but no differences in fruit responses or fungal growth between this concentration and 30 spores/µl were observed. Inoculated fruit were incubated at RT (at approximately 20–23°C) in high humidity (between 90 and 100%) chambers. For mock inoculations, the same procedure was followed but without the addition of the inoculum. The pericarp and epidermis of the blossom end (including both the inoculation point and/or the lesion area) were collected at 1 and 3 days post-inoculation (dpi), immediately frozen in liquid nitrogen, and stored at -80°C until use. One biological replicate consisted on average of eight fruit, and five biological replicates per treatment were obtained.

1.4.3 RNA extraction, cDNA library preparation, and RNA sequencing

Tomato fruit tissues were ground using a Retsch® Mixer Mill MM 400 (Retsch, Germany) and RNA was extracted from 1 g of fine-powdered tissue according to the procedure described in Blanco-Ulate et al. (2013). Fungal RNA from the in vitro cultures was extracted using TRIzol (Invitrogen, United States) and purified using the Quick-RNA MiniPrep Kit (Zymo Research, United States) following the procedure described in Morales-Cruz et al. (2015). The RNA concentration and purity were assessed with the

Qubit 3 (Invitrogen, United States) and the NanoDrop One Spectrophotometer (Thermo Scientific, United States), respectively. Gel electrophoresis was used to confirm the RNA was not degraded. Barcoded cDNA libraries were prepared using the Illumina TruSeq RNA Sample Preparation Kit v2 (Illumina, United States). Quality control of the cDNA libraries was performed with the High Sensitivity DNA Analysis Kit in the Agilent 2100 Bioanalyzer (Agilent Technologies, United States). 50-bp single-end libraries were sequenced on the Illumina HiSeq 4000 platform in the DNA Technologies Core of the UC Davis Genome Center. In total, 18 libraries were sequenced for B. cinerea (five for MG 1 dpi, four for RR 1 dpi, and three for MG 3 dpi, RR 3 dpi, and in vitro cultures), 17 libraries were sequenced for *F. acuminatum* (four for MG 1 dpi and RR 1 dpi, and three for MG 3 dpi, RR 3 dpi and in vitro cultures), and 17 libraries for *R. stolonifer* (five for RR 1 dpi and three for MG 1 dpi, MG 3 dpi, RR 3 dpi, and in vitro cultures).

1.4.4 De novo transcriptome assembly and annotation

Quality trimming (Q >30) of the raw reads was performed with sickle v1.33 (`https://github.com/najoshi/sickle`) and adapter sequences were removed with scythe v0.991 (`https://github.com/vsbuffalo/scythe`). Basic quality measurements were assessed with FastQC (`https://www.bioinformatics.babraham.ac.uk/projects/fastqc/`). In order to generate transcriptome assemblies for *F. acuminatum* and *R. stolonifer*, reads from samples infected with each of these pathogens were mapped to the tomato genome (ITAG3.2 - `http://solgenomics.net`) using STAR 2.6 (Dobin et al., 2013). Reads that failed to map to the tomato gene were pooled with the reads from the in vitro samples and used for de novo transcriptome assembly. Transcriptomes were assembled with Trinity 2.5.1 (Grabherr et al., 2011) using default parameters (i.e., no specified minimum contig length). Quality of the assemblies was assessed with BUSCO 3.0.2 (Waterhouse et al., 2018) using the "fungi odb9" dataset, while basic assembly metrics were obtained with Transrate 1.0.3 (Smith-Unna et al., 2016). Potential contaminant transcripts were identified via BLAST using both the blast nr database and the UniProt database. Transcripts with a top-scoring blast match to *Solanum* species were removed from the final transcriptomes.

Functional annotations for transcriptomes of all three fungi were created using Trinotate 3.0.1 (Bryant et al., 2017). The default Trinotate parameters (-max_target_seqs 1 -outfmt 6 -evalue 10^{-3}) were used to retrieve the best BLAST hits as well as annotations for Gene Ontology (GO) terms, Pfam families, Kyoto Encyclopedia of Genes and Genome (KEGG) pathways, EggNOG predictions, and SignalP sequences. Custom BLAST databases were incorporated according to the Trinotate manual for the Transporter Classification Database (TCDB - `http://www.tcdb.org/`) and the Pathogen-Host Interactions database (PHI - `http://www.phi-base.org/`). Custom HMMER alignment results for HMM profiles from dbCAN (`http://csbl.bmb.uga.edu/dbCAN/`) and fPoxDB (`http://peroxidase.riceblast.snu.ac.kr/`) were incorporated similarly.

1.4.5 RNA-seq nioinformatics pipeline

The bioinformatic pipeline was initiated by mapping parsed reads from the fungal-infected tomato samples to a combined transcriptome of tomato and the three pathogens using Bowtie2 (Langmead and Salzberg, 2012). The tomato transcriptome (build SL3.0 with ITAG 3.2 annotations; Consortium et al. (2012)) was obtained from `https://solgenomics.net/organism/Solanum_lycopersicum/genome`. For *B. cinerea* (strain B05.10), we used the predicted transcriptome ASM83294v1 (`http://fungi.ensembl.org/Botrytis_cinerea/Info/Index` Van Kan et al. (2017)). For *R. stolonifer* and *F. acuminatum*, the respective curated transcriptome assemblies were used. The in vitro samples were mapped to the pathogen transcriptomes alone. Count matrices were made from the Bowtie2 results using sam2counts.py (v0.91 - `https://github.com/vsbuffalo/sam2counts/`) and are available in Supplementary Table S1 at `https://www.frontiersin.org/articles/10.3389/fpls.2019.00223/full#supplementary-material`.

Count matrices were used as input for differential expression analysis with the Bioconductor package DESeq2 (Love et al., 2014) in R. Reads were normalized for library size after being filtered to exclude those that mapped to tomato. Gene expression comparisons were made between MG or RR and in vitro samples at 1 and 3 dpi. Differentially expressed genes (DEGs) were considered to be those with an adjusted P-value less than or equal to 0.05. Enrichment for GO terms was performed with the R package goseq

v1.32.0 (Young et al., 2010) with the use_genes_without_cat parameter set to TRUE. An over-represented *P*-value threshold of 0.05 was used to specify enriched genes.

1.4.6 RT-qPCR validation

cDNA was synthesized with an oligo-dT primer on 1 µg of RNA using the M-MLV Reverse Transcriptase (Promega, United States) in the SimpliAmp Thermal Cycler (Applied Biosystems, United States). Expression of the genes of interest was quantified through Real-Time Quantitative PCR (RT-qPCR) using PowerSYBR Green PCR Master Mix (Applied Biosystems, United States) in the QuantStudio3 (Applied Biosystems, United States). Primers for the genes of interest were designed using Primer-BLAST (Ye et al., 2012). Primer efficiency was confirmed to be higher than 90% using fourfold DNA or cDNA dilutions (0, 1:1, 1:4, 1:16, 1:64, and 1:256) in triplicate, while specificity was checked by analyzing the melting curves at temperatures ranging from 60 to 95°C. Relative gene expression was calculated using the formula $2^{(\text{reference gene Ct} - \text{gene of interest Ct})}$ The list of primers used in this study are listed in Supplementary Table S2 at `https://www.frontiersin.org/articles/10.3389/fpls.2019.00223/full#supplementary-material`.

1.4.7 Data availability

The transcriptome assemblies for *F. acuminatum* and *R. stolonifer* have been deposited at GenBank under the accessions GGXD00000000 and GGWM00000000, respectively. The versions described here are the first versions, GGXD01000000 and GGWM01000000. The RNA-Seq results, including the raw sequencing reads and the read mapping count matrices, have been deposited in the National Center for Biotechnology Information Gene Expression Omnibus (GEO) database (`http://www.ncbi.nlm.nih.gov/geo` - no. GSE122555).

1.5 Results

1.5.1 Tomato fruit susceptibility to fungal infections increases as a result of ripening

To determine if *F. acuminatum* and *R. stolonifer* show similar patterns of infections in tomato fruit as *B. cinerea* (Blanco-Ulate et al., 2013; Cantu et al., 2009), we did

side-by-side inoculations of fruit at two developmental stages: unripe (mature green, MG) and ripe (red ripe, RR). As displayed in Figure 1.1A, we confirmed that all fungi were unable to cause rotting in MG fruit but aggressively colonized RR fruit. These results were further validated by quantifying fungal biomass based on relative expression of fungal reference genes via qRT-PCR (Figure 1.1B). At 3 dpi, RR fruit inoculated with *B. cinerea* and *F. acuminatum* showed water-soaked lesions of approximately 15 mm covered by dense mycelia, whereas RR fruit inoculated with *R. stolonifer* were almost decomposed and entirely covered by mycelia. Although no lesions were observed in MG fruit when inoculated with any of the pathogens, some differences in fungal growth and tomato responses were observed. Inoculations with *B. cinerea* and *R. stolonifer* did not show any visible mycelia, whereas *F. acuminatum* inoculations showed limited hyphal growth without disease symptoms. All three fungi induced a necrotic ring surrounding the inoculation sites during the incompatible interaction with MG fruit, yet *F. acuminatum* inoculations caused dark and wide rings while fruit infected with *R. stolonifer* developed a weaker response. Because we were not able to visually detect any hyphal growth of *B. cinerea* and *R. stolonifer* in MG fruit, we used a microscope to observe whether the spores germinated in the inoculated wounds. At 1 dpi, *B. cinerea* spores were mainly ungerminated or in the process of germination (Figure 1.S1). By contrast, *F. acuminatum* and *R. stolonifer* already showed active hyphal growth, indicating that spores of these fungi germinate earlier on MG fruit. At 3 dpi, some hyphal growth was also observed for *B. cinerea*. Together, these observations suggest that the incompatibility of the interaction between these fungi and MG tomato fruit occurs after spore germination.

To provide initial support that both *F. acuminatum* and *R. stolonifer* are capable of inducing disease responses in the host, like *B. cinerea*, and do not merely behave as saprotrophs (i.e., feeding on dead tissue), we evaluated the expression of the host gene *SlWRKY33* (*Solyc09g014990*), which is well-known to be pathogen-responsive but is not induced by abiotic stresses (Zhou et al., 2015, 2014). To test that the induction of this gene occurred only as a result of inoculation and not wounding, we included a mock-inoculated control in our analyses. The expression patterns of *SlWRKY33* measured by

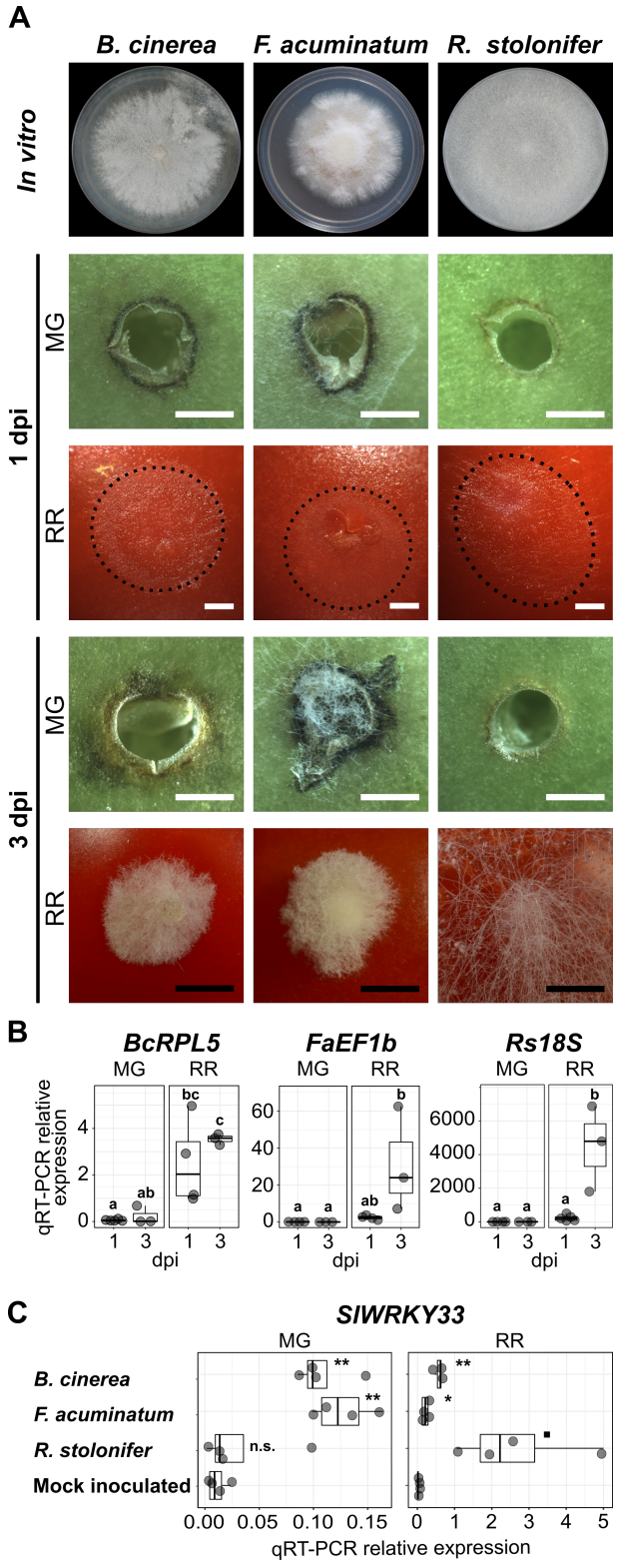

Figure 1.1: Caption presented on following page.

Figure 1.1: Fungal growth and disease development in tomato fruit. (A) Growth and lesion development of the three fungi in vitro and during inoculation, respectively. Fungi were grown on PDA in 100 mm Petri dishes. In vitro morphology represents the pre-sporulation stage used for this study at 3 (*Rhizopus stolonifer*), 5 (*Botrytis cinerea*) and 7 (*Fusarium acuminatum*) days post-plating. Fungal growth and lesion development during fruit inoculation is shown at 1 and 3 days post-inoculation (dpi) in mature green (MG) and red ripe (RR) fruit. The extent of mycelial growth is highlighted by dotted lines for 1 dpi RR fruit. White and black bars correspond to 1 and 5 mm, respectively. (B) Fungal biomass estimated by the relative expression of the reference genes *BcRPL5* (*Bcin01g09620*), *FaEF1b* (*FacuDN4188c0g1i4*), and *Rs18S* (*RstoDN6002c0g2i1*), normalized based on the tomato reference gene expression (*SlUBQ*, *Solyc12g04474*). Significant differences (P <0.05) between the biomass of the four treatments are denoted by letters. (C) Relative expression of the disease responsive tomato gene *SlWRKY33* (*Solyc09g014990*) in samples inoculated with the three fungi and in the mock-inoculated control. Symbols indicate statistical significance (n.s., not significant; ■ P <0.1; $*P$ <0.05; $**P$ <0.01) when comparing inoculations with each pathogen and the control.

qRT-PCR reflected the accumulation of fungal biomass and the presence of lesions in each of the treatments (Figure 1.1C). At 1 dpi, expression of *SlWRKY33* was induced by inoculation with both *B. cinerea* and *F. acuminatum* but not with *R. stolonifer* or mock inoculation in MG fruit. In RR fruit, pathogen-induced *SlWRKY33* was detected for all three pathogens at greater levels than found in MG fruit.

1.5.2 Novel transcriptomic resources for *F. acuminatum* and *R. stolonifer*

Our observations of lesion development, fungal biomass, and activation of pathogen responses led to the hypothesis that *F. acuminatum* and *R. stolonifer* display a similar necrotrophic behavior in tomato fruit as *B. cinerea*. Therefore, to discover pathogenicity or virulence factors in these fungi that are important for necrotrophic infections, we performed a genome-wide transcriptomic analysis of inoculated fruit at both time points

as well as in vitro cultures. Due to the lack of publicly available genomic data for *F. acuminatum* and *R. stolonifer*, we assembled de novo transcriptomes for both of these pathogens from our cDNA libraries following the Trinity pipeline (Grabherr et al. (2011); see Section "Materials and Methods" for details). Using the fungal ortholog dataset of the Benchmarking Universal Single-Copy Orthologs tool (BUSCO v3; Waterhouse et al. (2018)), we determined that our assemblies presented high completeness, with 88.2 and 90.3% of *F. acuminatum* and *R. stolonifer* matches being complete, respectively. Our *F. acuminatum* transcriptome contained 20,117 unique transcripts, while our *R. stolonifer* transcriptome contained 19,754 (see Table 1.1).

Table 1.1: Quantitative summary of de novo assembled transcriptomes of *F. acuminatum* and *R. stolonifer*.

	F. acuminatum	*R. stolonifer*
Transcripts in initial assembly	20,446	20,099
Removed contaminant transcripts	329	345
Transcripts in final assembly	20,117	19,754
Transcripts with ORF	9,617	11,468
N50 (bp)	1,825	1,412
Transcripts annotated	10,432	13,049

ORF, open reading frame. N50 refers to the minimum transcript length required to cover 50% of the transcriptome.

We then used homology-based annotation to obtain information on gene functions for each of the transcriptomes, including the *B. cinerea* B05.10 ASM83294v1 (Van Kan et al., 2017). We annotated transcripts based on nine separate functional classifications, including GO (Consortium, 2017), Pfam domains (El-Gebali et al., 2019), Pathogen-Host Interaction (PHI; Urban et al. (2017)), membrane transporters (Saier Jr et al., 2016), Carbohydrate-Active Enzymes (CAZymes; Lombard et al. (2014)), and fungal peroxidases (Choi et al., 2014). Each type of functional annotation was represented by a similar percentage of annotated transcripts across all pathogens (Figure 1.2). The specialized enzyme classifications of peroxidases and CAZymes made up a relatively small fraction of the annotated transcripts, whereas general functional classifications such as GO, Pfam, and KEGG descriptions were available for at least 70% of the annotated transcripts for all pathogens. Annotations for all three transcriptomes can be found in Supplementary Table S3 at `https://www.frontiersin.org/articles/10.3389/fpls.2019.00223/full#sup`

plementary-material. Although the *F. acuminatum* and *R. stolonifer* transcriptomes are preliminary and may require further curation and validation, we consider that they are a valuable resource to perform gene expression analyses and to shed light on the infection strategies utilized by these fungi.

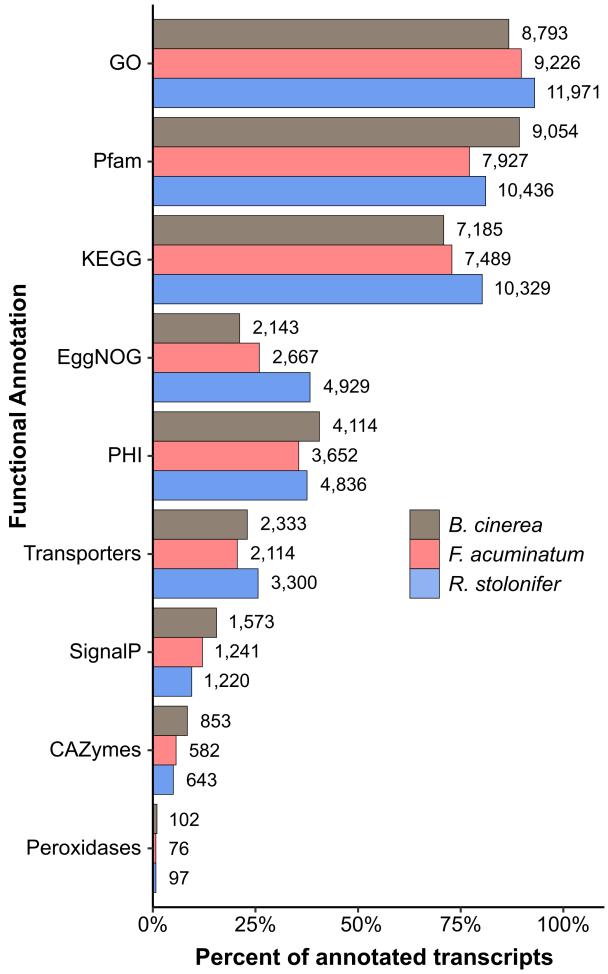

Figure 1.2: Summary of functional annotations across the *Botrytis cinerea*, *Fusarium acuminatum*, and *Rhizopus stolonifer* transcriptomes. Percent of all annotated transcripts in that transcriptome that contain at least one annotation for each categorization. GO, Gene Ontology; KEGG, Kyoto Encyclopedia of Genes and Genomes; PHI, Pathogen-Host Interaction; CAZymes, Carbohydrate-Active enZymes.

1.5.3 Fungal gene expression patterns are distinct during interactions with unripe and ripe fruit

First, we performed principal component analysis (PCA) to determine if the fungal-inoculated and in vitro samples could be discerned based on the expression of the fungal transcripts. The PCAs revealed that all samples clustered by treatment (Figure 1.3A). In most cases, the first component clearly differentiated the MG fruit from the RR fruit inoculations and the in vitro samples. Then, we determined DEGs (P_{adj}<.05) between inoculations of MG or RR fruit and in vitro cultures for each pathogen. Across all comparisons, we detected 6,488 *B. cinerea* DEGs (47.19% of its transcriptome), 6,154 *F. acuminatum* DEGs (30.59% of its transcriptome), and 8,777 *R. stolonifer* DEGs (44.43% of its transcriptome). The number of DEGs for *R. stolonifer* were mainly identified in the RR fruit comparisons, as the low amount of fungal biomass in MG fruit samples did not allow for an in-depth sequencing coverage of the fungal transcripts. To confirm the accuracy of the DEG analysis, we selected a subset of genes for each pathogen to validate their expression using a qRT-PCR approach (Supplementary Table S4 at `https://www.frontiersin.org/articles/10.3389/fpls.2019.00223/full#supplementary-material`). Our results confirmed that the gene expression values were consistent, showing significant Pearson correlation coefficients (r $\geq$ 0.7, P <0.05) and between the RNA-seq and the qPCR expression data (Figure 1.S2).

We further evaluated the fungal DEGs based on whether they were commonly or uniquely expressed under specific treatments, which can provide insight on particular sets of genes that are relevant during incompatible or compatible interactions (Supplementary Tables S5–S7 at `https://www.frontiersin.org/articles/10.3389/fpls.2019.00223/full#supplementary-material`). For each pathogen, genes uniquely upregulated in RR fruit (Figure 1.3B) constituted a sizable fraction of upregulated genes (58.80%, 49.19%, and 88.94% for *B. cinerea*, *F. acuminatum*, and *R. stolonifer*, respectively). This result may be influenced by the fact that RR fruit samples had more coverage of fungal transcripts in the RNA-seq experiment than MG fruit samples, which is a technical limitation of this type of study. Nevertheless, the comparisons of common and unique

DEGs among treatments for each of the pathogens support the results of the PCAs, indicating that these fungi display a specific behavior in each of the fruit stages at early and late time points after inoculation. We also identified upregulated DEGs shared across categories (224 for *B. cinerea*, 160 for *F. acuminatum*, and 30 for *R. stolonifer*) that are likely to represent core pathogenicity factors during fruit infections.

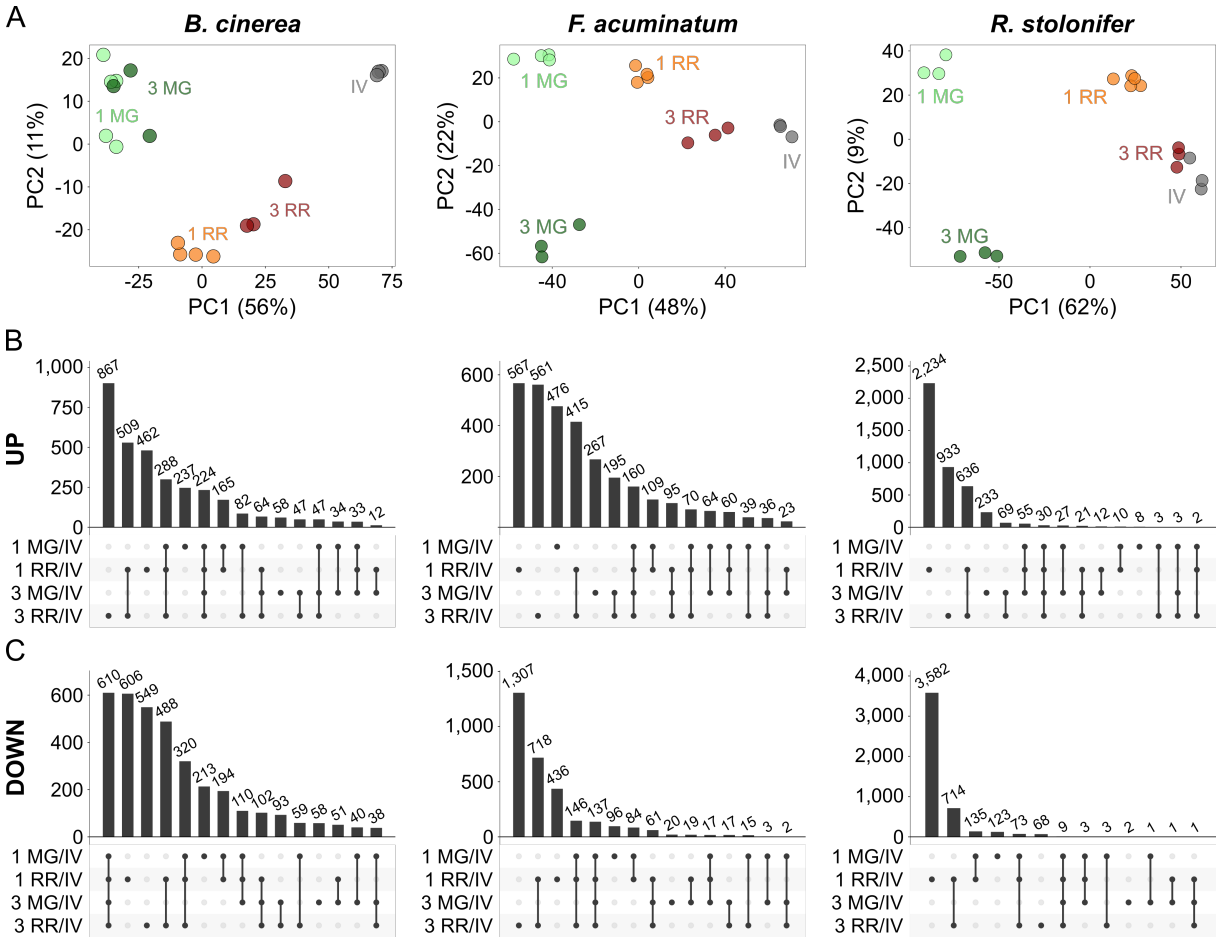

Figure 1.3: Principal component analysis (PCA) and intersections of differentially expressed genes (DEGs) during inoculations of tomato fruit. (A) PCA plots of variance-stabilized matrixes of mapped reads for each pathogen as generated by DESeq2. (B,C) UpSetR visualizations of intersections between the upregulated (B) and downregulated (C) DEGs of inoculated fruit at two time points versus in vitro comparisons for each pathogen. Intersections are displayed in descending order by number of genes.

1.5.4 Necrotrophic fungi utilize similar, yet distinct infection strategies in tomato fruit

To gain insight into key biological processes that are relevant during compatible or incompatible fruit infections, we performed GO enrichment analyses of the upregulated DEGs in all combinations of ripening stage (MG and RR) and dpi (1 and 3) for each pathogen (Supplementary Table S8 at `https://www.frontiersin.org/articles/10.3389/fpls.2019.00223/full#supplementary-material`). We mainly focused on GO terms of the "biological process" class that were significantly enriched (P <0.05, number of genes ≥ 2) and appeared to be involved in pathogenesis or fungal growth in the host tissues (Figure 1.4).

Upregulated DEGs from all comparisons, except for *R. stolonifer* MG inoculations, were enriched in oxidation-reduction processes (GO: 0055114). A closer inspection of these DEGs revealed functions that are likely to be involved with pathogenicity, such as catabolism of ROS [e.g., superoxide dismutases (SODs), catalases (CATs), peroxidases] and breakdown of cell wall molecules such as cellobiose and lignin (Supplementary Table S8 at `https://www.frontiersin.org/articles/10.3389/fpls.2019.00223/full#supplementary-material`). In *B. cinerea*, the SOD *BcSOD1* was induced in both MG and RR fruit at 1 and 3 dpi. Additionally, *BcSOD3* (*Bcin01g03830*) was upregulated only in MG fruit at 1 dpi, and *BcSOD2* (*Bcin01g03830*) is upregulated only at 1 dpi in MG and RR fruit. Although two potential SODs, *FacuDN9613c0g1i1* and *FacuDN4275c0g1i2*, were employed by F. acuminatum in all treatments except 1 dpi MG, none of the seven putative SODs identified in *R. stolonifer* were upregulated in any of the treatments. To further identify enzymatic scavengers of hydrogen peroxide (H_2O_2), we examined the upregulated DEGs of each pathogen which showed significant ($E \leq 10^{-3}$) similarity to members of the Fungal Peroxidase Database. This analysis revealed differences both in the classes of enzymes used in each pathogen and the treatments in which they were used. For example, in *B. cinerea*, only two known catalases, *BcCAT2* (*Bcin11g06450*) and *BcCAT4* (*Bcin05g00730*), were found to be upregulated during tomato fruit interaction. Both of these were only active in MG fruit. In contrast, *F. acuminatum* exhib-

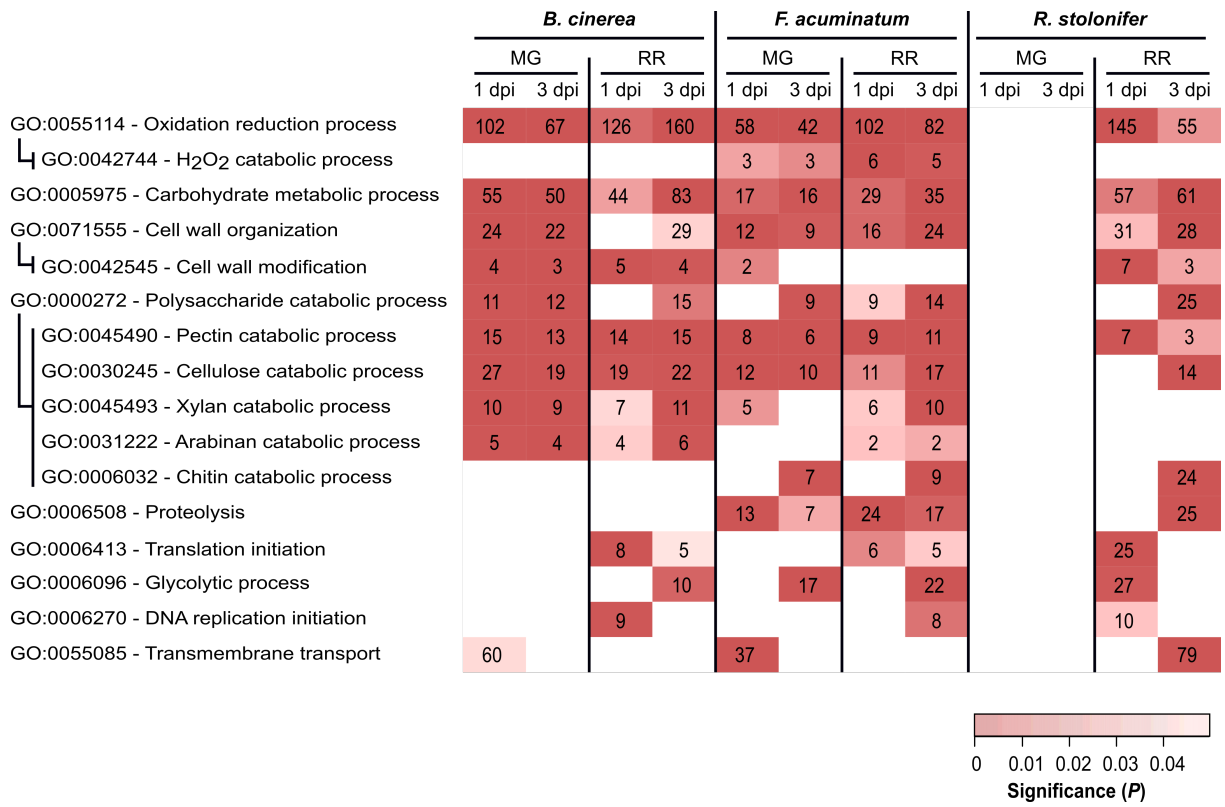

Figure 1.4: Subset of overrepresented Gene Ontology (GO) terms associated with pathogenicity and fungal growth among upregulated genes in *Botrytis cinerea*, *Fusarium acuminatum* and *Rhizopus stolonifer* inoculated samples. Indented GO terms are nested in the GO term above. Box color indicates the significance of enrichment, and values in the boxes indicate the number of upregulated genes in this comparison that share the indicated annotation. dpi, days post-inoculation; MG, mature green; RR, red ripe.

ited very strong induction ($\log_2$FC >9) of two predicted CATs, *FacuDN12367c0g1i1* and *FacuDN13048c0g1i1*, at 1 dpi in RR fruit but not in MG fruit, although a handful of CATs and catalase-peroxidases were upregulated less strongly across both MG and RR fruit. In all F. acuminatum-inoculated samples, there was also an enrichment of DEGs involved in hydrogen peroxide catabolism (GO: 0042744), further highlighting the importance of fungal responses to oxidative stress during fruit colonization. In *R. stolonifer*, peroxidases were only upregulated at 1 dpi in RR fruit and included two 2-cysteine peroxiredoxins (PRXs), one cytochrome C peroxidase, and one glutathione peroxidase (GPX).

Additionally, in all *B. cinerea*-inoculated samples, DEGs annotated with the oxidation - reduction process GO term included enzymes in the biosynthetic pathways for the phytotoxins botrydial and botcinic acid. Eight of these genes were strongly upregulated ($\log_2$FC >4) in all four treatments, indicating that *B. cinerea* may produce these toxins regardless of the ripening stage of the fruit. *F. acuminatum* genes annotated with this GO term included enzymes involved in the biosynthesis of the toxin fumonisin. Several of these genes (*FacuDN12063c0g1i1*, *FacuDN15813c0g1i1*, *FacuDN9039c0g1i1*) showed significant upregulation ($\log_2$FC >2) in infections of MG fruit at 1 dpi or RR fruit at both time points. Fungal proteolysis-related genes (GO: 0006508) were found to be enriched during MG and RR inoculations with *F. acuminatum* as well as RR inoculations with *R. stolonifer* at 3 dpi. Though not enriched, several genes with this GO term were also found to be expressed during fruit inoculation by *B. cinerea*, mostly in RR fruit. Across all treatments, *F. acuminatum* was found to produce 28 genes with this GO term, while *B. cinerea* was found to produce 29, and *R. stolonifer* produced 44 in RR fruit alone (Supplementary Table S8 at `https://www.frontiersin.org/articles/10.3389/fpls.2019.00223/full#supplementary-material`). Seven members of the *B. cinerea* aspartic proteinase family (ten Have et al., 2010) were upregulated in at least one of the fruit inoculations, though none were upregulated at 1 dpi in RR fruit. Thus, fungal proteases are likely to be a strategy used by all three pathogens.

Other GO terms served as a proxy for successful growth. Enrichments of genes involved in protein translation initiation (GO: 0006413), glycolytic process (GO: 0006096), and DNA replication initiation (GO: 0006270) were found in compatible interactions with RR fruit. Notably, DEGs involved in glycolytic process were enriched in MG inoculations for *F. acuminatum* at 1 dpi, which is consistent with visual observations of mycelium growth on inoculated fruit. A similar pattern was observed for the chitin catabolic process (GO: 0006032) term, which are involved in the continuous fungal cell wall remodeling during hyphal growth (Langner and Göhre, 2016).

Multiple GO terms relating to carbohydrate metabolism were found to be enriched across multiple fruit inoculation treatments. The corresponding genes included those in-

volved in breakdown of the cell wall polysaccharides, metabolism of host sugar sources, and production of fungal polysaccharides. As both the cell wall properties and sugar biochemistry differ between MG and RR fruit, we hypothesized that the fungi employ different classes of CAZymes depending on the ripening stage as already demonstrated for *B. cinerea* (Blanco-Ulate et al., 2014). To test this, we examined the expression profiles of CAZyme families among the DEGs for each pathogen (Figure 1.5 and Supplementary Table S9 at `https://www.frontiersin.org/articles/10.3389/fpls.2019.00223/full#supplementary-material`). CAZyme families involved in catabolism of cellulose, hemicellulose, pectin, and monosaccharides were detected, along with families with non-carbohydrate substrates and several responsible for polysaccharide biosynthesis. In *B. cinerea* and *F. acuminatum* inoculations, families involved in the degradation of cellulose (GH5, GH7, AA9) and hemicellulose (AA9 and multiple GHs) were more prominent during infections of MG fruit than RR fruit. Moreover, the CE5 family, which contains cutinases and acetylxylan esterases, was also especially utilized at 1 dpi in MG fruit. In *B. cinerea*, this family included the cutA gene previously shown to be expressed in tomato fruit infection (Van Kan et al., 1997). MG infections also exhibited higher percentages of families involved in the degradation of cellobiose, a disaccharide of β-1,4-linked glucose molecules that results from the breakdown of cellulose and glucan-based hemicelluloses. A similar trend was found for pectin-degrading families, particularly polygalacturonases (GH28) and pectate lyases (PL1 and PL3), though the PL1-4 subfamily appeared to be prominent in RR infections as well. Enzymes involved in metabolism of simple sugars, most notably GH32 in *F. acuminatum* and AA3-2 in *B. cinerea*, showed greater prominence in RR infections. Chitin and chitosan biosynthesis and processing families (GT2, GH18, CE4) were also detected in *B. cinerea* and *F. acuminatum*. In *B. cinerea*, chitin synthases (GT2) were generally equally expressed in all fruit inoculations, though chitin deacetylases (CE4), which produce chitosan, were only particularly prominent in RR infections at 3 dpi. In contrast,*F. acuminatum* produces multiple CE4 enzymes at 3 dpi in MG infections in addition to RR infections.

Other CAZy families also seemed to be featured heavily in fruit-pathogen interactions.

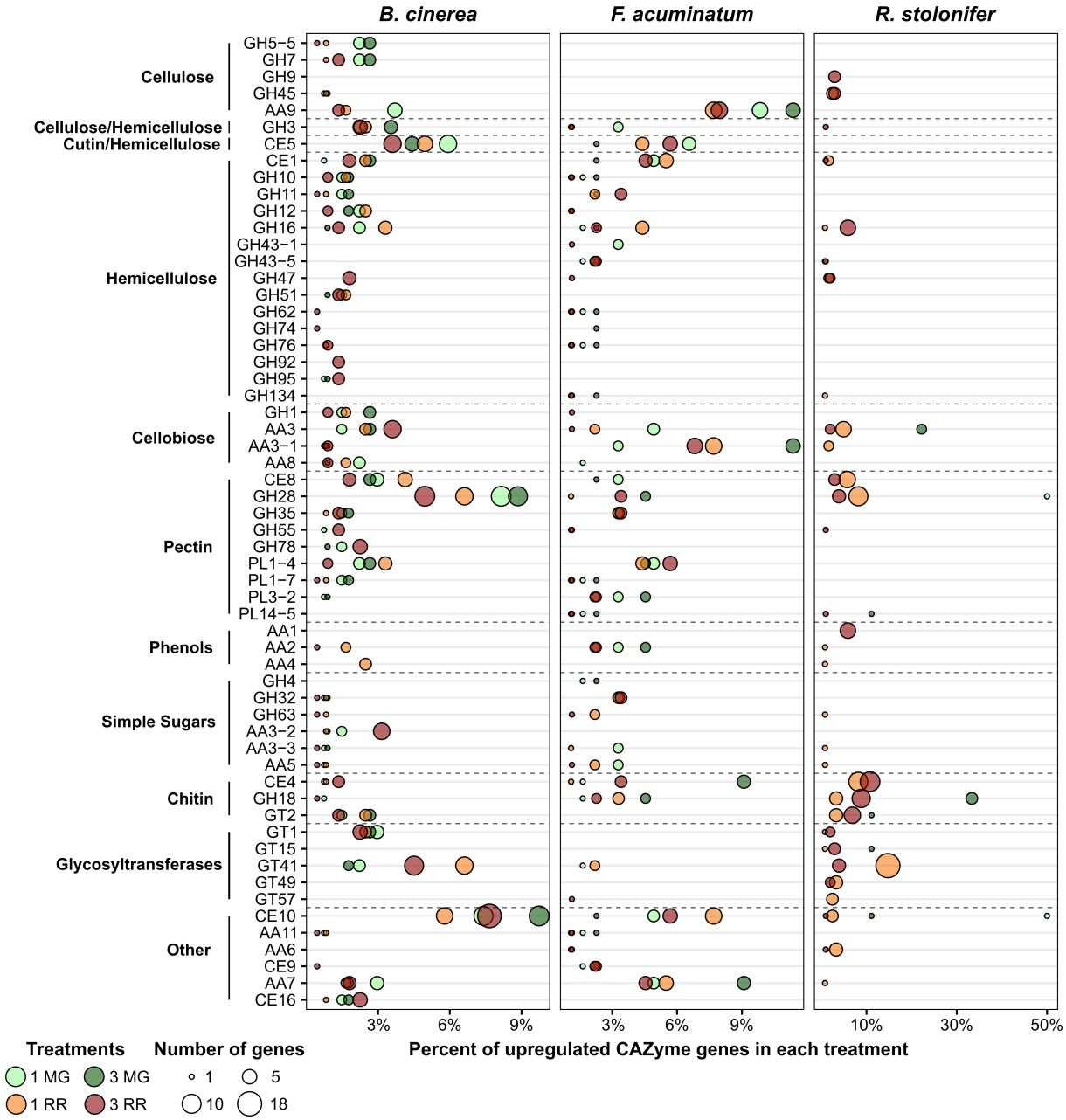

Figure 1.5: Upregulated CAZy family genes for each pathogen in the four treatments. Families and subfamilies from CAZy (`www.cazy.org`) are listed on the left. These are further nested into categories based on their substrates or activities. Each family is described by the percentage of all upregulated CAZyme genes it represents per treatment. Only families which constitute $\geq 2\%$ of upregulated CAZyme genes in at least one treatment are shown.

CE10 enzymes were especially prevalent in both *B. cinerea* and *F. acuminatum* infections. Members of the CE10 family include lipases, which catalyze the hydrolysis of fatty acids. The previously described *B. cinerea* gene *lip1* (Reis et al., 2005) was upregulated at both 1 and 3 dpi in MG fruit, but not RR fruit. Additionally, *B. cinerea* and *F. acuminatum* both produced multiple AA7 family enzymes in both MG and RR fruit. Many of these genes showed significant similarity to three genes of the PHI database: *ZEB1* in *F. graminearum*, *CTB5* from *Cercospora nicotianae*, and *sol5* from *Alternaria solani*. Each of these PHI genes is involved in the biosynthesis of polyketide mycotoxins in those plant pathogens (Chen et al., 2007; Kim et al., 2015; Park et al., 2015). Thus, these *B. cinerea* and *F. acuminatum* genes may be involved in similar roles.

Detection of CAZymes during infection by *R. stolonifer* was only possible in RR fruit due to the low number of DEGs determined in MG fruit. However, sizable numbers of genes from families detected in *B. cinerea* and *F. acuminatum* infections were also discovered in *R. stolonifer*. These include xyloglucanases (GH16), cellobiose dehydrogenases (AA3), pectin methylesterases (CE8), and polygalacturonases (GH28). In addition, multiple enzymes involved in chitin/chitosan biosynthesis were prevalent in RR fruit inoculations, which is indicative of the particularly aggressive hyphal growth of *R. stolonifer* on these fruit. In RR fruit at 3 dpi, *R. stolonifer* also produced six enzymes of the AA1 family, which consist of laccases, ferroxidases, and multi-copper oxidases. Each of these enzymes showed significant similarity to *FET3* enzymes from *Colletotrichum graminicola* in the PHI database and to genes of the TCDB class 2.A.108.1.4, the latter being iron transport multicopper oxidase FET5 precursors. This finding is also consistent with the enrichment of transmembrane transport genes (GO: 0055085) during RR infection at 3 dpi for *R. stolonifer*.

1.5.5 Infections of *non-ripening* tomato fruit are comparable to infections of unripe tomato fruit

We inoculated fruit of the *non-ripening* (*nor*) tomato mutant to verify the effect of the ripening stage on the infection success of *B. cinerea*, *F. acuminatum* and *R. stolonifer*. Fruit from the *nor* mutant do not show ripening-associated processes, such as carotenoid

and sugar accumulation or cell wall disassembly, and therefore resemble wild-type MG fruit even at a comparative RR-like stage. None of the three pathogens were able to infect *nor* fruit at any ripening stage (Figure 1.6 and Figure 1.S3). No hyphal growth of *B. cinerea* and *R. stolonifer* was apparent, whereas *F. acuminatum* formed visible mycelia especially at 3 dpi in MG and RR-like fruit. Like on wild-type MG fruit, all three fungi induced necrotic rings in *nor* fruit. When inoculated in RR-like fruit from *nor*, the three fungi displayed similar growth and morphology as in MG fruit from wild-type and *nor*, indicating that for compatible interactions to occur, tomato fruit needs to undergo certain ripening processes that facilitate fungal colonization and spread.

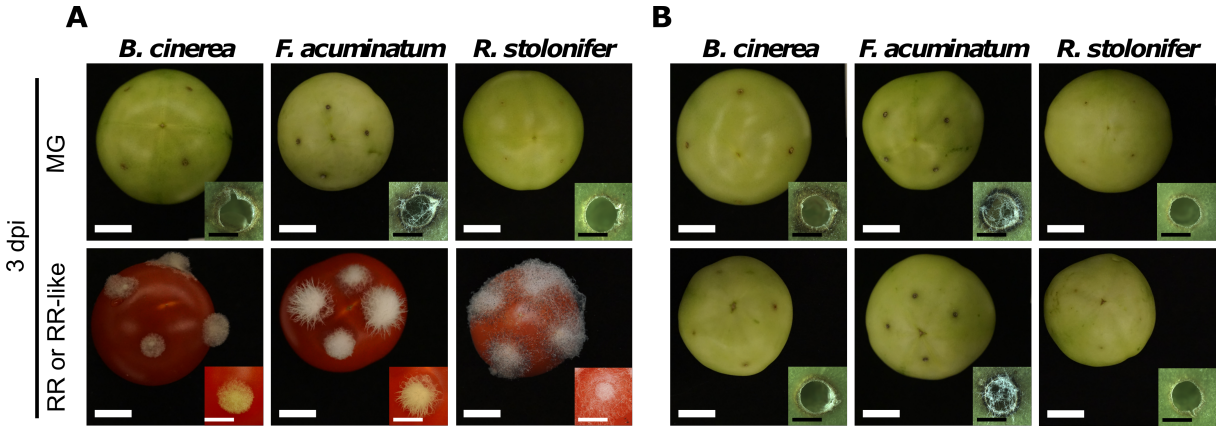

Figure 1.6: Fungal pathogens are unable to infect fruit from the *non-ripening* (*nor*) tomato mutant. (A) Shows inoculations of *Botrytis cinerea*, *Fusarium acuminatum* and *Rhizopus stolonifer* on mature green (MG) and red ripe (RR) wild-type tomato (cv. Ailsa Craig) fruit at 3 days post-inoculation (dpi). (B) Shows inoculations of the same fungi on MG and RR-like fruit from the isogenic *non-ripening* (*nor*) tomato mutant. White size bars correspond to 1 cm whereas black size bars correspond to 1 mm.

1.6 Discussion

Successful infections of *B. cinerea*, *F. acuminatum* and *R. stolonifer* in tomato fruit are dependent on the host developmental stage. In MG fruit, all three fungi were able to grow on the surface, but none of the pathogens was able to cause rot. In contrast, ripe tomato fruit represented a compatible system for infections as all three fungi induced

lesions that spread rapidly. This contrasting ability to cause disease in fruit has been previously reported for a variety of fungal pathogens, particularly those displaying necrotrophic behavior (Blanco-Ulate et al., 2016b; Cantu et al., 2008; Guidarelli et al., 2011; Prusky and Lichter, 2007). The tomato gene *SlWRKY33* has been shown in leaves to be expressed in response to *B. cinerea* inoculation, and deletion of this gene leads to increased susceptibility, indicating its role in defense response (Zhou et al., 2015). We demonstrated that, as in leaves, *B. cinerea* is capable of inducing *SlWRKY33* in MG and RR fruit. Furthermore, *F. acuminatum* also induced *SlWRKY33* in MG and RR fruit, and *R. stolonifer* did so substantially in RR fruit. These findings indicate that all three pathogens triggered disease responses in the host and that the strength of the response was reflective on the success of the infection process.

During interactions with tomato fruit, *B. cinerea*, *F. acuminatum*, and *R. stolonifer* employed a variety of pathogenicity and survival strategies that involved redox processes, carbohydrate catabolism, and proteolysis. Moreover, the degree to which particular strategies were used varied according to the ripening stage of the fruit, as certain processes were emphasized in either MG (such as pectin, cellulose, cellobiose. and hemicellulose breakdown by *B. cinerea* and *F. acuminatum*) or RR fruit (e.g., growth-related processes such as translation initiation, and DNA replication initiation and simple sugar catabolism). These observations suggest that the fungi can sense the physiological environment of the fruit and react accordingly with suitable infection, growth, or quiescence strategies. Though these fungi are incapable of causing disease symptoms in MG tomato fruit, this study demonstrates that they do make attempts to either establish infections or create a suitable environment in fruit for fungal growth and do not merely die on the host tissues. However, when the conditions in fruit are highly unsuitable (e.g., strong cell walls, prevalent antifungal compounds, active host defenses), the infection strategy of the fungal pathogen is often insufficient to cause successful infections. In many cases, when fungal pathogens encounter incompatible conditions, like in unripe fruit, they enter a quiescent phase with limited growth and activity (Prusky et al., 2013). During ripening, the physicochemical properties of the fruit tissues change, resulting in compatible conditions

for the fruit-pathogen interaction and the reactivation of quiescent pathogens (Prusky and Lichter, 2007). In this context, it would also be interesting to investigate the strategies employed by the three fungi during inoculations of other plant organs such as leaves. Our initial tests, however, indicated that both *F. acuminatum* and *R. stolonifer* are incapable of infecting tomato leaves even when leaves were senescing. This observation may suggest that the isolates of these two fungi are exclusive fruit pathogens and lack the molecular toolset to grow on leaves.

The redox environment of the plant-pathogen interface influences the outcome of the interaction. Upon pathogen detection, ROS are rapidly produced by the host, triggering a downstream signaling of various defense responses (Camejo et al., 2016). The enzymatic agents of this oxidative burst are respiratory burst oxidative homologs (RBOHs), which generate superoxide O–2 in the apoplast (Suzuki et al., 2011). This oxidative burst has been previously reported in incompatible tomato-*Botrytis* interactions (Asselbergh et al., 2007), including MG fruit, in which the appearance of a necrotic ring is associated with resistance to *B. cinerea* (Blanco-Ulate et al., 2013; Cantu et al., 2009). However, necrotrophic pathogens can exploit this ROS response by overwhelming the host with their own ROS production (Siegmund and Viefhues, 2016). In leaves of French bean (*Phaseolus vulgaris*), *B. cinerea* has been shown to produce ROS as virulence factors by activating the NADPH oxidases *BcnoxA* (*Bcin05g00350*) and *BcnoxB* (*Bcin02g04930*), coupled with the regulatory protein *BcnoxR* (*Bcin03g06840*; Siegmund et al. (2013)). Although we did not detect strong upregulation of these genes during inoculation of fruit, other ROS producing systems, including laccases (e.g., *Bclcc8*, *Bcin01g00800*) and glucose oxidases (e.g., *BcGOD1*, *Bcin14g05500*) were upregulated during inoculations of tomato fruit. In *F. acuminatum*, a *BcnoxA* homolog *FacuDN4838c0g1i1* and *BcnoxB* homolog *FacuDN3221c0g1i1* were induced in specific treatments. A BLAST search did not reveal any homologs of *BcnoxA* or *BcnoxB* in *R. stolonifer*, nor were any homologs of *Bclcc8* or *BcGOD1* detected in either *F. acuminatum* or *R. stolonifer*.

In addition to ROS generation machinery, fungal pathogens must protect themselves against the oxidative stress of the infection site. Methods of ROS scavenging in phy-

topathogenic fungi include enzymatic and non-enzymatic mechanisms (Heller and Tudzynski, 2011). SODs catalyze the conversion of O_2- produced by RBOHs into the less reactive hydrogen peroxide (H_2O_2). *B. cinerea* mutants lacking the *BcSOD1* (*Bcin03g03390*) gene have been shown to have reduced virulence on tomato leaves (López-Cruz et al., 2017). In tomato fruit, *BcSOD1* is upregulated for both MG and RR ripening stages, which suggests it is also a critical gene for fruit colonization. H_2O_2 can be converted to water by either catalases (CATs) or peroxidases such as GPXs or PRXs. All three pathogens demonstrated upregulation of specific mechanisms of catabolizing H_2O_2, but only *F. acuminatum* showed enrichment of genes involved in the H_2O_2 catabolic process. The usage of these H_2O_2 catabolizing systems varied between the pathogens. While *B. cinerea* utilized catalases in MG fruit at 1 dpi, *F. acuminatum* and *R. stolonifer* produced more catalases and peroxidases in RR fruit at 1 dpi.

In each pathogen, multiple genes involved in protein degradation were found to be upregulated during fruit inoculations. The strong enrichment of proteolysis-related genes may indicate that protein degradation is important for pathogenicity of *F. acuminatum* and *R. stolonifer* but not *B. cinerea*. Some pathogen-derived proteases, such as Sep1 and Mep1 in *Fusarium oxysporum*, are known to serve as suppressors of host-immune response in plant-pathogen interactions (Hou et al., 2018). Even though their specific roles in pathogenesis are not fully characterized, several aspartic proteinases in *B. cinerea* have been described (Ten Have et al., 2010). Three of the *B. cinerea* aspartic proteinases (*BcAP5*, *BcAP8*, and *BcAP9*) that we found to be induced in tomato fruit were also found to be upregulated during infection of grape berries (Kelloniemi et al., 2015). Aspartic proteinases were also found to be among the upregulated proteinases in *F. acuminatum* (4 genes) and *R. stolonifer* (31 genes), though all three pathogens appeared to utilize a diverse suite of proteinases of different families. Especially prominent in *F. acuminatum* and *R. stolonifer* were proteins with similarity to subtilisin-like proteases. This family of enzymes is mostly associated with plants and particularly plant defense, but subtilisin-like proteases involved in pathogenicity have been described for fungi as well (Figueiredo et al., 2018). Fungal plant pathogens are also known to express inhibitors of these types

of proteases as a counter-defense (Figueiredo et al., 2018) Since these inhibitors possess sequence similarity to the proteases themselves, the enzymes identified in *F. acuminatum* and *R. stolonifer* may be inhibitors, proteases, or a mixture of both. Additionally, proteases can help with host tissue decomposition by breaking down cell wall structural proteins or can serve in degradation of proteins to provide a source of nutrition for fungal growth (Lebeda et al., 2001). For example, the saprotrophic fungal species *Verticillium alboatrum* and *V. dahliae* were described to secrete proteases to break down structural proteins that stabilize the plant cell walls (St Leger et al., 1997). High proteolytic activity resulting in the degradation of proteins into free amino acids was also reported during fermentation of tempeh by several *Rhizopus* species (Baumann and Bisping, 1995).

Botrytis cinerea, *F. acuminatum*, and *R. stolonifer* also make use of a variety of CAZymes during interactions with the host. Several CAZyme families are involved in the breakdown of physical barriers present in the host tissues, namely the various cell wall components (cellulose, hemicellulose, and pectin), cell wall reinforcements (lignin), and the waxy fruit cuticle. Many of these enzymes, such as polygalacturonases, pectin methylesterases, pectate lyases, and endo-β-1,4-glucanases, mirror the activities of host enzymes active during the ripening-related softening of the fruit (Bennett and Labavitch, 2008). Others, such as cellulases, cutinases, and lipases, degrade components that are not typically degraded during ripening. Production of cellulases is also coupled with enzymes involved in degradation of cellobiose, the disaccharide product of cellulose breakdown. Both B. cinerea and F. acuminatum appear to focus on production of these latter CAZyme families (e.g., GH5-5, GH7, AA9, CE5, CE10) in MG fruit more than in RR fruit. This may be due to the greater strength and integrity of the cell wall in MG fruit, which requires the fungus to mount a larger attack on the physical barriers in order to penetrate into the cells.

Degradation of pectin is a hallmark feature of *B. cinerea* infection of plant tissues (Blanco-Ulate et al., 2014; Choquer et al., 2007; Lionetti et al., 2007; Shah et al., 2009). The principal enzymes responsible for this process are polygalacturonases (PGs, GH28), pectin methylesterases (PMEs, CE8), and pectate lyases (PLs, PL1, PL3). Both PGs

and PLs cleave the α-1,4-linkages in the homogalacturonan backbone of pectins. PMEs catalyze the removal of methylester groups on the C6 carbons of galacturonan, which allows for further degradation by PGs. Although overexpression of PME inhibitors in Arabidopsis leaves has been shown to increase resistance to *B. cinerea* (Lionetti et al., 2007), mutations in *Bcpme1* and *Bcpme2* do not appear to affect virulence in tomato leaves (Kars et al., 2005). In *B. cinerea*, all three classes of enzymes appear to be highly expressed in MG fruit but not as prominently in RR fruit. Not only do the GH28, PL1-7, and PL3-2 families constitute a greater fraction of upregulated CAZymes in MG fruit, but for PGs, PLs, and PMEs that are commonly upregulated in MG and RR fruit, upregulation is consistently greater (by differential expression analysis) in MG fruit over RR fruit. Additionally, although no *F. acuminatum* PGs were detected in MG, the two upregulated PMEs, *FacuDN5818c0g1i1* and *FacuDN10179c0g1i1*, were only active in MG fruit. Moreover, PL1-7 and PL3-2 genes were strongly expressed in MG fruit, with one PL3-2 gene, *FacuDN8473c0g1i1*, showing a $\log_2$FC of 10.29 at 1 dpi, the highest of any plant CWDE in this treatment. Only one *R. stolonifer* PG, *RstoDN2036c0g1i1*, was detected in MG fruit. However, given that this single *R. stolonifer* PG was one of only two CAZymes found in 1 dpi MG fruit, it is reasonable to believe PG activity in *R. stolonifer* is being underestimated due to low sequence coverage of fungal transcripts in this treatment. The absence of upregulation of any *R. stolonifer* pectate lyases in any fruit further underscores this point. Given the prominence of pectin degradation in *B. cinerea* and *F. acuminatum*, a more targeted analysis of *R. stolonifer* pectin degradation, especially in MG fruit, is warranted.

Degradation of the host cell wall in MG fruit by pathogen enzymes may accelerate ripening and in turn facilitate a more favorable environment for colonization. Pectin-derived oligosaccharides have been shown to induce ethylene production in tomato fruit (Bennett and Labavitch, 2008), which further upregulates expression of host CWDEs, including PG. *B. cinerea* can synthesize its own ethylene via the α-keto-γ-methylthiobutyric acid (KMBA) pathway (Cristescu et al., 2002), though it is still unknown whether the pathogen produces ethylene during interactions with the fruit. Ethylene production dur-

ing plant infection has also been reported via the KMBA pathway for species of *Fusarium* (Ansari et al., 2013; Tzeng and DeVay, 1984), but not, to our knowledge, for *R. stolonifer*. However, the specific genes involved in the KMBA pathway in *B. cinerea* or *Fusarium* spp. have yet to be elucidated.

As colonization proceeds, sugar substrates become available due to degradation of cell wall polysaccharides as well as increased access to stored sugars in the fruit. As a consequence, fungi actively infecting RR tomato fruit induced enzymes (GH32, AA3-2) that metabolize simple sugars. Sugar metabolism is accompanied by expression of CAZyme families involved in the production and modification of chitin, the structural component of fungal cell walls. Chitin production is known to be a hallmark of growth for fungal pathogens (Lenardon et al., 2010). Interestingly, chitin production and modification appear to be prominent not only in RR fruit for each pathogen, but also in MG fruit inoculated with *F. acuminatum*, where a much greater amount of mycelia growth was observed compared to the other two pathogens. The equal representation of CE4 enzymes in MG and RR fruit inoculated with *F. acuminatum* is reflective of the ability of this fungus of producing hyphae at either fruit ripening stage. The abundance of polysaccharide-building glycosyltransferases in RR infections with *R. stolonifer* is also likely connected to the abundant mycelial growth.

Other CAZyme families represent more specialized roles in the infection process. Production of enzymes in the AA7 family may be related to the production of polyketide toxins in *B. cinerea* and *R. stolonifer*. *B. cinerea* is known to produce botcinic acid, a polyketide mycotoxin, during infection (Dalmais et al., 2011). However, the AA7 genes detected to be upregulated in fruit infection here are not known members of the botcinic acid pathway, suggesting that *B. cinerea* may produce additional uncharacterized polyketide mycotoxins during fruit infection. Even though upregulated *F. acuminatum* genes involved in toxin production are not annotated as members of the AA7 family, fumonisins are products of polyketide metabolism (Alexander et al., 2009). The observed upregulation of fumonisin biosynthesis related genes (*FacuDN12063c0g1i1*, *FacuDN15813c0g1i1*, and *FacuDN9039c0g1i1*) indicates that *F. acuminatum* also produces polyketide mycotox-

ins during infection of unripe and ripe tomato fruit. However, we also observed upregulation of biosynthetic genes involved in production of trichothecenes (*FacuDN16662c0g1i1*, *FacuDN7264c0g1i1*, and *FacuDN16121c0g1i1*), which indicates that *F. acuminatum* also relies on other toxins during infection of tomato fruit concordant with the classification of *F. acuminatum* as strong toxin producer (Visconti et al., 1989). Additionally, the AA6 family that appears during RR infections of *F. acuminatum* and *R. stolonifer* may be involved in metabolism of host defense compounds. These enzymes are 1,4-benzoquinone reductases, which have been shown to function in fungal protection against destructive host-produced quinones (Gómez-Toribio et al., 2009; Jensen Jr et al., 2002; Lee et al., 2007).

Another physiological factor which may influence the success of infection is the pH of the pathogen-host interface. As the tomato fruit ripens, the apoplast becomes more acidic (Blanco-Ulate et al., 2016b). Furthermore, *B. cinerea* has been shown to acidify the host environment through the production and secretion of oxalic acid (Williamson et al., 2007). A key enzyme in oxalic acid biosynthesis is *BcOAH1* (*Bcin12g01020*), which encodes oxaloacetate hydrolase (Han et al., 2007). This gene is not upregulated during interaction with tomato fruit in any of the treatments. However, there is significant (P_{adj}) = 2.9 x 10^{-22}, $\log_2$FC = -4.52) downregulation of this gene in RR fruit compared to MG fruit. This suggests that, if *B. cinerea* utilizes oxalic acid to acidify tomato fruit, it does so to a much lesser extent in RR fruit where the pH is already comparatively acidic. In contrast, during infection of Arabidopsis roots, *F. oxysporum* relies on alkalinization via peptides known as rapid alkalinizing factors (RALFs; Masachis et al. (2016)). However, a BLAST search of RALF sequences, as was performed to identify fungal RALFs in Thynne et al. (2017), revealed no clear RALF genes in our transcriptome of *F. acuminatum*.

The importance of fruit ripening for the success of fungal infections was confirmed by comparing fungal growth and disease development in fruit from wild-type and a non-ripening mutant after fungal inoculation. Growth and morphology of *B. cinerea*, *F. acuminatum* and *R. stolonifer* on *nor* MG and RR-like tomato fruit was comparable to that on wild-type MG fruit. This result is in agreement with our previous report

that *nor* tomato fruit is resistant to *B. cinerea* infections (Cantu et al., 2009). The inability to infect non-ripening tomato fruit highlights the dependency of these fungi on the activation and progression of ripening events (e.g., cell wall disassembly during fruit softening, increased redox state, higher available sugars) that transform the host tissues into a favorable environment for disease development.

Altogether, our results confirm that infection success of the three pathogens *B. cinerea*, *F. acuminatum* and *R. stolonifer* largely depends on fruit ripening stage. This is due to all three pathogens sharing similar lifestyles and necrotrophic infection strategies. However, the capacity to infect different plant tissues differs between the three fungi. *B. cinerea* shows distinct strategies in both ripening stages likely due to its ability to induce susceptibility in the host (Cantu et al., 2009), whereas *R. stolonifer* is active almost exclusively in RR fruit. The ability of *F. acuminatum* to infect both MG and RR fruit may be reflective of its especially wide host range, which includes insects in addition to fruit (Logrieco et al., 1992; Rashid et al., 2016). A summary of infection strategies utilized by the three pathogens during infection of MG and RR tomato fruit is shown in Table 1.2. Further research on which processes identified are required for successful infection would lead to a greater understanding of fruit-pathogen interactions and, ultimately, strategies for their management.

Table 1.2: Summary of strategies utilized by *Botrytis cinerea*, *Fusarium acuminatum* and *Rhizopus stolonifer* during infection of unripe (MG) and ripe (RR) tomato fruit.

Infection strategies in fruit	*B. cinerea*		*F. acuminatum*		*R. stolonifer*	
	MG	RR	MG	RR	MG	RR
ROS production (e.g., NADPH oxidases, laccases)	✓	✓	✓	✓		
ROS detoxification (e.g., catalases, peroxidases)	✓		✓	✓		✓
Proteolysis (e.g., aspartic or subtilisin-like proteases)			✓	✓		✓
Cell wall degradation (e.g., polygalacturonases, cellulases)	✓	✓	✓	✓		✓
Sugar metabolism (e.g., invertases, glucose oxidase)		✓	✓	✓		✓
Toxin production (e.g., polyketides, trichothecenes)	✓	✓	✓	✓		
pH alteration (e.g. oxalic acid production)	✓					

References

Alexander, N. J., Proctor, R. H., and McCormick, S. P. (2009). Genes, gene clusters, and biosynthesis of trichothecenes and fumonisins in *Fusarium*. *Toxin Reviews*, 28(2-

3):198–215.

Alkan, N. and Fortes, A. M. (2015). Insights into molecular and metabolic events associated with fruit response to post-harvest fungal pathogens. *Frontiers in Plant Science*, 6:889.

Altomare, C., Logrieco, A., Petrini, O., and Bottalico, A. (1997). Taxonomic relationships among the toxigenic species *Fusarium acuminatum*, *Fusarium sporotrichioides* and *Fusarium tricinctum* by isozyme analysis and RAPD assay. *Canadian Journal of Botany*, 75(10):1674–1684.

Ansari, M. W., Shukla, A., Pant, R. C., and Tuteja, N. (2013). First evidence of ethylene production by *Fusarium mangiferae* associated with mango malformation. *Plant Signaling & Behavior*, 8(1):e22673.

Asselbergh, B., Curvers, K., França, S. C., Audenaert, K., Vuylsteke, M., Van Breusegem, F., and Höfte, M. (2007). Resistance to *Botrytis cinerea* in sitiens, an abscisic acid-deficient tomato mutant, involves timely production of hydrogen peroxide and cell wall modifications in the epidermis. *Plant Physiology*, 144(4):1863–1877.

Baumann, U. and Bisping, B. (1995). Proteolysis during tempe fermentation. *Food Microbiology*, 12:39–47.

Bautista-Baños, S., Bosquez-Molina, E., and Barrera-Necha, L. L. (2014). *Rhizopus stolonifer* (soft rot). In *Postharvest Decay*, pages 1–44. Elsevier.

Bautista-Baños, S., Velaquez-Del Valle, M. G., Hernandez-Lauzardoa, A. N., and Barka, E. A. (2008). The *Rhizopus stolonifer*-tomato interaction.

Bennett, A. B. and Labavitch, J. M. (2008). Ethylene and ripening-regulated expression and function of fruit cell wall modifying proteins. *Plant Science*, 175(1-2):130–136.

Blanco-Ulate, B., Labavitch, J. M., Vincenti, E., Powell, A. L. T., and Cantu, D. (2016a). Hitting the wall: Plant cell walls during *Botrytis cinerea* infections. In Fillinger, S.

and Elad, Y., editors, *Botrytis - the Fungus, the Pathogen and its Management in Agricultural Systems*, pages 361–386. Springer International Publishing.

Blanco-Ulate, B., Morales-Cruz, A., Amrine, K. C., Labavitch, J. M., Powell, A. L., and Cantu, D. (2014). Genome-wide transcriptional profiling of *Botrytis cinerea* genes targeting plant cell walls during infections of different hosts. *Frontiers in Plant Science*, 5:435.

Blanco-Ulate, B., Vincenti, E., Cantu, D., and Powell, A. L. T. (2016b). Ripening of tomato fruit and susceptibility to *Botrytis cinerea*. In Fillinger, S. and Elad, Y., editors, *Botrytis - the Fungus, the Pathogen and its Management in Agricultural Systems*, pages 387–412. Springer International Publishing.

Blanco-Ulate, B., Vincenti, E., Powell, A. L., and Cantu, D. (2013). Tomato transcriptome and mutant analyses suggest a role for plant stress hormones in the interaction between fruit and *Botrytis cinerea*. *Frontiers in Plant Science*, 4:142.

Bryant, D. M., Johnson, K., DiTommaso, T., Tickle, T., Couger, M. B., Payzin-Dogru, D., Lee, T. J., Leigh, N. D., Kuo, T.-H., Davis, F. G., et al. (2017). A tissue-mapped axolotl de novo transcriptome enables identification of limb regeneration factors. *Cell Reports*, 18(3):762–776.

Camejo, D., Guzmán-Cedeño, Á., and Moreno, A. (2016). Reactive oxygen species, essential molecules, during plant–pathogen interactions. *Plant Physiology and Biochemistry*, 103:10–23.

Cantu, D., Blanco-Ulate, B., Yang, L., Labavitch, J. M., Bennett, A. B., and Powell, A. L. (2009). Ripening-regulated susceptibility of tomato fruit to *Botrytis cinerea* requires NOR but not RIN or ethylene. *Plant Physiology*, 150(3):1434–1449.

Cantu, D., Vicente, A. R., Greve, L., Dewey, F., Bennett, A., Labavitch, J., and Powell, A. (2008). The intersection between cell wall disassembly, ripening, and fruit susceptibility to *Botrytis cinerea*. *Proceedings of the National Academy of Sciences*, 105(3):859–864.

Chen, H.-Q., Lee, M.-H., and Chung, K.-R. (2007). Functional characterization of three genes encoding putative oxidoreductases required for cercosporin toxin biosynthesis in the fungus *Cercospora nicotianae*. *Microbiology*, 153(8):2781–2790.

Choi, J., Détry, N., Kim, K.-T., Asiegbu, F. O., Valkonen, J. P., and Lee, Y.-H. (2014). fPoxDB: fungal peroxidase database for comparative genomics. *BMC Microbiology*, 14(1):117.

Choquer, M., Fournier, E., Kunz, C., Levis, C., Pradier, J.-M., Simon, A., and Viaud, M. (2007). *Botrytis cinerea* virulence factors: new insights into a necrotrophic and polyphageous pathogen. *FEMS Microbiology Letters*, 277(1):1–10.

Consortium, G. O. (2017). Expansion of the gene ontology knowledgebase and resources. *Nucleic Acids Research*, 45(D1):D331–D338.

Consortium, T. G. et al. (2012). The tomato genome sequence provides insights into fleshy fruit evolution. *Nature*, 485(7400):635.

Cristescu, S. M., De Martinis, D., te Lintel Hekkert, S., Parker, D. H., and Harren, F. J. (2002). Ethylene production by *Botrytis cinerea* in vitro and in tomatoes. *Applied and Environmental Microbiology*, 68(11):5342–5350.

Dalmais, B., Schumacher, J., Moraga, J., Le Pecheur, P., Tudzynski, B., Collado, I. G., and Viaud, M. (2011). The *Botrytis cinerea* phytotoxin botcinic acid requires two polyketide synthases for production and has a redundant role in virulence with botrydial. *Molecular Plant Pathology*, 12(6):564–579.

Dean, R., Van Kan, J. A., Pretorius, Z. A., Hammond-Kosack, K. E., Di Pietro, A., Spanu, P. D., Rudd, J. J., Dickman, M., Kahmann, R., Ellis, J., et al. (2012). The top 10 fungal pathogens in molecular plant pathology. *Molecular Plant Pathology*, 13(4):414–430.

Dobin, A., Davis, C. A., Schlesinger, F., Drenkow, J., Zaleski, C., Jha, S., Batut, P., Chaisson, M., and Gingeras, T. R. (2013). STAR: ultrafast universal RNA-seq aligner. *Bioinformatics*, 29(1):15–21.

Dyakov, Y. T. (2007). Overview on parasitism. In *Comprehensive and Molecular Phytopathology*, pages 3–17. Elsevier.

El-Gebali, S., Mistry, J., Bateman, A., Eddy, S. R., Luciani, A., Potter, S. C., Qureshi, M., Richardson, L. J., Salazar, G. A., Smart, A., et al. (2019). The Pfam protein families database in 2019. *Nucleic Acids Research*, 47(D1):D427–D432.

Ferrari, S., Galletti, R., Denoux, C., De Lorenzo, G., Ausubel, F. M., and Dewdney, J. (2007). Resistance to *Botrytis cinerea* induced in *Arabidopsis* by elicitors is independent of salicylic acid, ethylene, or jasmonate signaling but requires PHYTOALEXIN DEFICIENT3. *Plant Physiology*, 144(1):367–379.

Figueiredo, J., Sousa Silva, M., and Figueiredo, A. (2018). Subtilisin-like proteases in plant defence: The past, the present and beyond. *Molecular Plant Pathology*, 19(4):1017–1028.

Fillinger, S. and Elad, Y. (2016). *Botrytis: the fungus, the pathogen and its management in agricultural systems*. Springer.

Glazebrook, J. (2005). Contrasting mechanisms of defense against biotrophic and necrotrophic pathogens. *Annual Review of Phytopathology.*, 43:205–227.

Gómez-Toribio, V., García-Martín, A. B., Martínez, M. J., Martínez, Á. T., and Guillén, F. (2009). Induction of extracellular hydroxyl radical production by white-rot fungi through quinone redox cycling. *Applied and Environmental Microbiology*, 75(12):3944–3953.

Grabherr, M. G., Haas, B. J., Yassour, M., Levin, J. Z., Thompson, D. A., Amit, I., Adiconis, X., Fan, L., Raychowdhury, R., Zeng, Q., et al. (2011). Full-length transcriptome assembly from RNA-seq data without a reference genome. *Nature Biotechnology*, 29(7):644–652.

Guidarelli, M., Carbone, F., Mourgues, F., Perrotta, G., Rosati, C., Bertolini, P., and Baraldi, E. (2011). *Colletotrichum acutatum* interactions with unripe and ripe straw-

berry fruits and differential responses at histological and transcriptional levels. *Plant Pathology*, 60(4):685–697.

Han, Y., Joosten, H.-J., Niu, W., Zhao, Z., Mariano, P. S., McCalman, M., Van Kan, J., Schaap, P. J., and Dunaway-Mariano, D. (2007). Oxaloacetate hydrolase, the C–C bond lyase of oxalate secreting fungi. *Journal of Biological Chemistry*, 282(13):9581–9590.

Heller, J. and Tudzynski, P. (2011). Reactive oxygen species in phytopathogenic fungi: signaling, development, and disease. *Annual review of phytopathology*, 49:369–390.

Hou, S., Jamieson, P., and He, P. (2018). The cloak, dagger, and shield: proteases in plant–pathogen interactions. *Biochemical Journal*, 475(15):2491–2509.

Jensen Jr, K. A., Ryan, Z. C., Wymelenberg, A. V., Cullen, D., and Hammel, K. E. (2002). An NADH: quinone oxidoreductase active during biodegradation by the brown-rot basidiomycete *Gloeophyllum trabeum*. *Applied and Environmental Microbiology*, 68(6):2699–2703.

Jimenez, M., Logrieco, A., and Bottalico, A. (1993). Occurrence and pathogenicity of *Fusarium* species in banana fruits. *Journal of Phytopathology*, 137(3):214–220.

Kars, I., McCalman, M., Wagemakers, L., and van Kan, J. A. (2005). Functional analysis of *Botrytis cinerea* pectin methylesterase genes by PCR-based targeted mutagenesis: Bcpme1 and Bcpme2 are dispensable for virulence of strain B05. 10. *Molecular Plant Pathology*, 6(6):641–652.

Kelloniemi, J., Trouvelot, S., Héloir, M.-C., Simon, A., Dalmais, B., Frettinger, P., Cimerman, A., Fermaud, M., Roudet, J., Baulande, S., et al. (2015). Analysis of the molecular dialogue between gray mold (*Botrytis cinerea*) and grapevine (*Vitis vinifera*) reveals a clear shift in defense mechanisms during berry ripening. *Molecular Plant-Microbe Interactions*, 28(11):1167–1180.

Kim, W., Park, C.-M., Park, J.-J., Akamatsu, H. O., Peever, T. L., Xian, M., Gang, D. R., Vandemark, G., and Chen, W. (2015). Functional analyses of the Diels-Alderase

gene sol5 of *Ascochyta rabiei* and *Alternaria solani* indicate that the solanapyrone phytotoxins are not required for pathogenicity. *Molecular Plant-Microbe Interactions*, 28(4):482–496.

Langmead, B. and Salzberg, S. L. (2012). Fast gapped-read alignment with Bowtie 2. *Nature Methods*, 9(4):357.

Lebeda, A., Luhová, L., Sedlářová, M., and Jančová, D. (2001). The role of enzymes in plant-fungal pathogens interactions/Die Rolle der Enzyme in den Beziehungen zwischen Pflanzen und pilzlichen Erregern. *Zeitschrift für Pflanzenkrankheiten und Pflanzenschutz/Journal of Plant Diseases and Protection*, pages 89–111.

Lee, S.-S., Moon, D.-S., Choi, H. T., and Song, H.-G. (2007). Purification and characterization of an intracellular NADH: quinone reductase from *Trametes versicolor*. *The Journal of Microbiology*, 45(4):333–338.

Lenardon, M. D., Munro, C. A., and Gow, N. A. (2010). Chitin synthesis and fungal pathogenesis. *Current Opinion in Microbiology*, 13(4):416–423.

Lionetti, V., Raiola, A., Camardella, L., Giovane, A., Obel, N., Pauly, M., Favaron, F., Cervone, F., and Bellincampi, D. (2007). Overexpression of pectin methylesterase inhibitors in *Arabidopsis* restricts fungal infection by *Botrytis cinerea*. *Plant Physiology*, 143(4):1871–1880.

Logrieco, A., Altomare, C., Moretti, A., and Bottalico, A. (1992). Cultural and toxigenic variability in *Fusarium acuminatum*. *Mycological Research*, 96(6):518–523.

Lombard, V., Golaconda Ramulu, H., Drula, E., Coutinho, P. M., and Henrissat, B. (2014). The carbohydrate-active enzymes database (CAZy) in 2013. *Nucleic Acids Research*, 42(D1):D490–D495.

López-Cruz, J., Óscar, C.-S., Emma, F.-C., Pilar, G.-A., and Carmen, G.-B. (2017). Absence of Cu–Zn superoxide dismutase BCSOD1 reduces *Botrytis cinerea* virulence

in *Arabidopsis* and tomato plants, revealing interplay among reactive oxygen species, callose and signalling pathways. *Molecular Plant Pathology*, 18(1):16–31.

Love, M. I., Huber, W., and Anders, S. (2014). Moderated estimation of fold change and dispersion for RNA-seq data with DESeq2. *Genome Biology*, 15(12):550.

Marín, P., Moretti, A., Ritieni, A., Jurado, M., Vázquez, C., and González-Jaén, M. T. (2012). Phylogenetic analyses and toxigenic profiles of *Fusarium equiseti* and *Fusarium acuminatum* isolated from cereals from Southern Europe. *Food Microbiology*, 31(2):229–237.

Masachis, S., Segorbe, D., Turrà, D., Leon-Ruiz, M., Fürst, U., El Ghalid, M., Leonard, G., López-Berges, M. S., Richards, T. A., Felix, G., et al. (2016). A fungal pathogen secretes plant alkalinizing peptides to increase infection. *Nature Microbiology*, 1(6):1–9.

Nabi, S., Raja, W., Kumawat, K., Mir, J., Sharma, O., Singh, D., and Sheikh, M. (2017). Post harvest diseases of temperate fruits and their management strategies-a review.

Nakajima, M. and Akutsu, K. (2014). Virulence factors of *Botrytis cinerea*. *Journal of General Plant Pathology*, 80(1):15–23.

Oliver, R. P. and Ipcho, S. V. S. (2004). *Arabidopsis* pathology breathes new life into the necrotrophs-vs.-biotrophs classification of fungal pathogens. *Molecular Plant Pathology*, 5(4):347–352.

Park, A. R., Son, H., Min, K., Park, J., Goo, J. H., Rhee, S., Chae, S.-K., and Lee, Y.-W. (2015). Autoregulation of ZEB 2 expression for zearalenone production in *Fusarium graminearum*. *Molecular Microbiology*, 97(5):942–956.

Perfect, S. E. and Green, J. R. (2001). Infection structures of biotrophic and hemibiotrophic fungal plant pathogens. *Molecular Plant Pathology*, 2(2):101–108.

Prusky, D., Alkan, N., Mengiste, T., and Fluhr, R. (2013). Quiescent and necrotrophic lifestyle choice during postharvest disease development. *Annual Review of Phytopathology*, 51:155–176.

Prusky, D. and Lichter, A. (2007). Activation of quiescent infections by postharvest pathogens during transition from the biotrophic to the necrotrophic stage. *FEMS Microbiology Letters*, 268(1):1–8.

Rashid, T. S., Sijam, K., Awla, H. K., Saud, H. M., and Kadir, J. (2016). Pathogenicity assay and molecular identification of fungi and bacteria associated with diseases of tomato in Malaysia. *American Journal of Plant Sciences*, 7(6):949–957.

Reis, H., Pfiffi, S., and Hahn, M. (2005). Molecular and functional characterization of a secreted lipase from *Botrytis cinerea*. *Molecular Plant Pathology*, 6(3):257–267.

Rossi, F. R., Krapp, A. R., Bisaro, F., Maiale, S. J., Pieckenstain, F. L., and Carrillo, N. (2017). Reactive oxygen species generated in chloroplasts contribute to tobacco leaf infection by the necrotrophic fungus *Botrytis cinerea*. *The Plant Journal*, 92(5):761–773.

Saier Jr, M. H., Reddy, V. S., Tsu, B. V., Ahmed, M. S., Li, C., and Moreno-Hagelsieb, G. (2016). The transporter classification database (TCDB): recent advances. *Nucleic Acids Research*, 44(D1):D372–D379.

Shah, P., Gutierrez-Sanchez, G., Orlando, R., and Bergmann, C. (2009). A proteomic study of pectin-degrading enzymes secreted by *Botrytis cinerea* grown in liquid culture. *Proteomics*, 9(11):3126–3135.

Siegmund, U., Heller, J., van Kann, J. A., and Tudzynski, P. (2013). The NADPH oxidase complexes in *Botrytis cinerea*: evidence for a close association with the ER and the tetraspanin Pls1. *PloS One*, 8(2):e55879.

Siegmund, U. and Viefhues, A. (2016). Reactive oxygen species in the *Botrytis*–host interaction. In Fillinger, S. and Elad, Y., editors, *Botrytis - the Fungus, the Pathogen and its Management in Agricultural Systems*, pages 269–289. Springer International Publishing.

Smith-Unna, R., Boursnell, C., Patro, R., Hibberd, J. M., and Kelly, S. (2016). TransRate: reference-free quality assessment of de novo transcriptome assemblies. *Genome Research*, 26(8):1134–1144.

St Leger, R. J., Joshi, L., and Roberts, D. W. (1997). Adaptation of proteases and carbohydrases of saprophytic, phytopathogenic and entomopathogenic fungi to the requirements of their ecological niches. *Microbiology*, 143(6):1983–1992.

Suzuki, N., Miller, G., Morales, J., Shulaev, V., Torres, M. A., and Mittler, R. (2011). Respiratory burst oxidases: the engines of ROS signaling. *Current Opinion in Plant Biology*, 14(6):691–699.

Swartzberg, D., Kirshner, B., Rav-David, D., Elad, Y., and Granot, D. (2008). *Botrytis cinerea* induces senescence and is inhibited by autoregulated expression of the IPT gene. *European Journal of Plant Pathology*, 120(3):289–297.

Ten Have, A., Espino, J. J., Dekkers, E., Van Sluyter, S. C., Brito, N., Kay, J., González, C., and van Kan, J. A. (2010). The *Botrytis cinerea* aspartic proteinase family. *Fungal Genetics and Biology*, 47(1):53–65.

Thynne, E., Saur, I. M., Simbaqueba, J., Ogilvie, H. A., Gonzalez-Cendales, Y., Mead, O., Taranto, A., Catanzariti, A.-M., McDonald, M. C., Schwessinger, B., et al. (2017). Fungal phytopathogens encode functional homologues of plant rapid alkalinization factor (RALF) peptides. *Molecular Plant Pathology*, 18(6):811–824.

Tzeng, D. D. and DeVay, J. E. (1984). Ethylene production and toxigenicity of methionine and its derivatives with riboflavin in cultures of *Verticillium*, *Fusarium* and *Colletotrichum* species exposed to light. *Physiologia Plantarum*, 62(4):545–552.

Urban, M., Cuzick, A., Rutherford, K., Irvine, A., Pedro, H., Pant, R., Sadanadan, V., Khamari, L., Billal, S., Mohanty, S., et al. (2017). PHI-base: a new interface and further additions for the multi-species pathogen–host interactions database. *Nucleic Acids Research*, 45(D1):D604–D610.

Van Kan, J., Van't Klooster, J., Wagemakers, C., Dees, D., and Van der Vlugt-Bergmans, C. (1997). Cutinase A of *Botrytis cinerea* is expressed, but not essential, during penetration of gerbera and tomato. *Molecular Plant-Microbe Interactions*, 10(1):30–38.

van Kan, J. A. (2006). Licensed to kill: the lifestyle of a necrotrophic plant pathogen. *Trends in Plant Science*, 11(5):247–253.

Van Kan, J. A., Shaw, M. W., and Grant-Downton, R. T. (2014). Botrytis species: relentless necrotrophic thugs or endophytes gone rogue? *Molecular Plant Pathology*, 15(9):957–961.

Van Kan, J. A., Stassen, J. H., Mosbach, A., Van Der Lee, T. A., Faino, L., Farmer, A. D., Papasotiriou, D. G., Zhou, S., Seidl, M. F., Cottam, E., et al. (2017). A gapless genome sequence of the fungus *Botrytis cinerea*. *Molecular Plant Pathology*, 18(1):75–89.

Veloso, J. and van Kan, J. A. (2018). Many shades of grey in *Botrytis*–host plant interactions. *Trends in Plant Science*, 23(7):613–622.

Visconti, A., Mirocha, C. J., Logrieco, A., Bottalico, A., and Solfrizzo, M. (1989). Mycotoxins produced by *Fusarium acuminatum*. isolation and characterization of acuminatin: a new trichothecene. *Journal of Agricultural and Food Chemistry*, 37(5):1348–1351.

Waterhouse, R. M., Seppey, M., Simão, F. A., Manni, M., Ioannidis, P., Klioutchnikov, G., Kriventseva, E. V., and Zdobnov, E. M. (2018). BUSCO applications from quality assessments to gene prediction and phylogenomics. *Molecular Biology and Evolution*, 35(3):543–548.

Weiberg, A., Wang, M., Lin, F.-M., Zhao, H., Zhang, Z., Kaloshian, I., Huang, H.-D., and Jin, H. (2013). Fungal small RNAs suppress plant immunity by hijacking host RNA interference pathways. *Science*, 342(6154):118–123.

Williamson, B., Tudzynski, B., Tudzynski, P., and Van Kan, J. A. (2007). *Botrytis cinerea*: the cause of grey mould disease. *Molecular Plant Pathology*, 8(5):561–580.

Ye, J., Coulouris, G., Zaretskaya, I., Cutcutache, I., Rozen, S., and Madden, T. L. (2012). Primer-BLAST: a tool to design target-specific primers for polymerase chain reaction. *BMC Bioinformatics*, 13(1):134.

Young, M. D., Wakefield, M. J., Smyth, G. K., and Oshlack, A. (2010). Gene ontology analysis for rna-seq: accounting for selection bias. *Genome Biology*, 11(2):R14.

Zhou, J., Wang, J., Zheng, Z., Fan, B., Yu, J.-Q., and Chen, Z. (2015). Characterization of the promoter and extended C-terminal domain of *Arabidopsis* WRKY33 and functional analysis of tomato WRKY33 homologues in plant stress responses. *Journal of Experimental Botany*, 66(15):4567–4583.

Zhou, J., Yu, J.-Q., and Chen, Z. (2014). The perplexing role of autophagy in plant innate immune responses. *Molecular Plant Pathology*, 15(6):637–645.

1.7 Supplemental Material

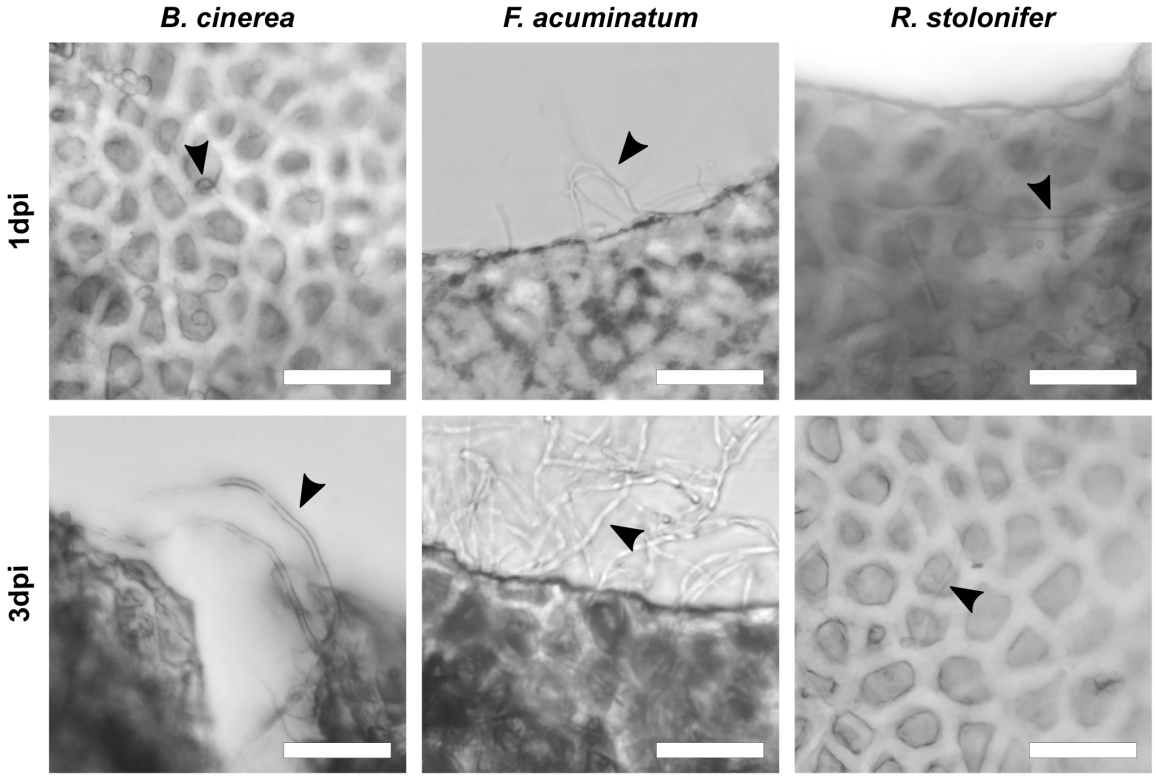

Figure 1.S1: Mycelial growth in mature green tomato fruit. Hyphae and spores are indicated by arrowheads in each panel. The size bars correspond to 0.5 mm and dpi corresponds to days post inoculation.

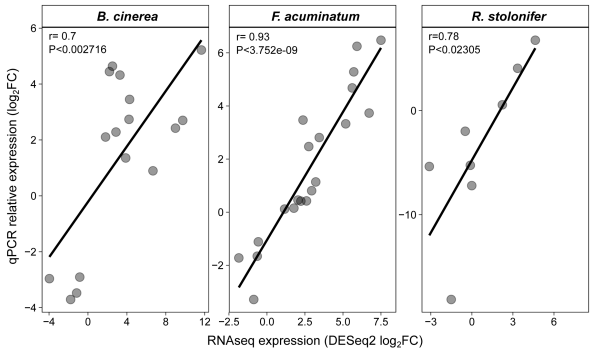

Figure 1.S2: Correlation between the qPCR data and the RNAseq data validate the Differential Gene Expression analysis. For each gene, fold change of the gene expression was calculated as $\log_2$(expression on MG or RR tissue/expression IV). r, Pearson correlation coefficient; *P*, *P*-value.

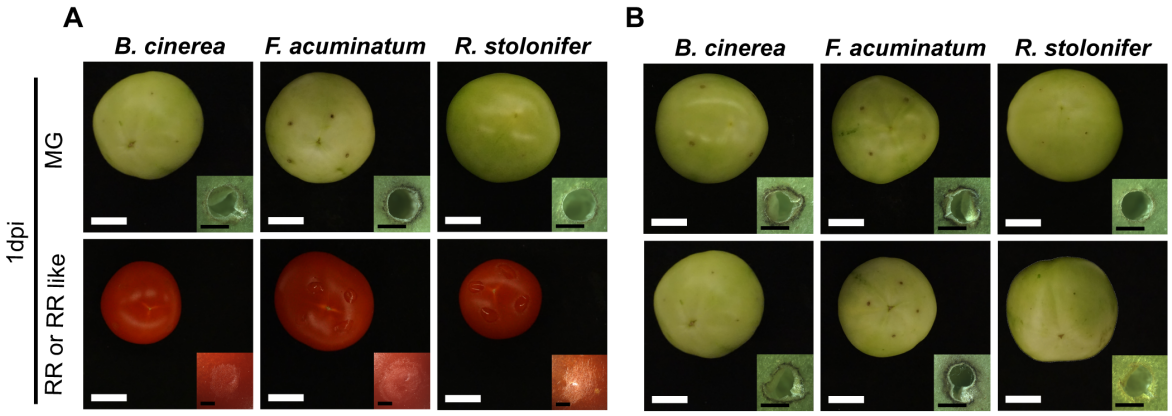

Figure 1.S3: Fungal pathogens do not cause disease on fruit from the *non-ripening* (*nor*) tomato mutant. (A) Inoculations of *Botrytis cinerea*, *Fusarium acuminatum* and *Rhizopus stolonifer* on mature green (MG) and red ripe (RR) wild-type tomato (cv. Ailsa Craig) fruit at 1 days post-inoculation (dpi). (B) Inoculations of the same fungi on MG and RR-like fruit from the isogenic *non-ripening* (*nor*) tomato mutant. White size bars correspond to 1 cm whereas black size bars correspond to 1 mm.

Chapter 2

Host susceptibility factors render ripe tomato fruit vulnerable to fungal disease despite active immune responses

2.1 Publication Statement

The content of this chapter was peer-reviewed and published as follows:

Silva, C. J., van den Abeele, C., Ortega-Salazar, I., Papin, V., Adaskaveg, J. A., Wang, D., Casteel, C. L., Seymour, G. B., and Blanco-Ulate, B. (2021). Host susceptibility factors render ripe tomato fruit vulnerable to fungal disease despite active immune responses. *Journal of Experimental Botany*, 72(7):2696–2709.

For this publication, I wrote the paper and was credited as first author. Additionally, I performed the fungal inoculations, prepared the RNA-Seq libraries, performed all bioinformatics and statistical analyses.

2.2 Abstract

The increased susceptibility of ripe fruit to fungal pathogens poses a substantial threat to crop production and marketability. Here, we coupled transcriptomic analyses with mutant studies to uncover critical processes associated with defense and susceptibility in tomato (*Solanum lycopersicum*) fruit. Using unripe and ripe fruit inoculated with three fungal pathogens, we identified common pathogen responses reliant on chitinases, WRKY transcription factors, and reactive oxygen species detoxification. We established that the magnitude and diversity of defense responses do not significantly impact the interaction

outcome, as susceptible ripe fruit mounted a strong immune response to pathogen infection. Then, to distinguish features of ripening that may be responsible for susceptibility, we utilized nonripening tomato mutants that displayed different susceptibility patterns to fungal infection. Based on transcriptional and hormone profiling, susceptible tomato genotypes had losses in the maintenance of cellular redox homeostasis, while jasmonic acid accumulation and signaling coincided with defense activation in resistant fruit. We identified and validated a susceptibility factor, pectate lyase (*PL*). CRISPR-based knockouts of *PL*, but not polygalacturonase (*PG2a*), reduced susceptibility of ripe fruit by >50%. This study suggests that targeting specific genes that promote susceptibility is a viable strategy to improve the resistance of tomato fruit against fungal disease.

2.3 Introduction

Half of all fruit and vegetables produced globally are lost each year (Gustavsson et al., 2011). While the causes of losses vary by region and commodity, fungal phytopathogens have a widespread role, as 20–25% of all harvested fruit and vegetables are lost to rotting caused by such fungi (Sharma et al., 2009). In fleshy fruits, this issue is exacerbated because, in general, fruit become more susceptible to fungal pathogens as they ripen (Blanco-Ulate et al., 2016b; Prusky, 1996). Ripening-associated susceptibility has been demonstrated in multiple commodities including climacteric fruits such as tomato, stone fruit, banana, apple, and pear, as well as non-climacteric fruits such as strawberry, cantaloupe, citrus, and pineapple (Alkan et al., 2015; Barral et al., 2019; Cantu et al., 2009; Chiu et al., 2013; Gell et al., 2008; Lafuente et al., 2019; Lassois et al., 2010; Morales et al., 2008; Petrasch et al., 2019a; Zhang et al., 1999).

The most devastating postharvest pathogens in fruit are those with necrotrophic lifestyles, which deliberately kill host tissue, resulting in rotting. Example pathogens include the model necrotrophic fungi *Botrytis cinerea* and *Sclerotinia sclerotiorum* as well as *Monilinia* spp., *Alternaria* spp., *Rhizopus* spp., *Penicillium* spp., and *Fusarium* spp. (Bautista-Baños et al., 2014; Liang and Rollins, 2018; Nunes, 2012; Petrasch et al., 2019b; van Kan et al., 2014). Plant immune responses against necrotrophic fungi are

multilayered, involving (i) recognition of pathogen-associated molecular patterns, such as chitin or chitosan, by pattern recognition receptors, (ii) intracellular signaling through mitogen-activated protein (MAP) kinase cascades, (iii) induction of downstream defenses by coordinated activity of phytohormones, particularly ethylene and jasmonic acid (JA), (iv) cell wall fortifications, and (v) production of various secondary metabolites and antifungal proteins (AbuQamar et al., 2017; Mbengue et al., 2016; Pandey et al., 2016; van der Ent and Pieterse, 2012; Veloso and van Kan, 2018). However, most defense strategies have been studied in leaves, and their utilization and effectiveness in fruit have been assessed only with single pathogens (Ahmadi-Afzadi et al., 2018; Alkan et al., 2015; Cantu et al., 2009).

The outcome of any fruit–necrotroph interaction relies on the balance between the presence or induction of defenses and the contributions of susceptibility factors. Though induced defenses are heavily studied in plant immunity, the impact of preformed (or 'constitutive') defenses and susceptibility factors are less researched (van Schie and Takken, 2014). Preformed defenses include structural barriers, such as the cell wall and cuticle, and the accumulation of secondary metabolites (Veronese et al., 2003; Wittstock and Gershenzon, 2002), while susceptibility factors include the abundance of simple sugars and organic acids or activity of host cell wall modifying proteins (Cantu et al., 2008; Centeno et al., 2011). A sufficient understanding of ripening-associated susceptibility requires a characterization of the ripening program's impact on (i) the ability of the host to express necessary defense genes upon pathogen challenge, (ii) the integrity of preformed defenses, and (iii) the abundance of susceptibility factors.

In this study, we first applied a transcriptomic approach to characterize core tomato fruit responses to three fungal pathogens and changes in gene expression that occur during ripening to promote susceptibility. To identify core responses that are not merely pathogen-specific, we used three pathogens with necrotrophic infection strategies: *B. cinerea*, *Rhizopus stolonifer*, and *Fusarium acuminatum*. Using well-established defense gene classifications, we developed profiles of host defense gene expression responses in unripe and ripe fruit. We then determined the susceptibility phenotypes of three non-

ripening mutants: *Colorless non-ripening* (*Cnr*), *ripening inhibitor* (*rin*), and *non-ripening* (*nor*), which have unique defects in ripening features (Gao et al., 2020, 2019; Giovannoni et al., 2004; Ito et al., 2017; Manning et al., 2006; Vrebalov et al., 2002; Wang et al., 2019b). After demonstrating that each mutant has distinct susceptibility to disease, we identified ripening genes whose expression changes may impact the disease outcome. By integrating our transcriptomic data and mutant analyses, we found preformed defenses and susceptibility factor candidates associated with *B. cinerea* infections. Using CRISPR-based mutants, we established that one candidate, the pectin-degrading enzyme pectate lyase, is indeed a disease susceptibility factor in ripe tomato fruit.

2.4 Materials and Methods

2.4.1 Plant material

Tomato (*Solanum lycopersicum*) cv. 'Ailsa Craig' (AC), isogenic non-ripening mutants *rin*, *nor*, and *Cnr*, and CRISPR-based *PL* (PL5-4) and *PG2a* (PG21) mutants with azygous control plants (Wang et al., 2019a) were grown under standard field conditions in the Department of Plant Sciences Field Facilities at the University of California, Davis. Fruit were tagged at 3 d post-anthesis (dpa) and harvested at 31 dpa for mature green (MG) and at 42 dpa for red ripe (RR) or equivalent for ripening mutants. For all tomato genotypes, fruit ripening stages were visually assessed based on color, and quality attributes were measured at the time of harvest (see Supplementary Tables S1, S2 at `https://academic.oup.com/jxb/article/72/7/2696/6104152#233260137`). Color was also assessed quantitatively using a Minolta CR-400 chroma meter (Konica Minolta Sensing Inc., Japan) and recorded in the L*a*b color space for the non-ripening fruit (n=24–48 fruit). Firmness was evaluated with a TA.XT2i Texture Analyzer (Texture Technologies, USA) using a TA-25 cylinder probe, a trigger force of 0.045 N and a test speed of 2.00 mm s^{-1}. Non-ripening fruit (n=20–25 fruit) were evaluated at both stages, azygous and CRISPR lines (n=32 fruit) only at the RR stage. Soluble solids, titratable acidity (TA) levels, and pH were determined from the juice of the same fruit used for firmness measurements (n=4–9 replicates of a pool of 5–8 fruit each). Soluble solids were

measured as degrees Brix with a Reichert AR6 Series automatic bench refractometer (Reichert Inc., USA). TA and pH were measured with the TIM850 Titration Manager (Radiometer Analytics, Germany). Four grams of juice diluted in 20 ml deionized water were titrated to determine TA based on citric acid equivalents. Significant differences in physiological parameters between genotypes were determined with analysis of variance (ANOVA) followed by post hoc testing (Tukey's honestly significant difference, HSD) using R (R Foundation for Statistical Computing, Vienna, Austria).

2.4.2 Fungal culture and fruit inoculation

Rhizopus stolonifer and *F. acuminatum* isolates were taken from rotting fruit and identified through morphological and sequencing methods (Petrasch et al., 2019b). *Botrytis cinerea* (B05.10), *R. stolonifer*, and *F. acuminatum* cultures were grown on 1% potato dextrose agar media. Conidia were harvested from sporulating cultures in 0.01% Tween-20 (Sigma-Aldrich, USA) and counted. Fruit were disinfected and inoculated as described in Petrasch et al. (2019b) using 500, 30, and 1000 conidia μl^{-1} for *B. cinerea*, *R. stolonifer*, and *F. acuminatum*, respectively. Each fruit used to measure disease incidence and severity was punctured at six sites; each fruit used for RNA extraction and transcriptomic analysis was punctured at 15 sites. No inoculum was introduced at puncture sites on wounded fruit. Healthy controls were not wounded or inoculated. Fruit were incubated for up to 3 d at 25 °C in high-humidity containers (90% relative humidity). Five replicates (n=8–10 fruit each) of each treatment were generated for transcriptomic analysis, while four replicates (n=10–12 fruit each) were used for measurements of disease progression.

2.4.3 Disease incidence and severity measurements

Fruit disease incidence and severity were measured at 1, 2, and 3 d postinoculation (dpi). Disease incidence was the percentage of inoculated sites displaying visual signs of tissue maceration or soft rot. Disease severity was calculated as the average lesion diameter (in mm) of each inoculated site displaying signs of rot. Significant differences in disease incidence and severity between genotypes were assessed for each pathogen with ANOVA followed by Tukey's HSD using R.

2.4.4 RNA extraction and library preparation

At 1 dpi, fruit pericarp and epidermal tissue of the blossom end halves of healthy, wounded, and infected fruit were collected and immediately frozen in liquid nitrogen and lysed using a Retsch Mixer Mill MM 400 (Retsch, Germany). RNA was extracted from 1 g of ground material as described in Blanco-Ulate et al. (2013). The purity and concentration of the extracted RNA were determined with a NanoDrop One Spectrophotometer (Thermo Fisher Scientific, USA) and a precise concentration measurement was made with a Qubit 3 fluorometer (Thermo Fisher Scientific). The integrity of the RNA was confirmed by agarose gel electrophoresis.

One hundred and twenty-six cDNA libraries were prepared using the Illumina TruSeq RNA Sample Preparation Kit v.2 (Illumina, USA) from isolated RNA (n=3–8 libraries per treatment). Each library was barcoded and analysed with the High Sensitivity DNA Analysis Kit for the Agilent 2100 Bioanalyzer (Agilent Technologies, USA). Libraries were sequenced as single-end 50-bp reads on an Illumina HiSeq 4000 platform by the DNA Technologies Core at the UC Davis Genome Center.

2.4.5 RNA sequencing and data processing

Raw sequencing reads were trimmed for quality and adapter sequences using Trimmomatic v0.33 (Bolger et al., 2014) with the following parameters: maximum seed mismatches=2, palindrome clip threshold=30, simple clip threshold=10, minimum leading quality=3, minimum trailing quality=3, window size=4, required quality=15, and minimum length=36. Trimmed reads were mapped using Bowtie2 (Langmead and Salzberg, 2012) to combined transcriptomes of tomato (SL4.0 release; `http://solgenomics.net`) and one of the three pathogens: *B. cinerea* (`http://fungi.ensembl.org/Botrytis_cinerea/Info/Index`), *F. acuminatum* (Petrasch et al., 2019b), or *R. stolonifer* (Petrasch et al., 2019b). Count matrices were made from the Bowtie2 results using sam2counts.py v0.91 (`https://github.com/vsbuffalo/sam2counts/`). Only reads that mapped to the tomato transcriptome were used in the following analyses. A summary of the read mapping results can be found in Supplementary Table S3 at `https://academic.oup.com/jxb/article/72/7/2696/6104152#233260137`.

2.4.6 Differential expression analysis

The Bioconductor package DESeq2 (Love et al., 2014) was used to perform normalization of read counts and differential expression analyses for various treatment comparisons. Differentially expressed (DE) genes for each comparison were those with an adjusted P-value of <0.05.

2.4.7 Functional annotation and enrichment analyses

Gene Ontology (GO) terms were retrieved from SolGenomics. Annotations for transcription factors and kinases were generated using the automatic annotation tool from iTAK (Zheng et al., 2016). NBS-LRR family members were identified from Andolfo et al. (2014). Kyoto Encyclopedia of Genes and Genomes (KEGG) annotations were determined using the KEGG Automatic Annotation Server (Moriya et al., 2007), and hormone annotations were derived from these (see Supplementary Table S4 at `https://academic.oup.com/jxb/article/72/7/2696/6104152#233260137`). GO enrichments were performed with the goseq package in R (Young et al., 2010), while enrichments for all other annotations were performed using Fisher's test with resulting P-values adjusted via the Benjamini–Hochberg method (Benjamini and Hochberg, 1995).

2.4.8 Measurement of phytohormones

Ethylene emission was measured in MG and RR fruit (n=4 replicates of a pool of 8–10 fruit each) from the day of harvest through 3 dpi. Headspace gas (3 ml) from weighed fruit in sealed 1 liter containers was extracted after 30–90 min in a Shimadzu CG-8A gas chromatograph (Shimadzu Scientific Instruments, Kyoto, Japan). Sample peaks were measured against an ethylene standard of 1 ppm. Ethylene production was calculated from the peak height, fruit mass, and incubation time. JA was measured using liquid chromatography coupled to tandem mass spectrometry and internal standards as in Patton et al. (2020) with modifications (n=4 replicates of a pool of 8–10 fruit each). Briefly, frozen tissue was lyophilized, weighed and extracted in isopropanol: H2O: HCL1mol (2:1:0.005) with 100 µl of internal standard solution (1000 pg) as previously described (Casteel et al., 2015). Samples were evaporated to dryness, resuspended in 100 µl of MeOH, filtered,

and 10 µl samples injected into an Agilent 6420 Triple Quad Mass Spectrometer (Agilent Technologies, USA). A Zorbax Extend-C18 column 3.0×150 mm (Agilent) with 0.1% formic acid in water (A) and 0.1% (v/v) formic acid in acetonitrile (B) at a flow rate of 600 ml min–1 was used. The gradient was 0–1 min, 20% B; 1–10 min, linear gradient to 100% B; 10–13 min, 100% A. Differences in hormone levels among treatments, ripening stages, and time points were assessed by ANOVA followed by Tukey's HSD using R.

2.4.9 Data availability

The datasets for this study have been deposited in the Gene Expression Omnibus (GEO) database under the accession GSE148217.

2.5 Results

2.5.1 Susceptibility of tomato fruit to fungal infections by *Botrytis cinerea*, *Fusarium acuminatum*, and *Rhizopus stolonifer* increases during ripening

To characterize tomato fruit responses to fungal infection at unripe (MG) and ripe (RR) stages, we inoculated fruit (cv. 'Ailsa Craig') with *B. cinerea*, *F. acuminatum*, or *R. stolonifer* spores. Each pathogen successfully infected RR fruit, producing visible water-soaked lesions and mycelial growth by 3 dpi, whereas MG fruit remained resistant and, except in samples inoculated with *R. stolonifer*, had a dark, necrotic ring around the inoculation sites (Figure 2.1A), a feature of the pathogen response that did not appear in wounded fruit. Thus, MG fruit resistance and RR fruit susceptibility are a feature common to multiple necrotrophic infections. We hypothesized that these susceptibility phenotypes are the result of (i) differences in immune responses at each ripening stage and (ii) developmental processes during ripening that alter the levels of preformed defenses and susceptibility factors. First, we assumed that, compared with a robust immune response in MG fruit, RR fruit have a weaker response, consisting of fewer genes induced, less diverse functionality, and absent expression of critical genes. Additionally, we predicted that ripening may decrease the expression of preformed defenses and increase the expression of susceptibility factors, which create a more favorable environment for infection.

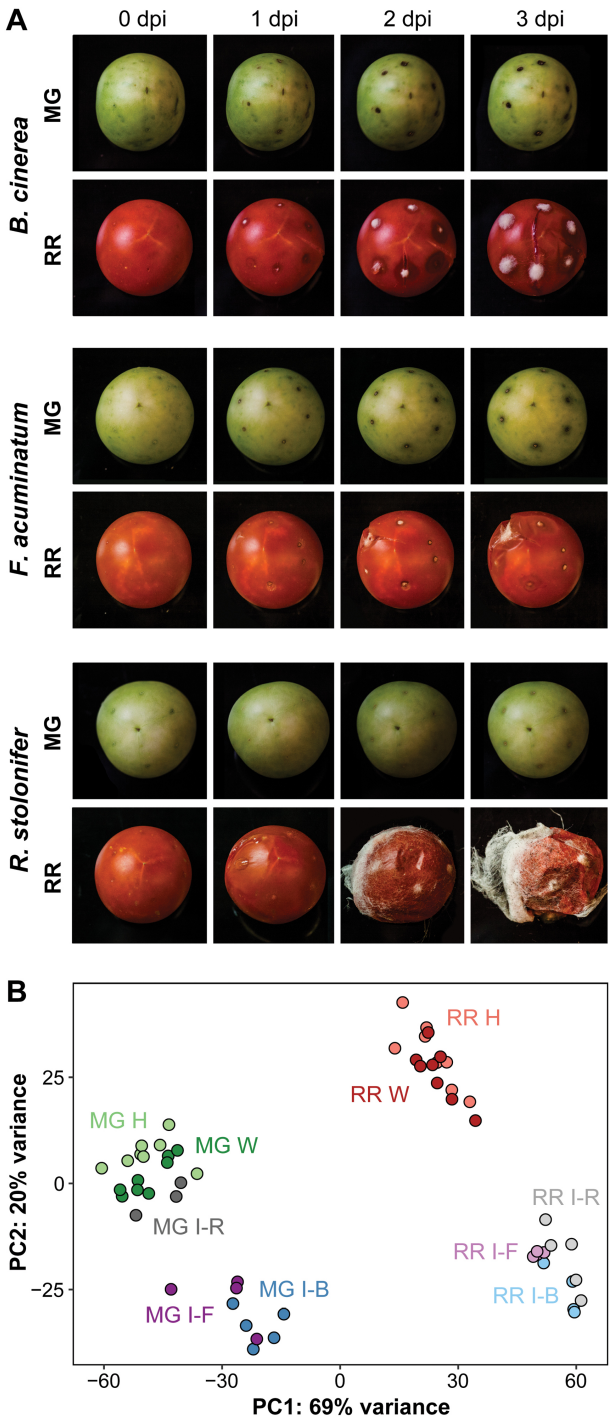

Figure 2.1: Tomato fruit responses to *B. cinerea*, *F. acuminatum*, and *R. stolonifer*. (A) Disease progression in inoculated mature green (MG) and red ripe (RR) fruit each day up to 3 d post-inoculation (dpi). (B) Principal component analysis of total mapped RNA-Seq tomato reads. Color corresponds to treatment. H, healthy; I, inoculated 1 dpi; W, wounded; B, *B. cinerea*; F, *F. acuminatum*; R, *R. stolonifer*.

2.5.2 Susceptible ripe fruit respond to pathogens with a larger, more diverse set of defense genes than resistant unripe fruit

To test if immune responses to fungal pathogens are compromised in RR compared with MG fruit, we sequenced mRNA from *B. cinerea*-, *F. acuminatum*-, and *R. stolonifer*-inoculated fruit at 1 dpi, an early time point at which either a resistant or a susceptible phenotype becomes apparent. We included healthy and wounded MG and RR fruit from the same time point as controls. A principal component analysis (PCA) of the mapped normalized reads for all tomato genes (Figure 2.1B) revealed that the major driver separating sample data was the ripening stage (PC1, 69%), while inoculation status accounted for less of the separation (PC2, 20%). The one exception to this pattern was the *R. stolonifer*-inoculated MG samples, which clustered with the healthy and wounded MG samples, suggesting that unripe fruit did not display strong responses to this pathogen and yet remained resistant. However, quantification of normalized pathogen reads (see Supplementary Figure 2.S1A) confirmed that all three pathogens were detectable at 1 dpi even in MG samples.

To identify the responses for each ripening stage common to all three pathogens, we performed a differential expression analysis between inoculated and healthy samples for MG and RR fruit. We chose the healthy samples as controls for these comparisons in order to capture responses to necrotrophic infection, which may share features with mechanical wounding. Of all 34,075 protein-coding genes found in the tomato transcriptome, 9,366 (27.5%) were found to be differentially expressed (P_{adj} <0.05) in response to inoculation in fruit at 1 dpi in at least one comparison (see Supplementary Table S4 at `https://academic.oup.com/jxb/article/72/7/2696/6104152#233260137`). Of these, 475 genes were significantly up-regulated in MG fruit in response to all three pathogens, corresponding to the MG core response (Figure 2.2A), whereas 1,538 genes formed the RR core response (Figure 2.2B). The MG core response overlapped substantially with the wounding response in MG fruit (Supplementary Figure 2.S1B), which suggests that unripe fruit activate similar functions when responding to pathogen attack and mechanical damage. However, this large overlap is also due to the similarity

between the gene expression profiles of wounded and *R. stolonifer*-inoculated samples as seen in the PCA (Figure 2.1B). In contrast, the lack of a strong wounding response in RR fruit indicates that nearly all RR core response genes were strictly pathogen-related (Supplementary Figure 2.S1B). Downregulated genes in response to infection were largely unique to each pathogen, with only 57 and 225 down-regulated across all three pathogens in MG and RR fruit, respectively, and thus we decided to continue our analysis only on the up-regulated core response genes. Complete lists of gene set intersections of up-regulated and down-regulated genes are in given in Supplementary Table S5 at `https://academic.oup.com/jxb/article/72/7/2696/6104152#233260137`.

We then assessed the MG and RR core responses for the presence of various well-established gene classifications related to pathogen defense, including selected GO terms, KEGG pathways, transcription factor (TF) families, hormone biosynthesis, signaling and response genes, and receptor-like kinase (RLK) genes (Figure 2.2C). For each category, we performed enrichment analyses (P_{adj} <0.05) to identify classifications of particular importance in both MG and RR core responses. A total of 70 defense genes were identified in the MG core response. Interestingly, these were enriched in only two categories: chitin catabolic process (GO:0006032) and RLK genes. The RR core response was enriched in 13 defense categories, including the plant–pathogen interaction (sly04626) and MAP kinase signaling pathways (sly04016), secondary metabolite biosynthesis pathways (sly00900, sly00941, sly00945), WRKY and ethylene responsive factor (ERF) transcription factors, RLKs, and JA biosynthesis. Altogether, 302 defense genes were identified among the RR core response. Thus, in contrast to their respective susceptibility phenotypes, RR fruit appear to mount a more robust and diverse immune response than MG fruit early during inoculation, demonstrating that, contrary to our initial hypothesis, weakened immune responses in RR fruit are not a contributor to ripening-associated susceptibility.

However, it is possible that tomato fruit resistance to necrotrophs could be determined by a small number of genes that were exclusive to the MG core response. Out of the 70 defense genes in the MG core response, 27 were not found in the RR core response (Figure 2.3). These 27 genes are heterogeneous, representing 12 different defense

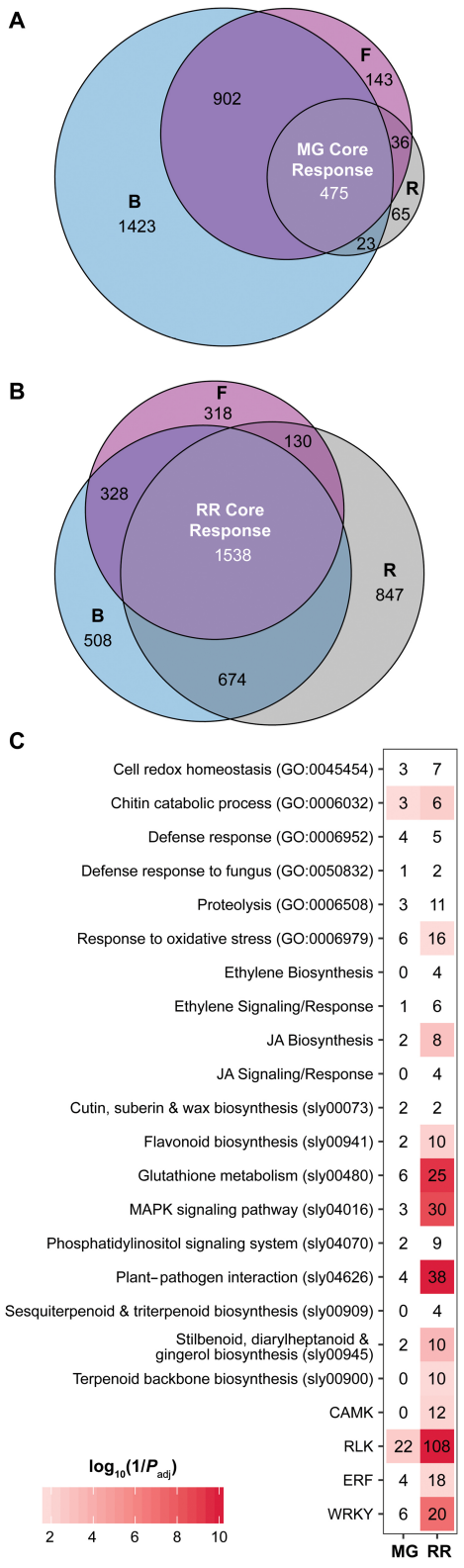

Figure 2.2: Caption presented on following page.

Figure 2.2: Tomato core responses to fungal inoculations. (A, B) Euler diagram of tomato genes up-regulated in response to inoculation in mature green (MG) (A) or red ripe (RR) (B) fruit. B, *B. cinerea*; F, *F. acuminatum*; R, *R. stolonifer*. Core responses are shown in white. (C) Enrichments of various defense-related classes in the MG and RR core responses. The scale is the $\log_{10}(1/P_{adj})$. Values greater than 10 were converted to 10 for scaling purposes. Numbers in each tile indicate the number of genes within each classification. CAMK, calmodulin-dependent protein kinase; ERF, ethylene responsive factor; JA, jasmonic acid; MAPK, mitogenactivated protein kinase; RLK, receptor-like kinase.

categories. Notable genes in this category include a three-gene cluster of PR-10 family proteins (GO:0006952), a chitinase previously identified during infections of tomato with *Cladiosporum fulvum* (*Solyc10g055810*, Danhash et al. (1993)), and an ERF active at the onset of ripening (Liu et al., 2015a). Although these 27 genes were not in the RR core response, most of them were induced during RR infections by one or two of the pathogens studied. Only seven were not up-regulated by any of the three pathogens in RR fruit, including the ERF mentioned above (*Solyc03g118190*), as well as three RLK genes, two glutaredoxin genes involved in the response to oxidative stress, and a cysteine protease. Given that each of these genes belongs to a large family of genes whose members are often functionally redundant, and their average expression levels in infected MG fruit were fairly low (normalized read counts 8.13–149.07), we consider it unlikely that the lack of these genes in the RR core response contributes heavily to susceptibility.

Additionally, the induction of defense genes in the RR core response could be ineffective if their expression levels were too weak compared with those seen in resistant MG fruit. We evaluated the levels of gene expression in inoculated RR fruit via a differential expression comparison (P_{adj} <0.05) to inoculated MG fruit. Of all the RR core defense genes identified above, 269/302 (89.1%) were expressed at equal or greater levels (average $\log_2$FC=2.16) in inoculated RR fruit compared with inoculated MG fruit for all three pathogens. Conversely, 33/302 (11.9%) of these defense genes were expressed at higher levels in MG fruit compared with RR fruit for at least one of the three pathogens (see

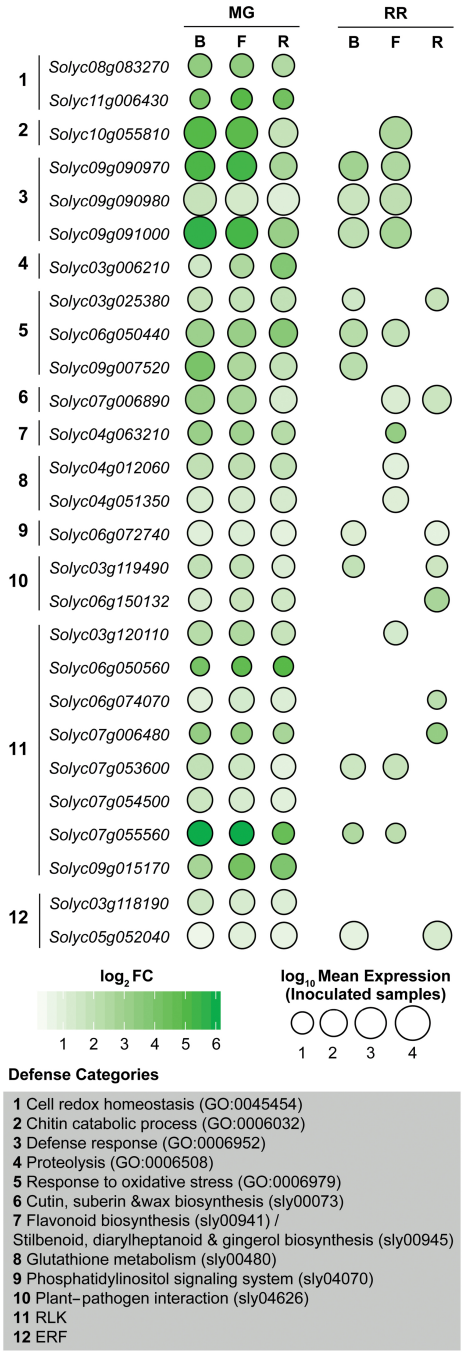

Figure 2.3: Defense genes in the mature green (MG) core response that are not in the red ripe (RR) core response. Circle sizes are proportional to the average normalized read count values from the inoculated fruit samples. B, B. cinerea; F, F. acuminatum; R, R. stolonifer; ERF, ethylene responsive factor; RLK, receptor-like kinase.

Supplementary Table S6 at https://academic.oup.com/jxb/article/72/7/2696/6104152#233260137). These genes are diverse, representing 15 different defense categories. Prominent genes in this category include *TAP1* (*Solyc02g079500*) and *TAP2* (*Solyc02g079510*), two peroxidases associated with defensive suberization in tomato (Kesanakurti et al., 2012; Roberts and Kolattukudy, 1989); *CHI3* (*Solyc02g082920*) and *CHI17* (*Solyc02g082930*), two chitinases associated with *C. fulvum* infection (Danhash et al., 1993); and the JA biosynthesis gene *OPR3* (*Solyc07g007870*). While it is possible that resistance may be determined by these genes, these results indicated that the differences in immune responses observed between MG and RR fruit are not likely solely responsible for differences in susceptibility, and, therefore, we considered the alternate hypothesis.

2.5.3 Defects in the regulation of ripening indicate that only some ripening processes promote susceptibility to fungal disease

We explored the possibility that the increase in susceptibility to fungal pathogens is heavily influenced by a decline of preformed defenses and accumulation of susceptibility factors that occur during fruit ripening prior to pathogen challenge. Due to the complexity of the ripening program, we utilized isogenic non-ripening tomato mutants as tools to identify specific developmental features that are integral to fruit resistance or susceptibility. The *Cnr*, *rin*, and *nor* mutants produce fruit that lack most of the characteristic changes associated with normal ripening, such as color, texture, acidity, sugar accumulation, and ethylene production, but yet are phenotypically different from one another (see Supplementary Table S1 at https://academic.oup.com/jxb/article/72/7/2696/6104152#233260137). All three mutant lines likely result from spontaneous gain-of-function mutations in transcription factors with key roles in the regulation of ripening (Gao et al., 2020, 2019; Ito et al., 2017; Wang et al., 2019b).

We inoculated fruit of these mutant genotypes at comparable stages to MG and RR wild-type fruit (i.e. 'MG-like' and 'RR-like') with *B. cinerea*, *F. acuminatum*, and *R. stolonifer* and measured disease incidence and severity up to 3 dpi (Figure 2.4). For all three pathogens at both MG-like and RR-like stages, only *nor* fruit were consistently

resistant to infection. MG-like fruit of *Cnr* were the only unripe fruit susceptible to any pathogen, with both *B. cinerea* and *F. acuminatum* able to produce lesions on a significant number of these fruit. Consistent with this, *Cnr* RR-like were more susceptible than wild-type RR fruit to *B. cinerea*, with average disease severity (i.e. lesion size) nearly twice as great at 3 dpi (Figure 2.4A). The fruit of *rin* at both MG-like and RR-like stages showed similar or slightly lower susceptibility to all pathogens when compared with wild-type, with the exception of a significant reduction in disease incidence to *F. acuminatum* at the RR-like stage. Because some ripening processes may promote susceptibility, others may maintain resistance, and others may have no impact, we hypothesized that the *Cnr*, *rin*, and *nor* mutations differentially affect ripening-associated genes or pathways that are critical to tip the balance towards either susceptibility or resistance.

We sequenced mRNA from *B. cinerea*-inoculated and healthy fruit from the non-ripening mutants at MG-like and RR-like stages at 1 dpi. We chose *B. cinerea* inoculations because this pathogen showed the clearest differences in susceptibility phenotypes between these genotypes. We first characterized transcriptional responses of mutant fruit to pathogen challenge by using enrichment analysis of defense-related processes to determine if differences in immune responses could explain the distinct susceptibility phenotypes (Supplementary Figure 2.S2A). In most cases, the mutant fruit exhibited similar patterns of defense classification enrichments as wild-type fruit in both stages, with some notable exceptions. Compared with the other genotype–stage combinations, *Cnr* MG-like responses were deficient (i.e. less enriched) in the expression of genes from several prominent defense classifications, including chitin catabolic process (GO:0006032), the plant–pathogen interaction (sly04626) and glutathione metabolism (sly00480) pathways, ERF and WRKY transcription factors, and RLK and CAMK genes. Given that *Cnr* fruit were the only genotype at the MG-like stage to display susceptibility to *B. cinerea* infection, it can be suggested that these defense processes may be necessary for resistance in unripe fruit. However, these processes were enriched in the susceptible RR-like fruit of *Cnr* and *rin*, as well as wild-type RR fruit, which clearly indicates that they are not sufficient to result in a resistant outcome.

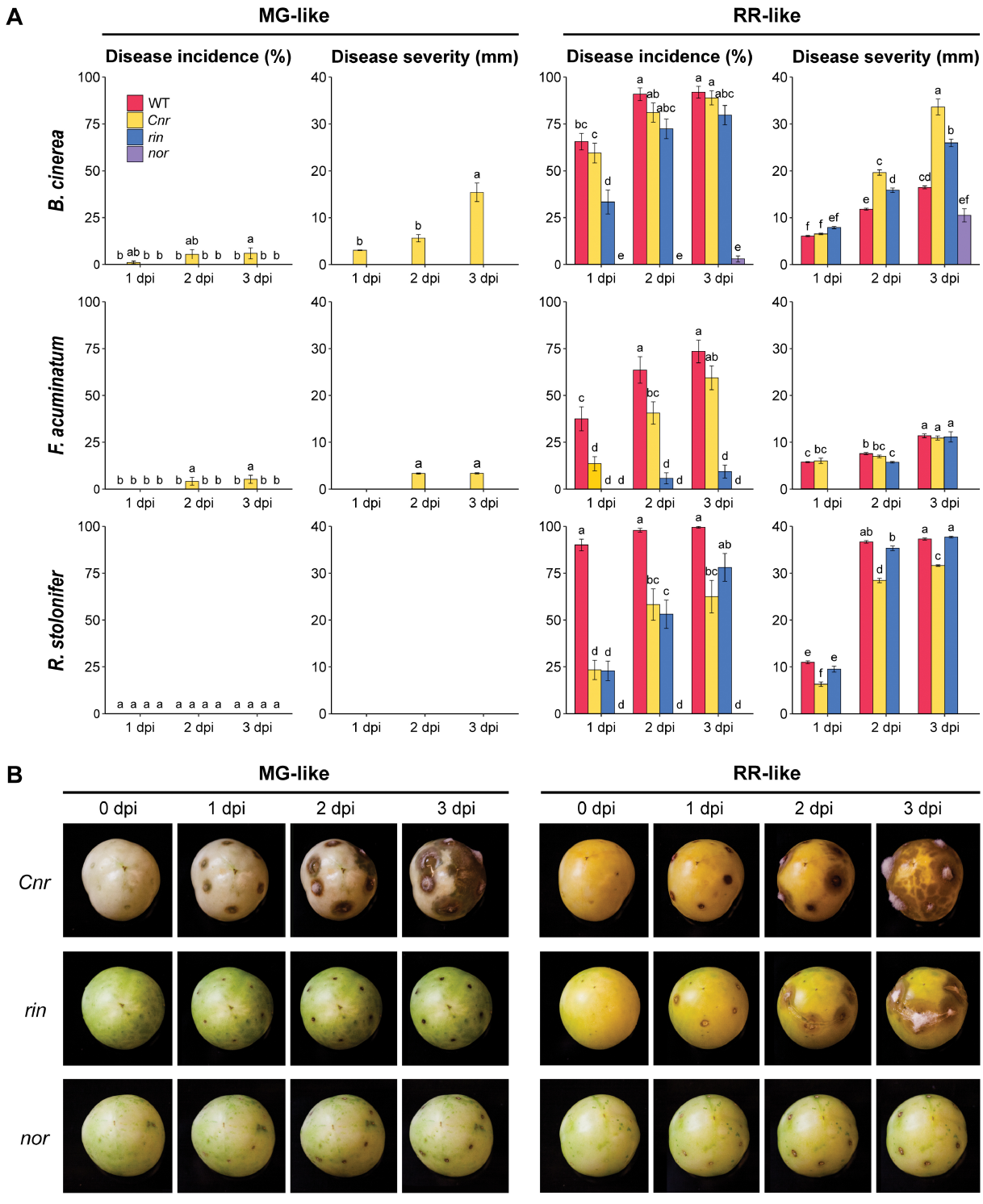

Figure 2.4: Caption presented on following page.

Figure 2.4: Susceptibility of the non-ripening mutants *Cnr*, *rin*, and *nor* to fungal infections. (A) Disease incidence and severity measurements for MG-like (left) and RR-like (right) fruit. Wild-type values are included for comparison. (B) Disease progression of *B. cinerea*-inoculated MG-like and RR-like fruit each day up to 3 d post-inoculation. Letters represent statistical differences between genotypes for each pathogen in study ($P < 0.05$).

The role of ethylene and JA showed some variation amongst the mutants. For example, the responses of resistant *nor* fruit in both MG-like and RR-like fruit were noticeably less enriched in ethylene-associated pathways and more enriched in JA-associated pathways. These results suggest that JA-mediated defenses may contribute to tomato fruit resistance in the absence of ethylene, and that the *nor* mutation may activate JA-associated resistance. In support of this observation, levels of JA in healthy fruit appeared to be linked to resistance: they were highest in RR-like *nor* fruit, and only *nor* fruit experienced an increase in JA in the transition from MG-like to RR-like (see Supplementary Table S7 at `https://academic.oup.com/jxb/article/72/7/2696/6104152#233260137`). Ethylene levels increase dramatically during ripening in wild-type fruit, but they remain low in all three non-ripening mutants (Supplementary Figure 2.S2B). However, both *Cnr* and *rin* mutants produce ethylene in response to *B. cinerea* inoculation, with ethylene production in inoculated *Cnr* MG-like fruit reaching levels nearly three times greater than wild-type MG fruit by 3 dpi. Moreover, ethylene signaling/response genes are highly enriched in *Cnr* MG-like fruit responses (Supplementary Figure 2.S2A). In contrast, healthy *nor* fruit did not produce substantial amounts of ethylene at either stage, and inoculation in *nor* fruit did not appear to induce significant ethylene production as in *rin* and *Cnr* fruit. These results indicate that high levels of ethylene are not required for *B. cinerea* resistance and most likely promote susceptibility. Regardless, the combination of hormone activity and defense gene enrichment suggests that, with the exception of *Cnr* MG-like fruit, resistance or susceptibility in the non-ripening mutants cannot be merely explained by the presence and/or magnitude of immune responses.

2.5.4 Fruit infections are promoted by a decrease in preformed defenses and an increase in susceptibility factors during ripening

To identify genes that are involved in resistance or susceptibility that change during tomato fruit ripening, we used a differential expression analysis (P_{adj} <0.05) comparing healthy RR/RR-like to healthy MG/MG-like fruit for each wildtype and mutant line. In wild-type fruit, 6,574 genes were significantly down-regulated in RR fruit compared with MG, while 5,674 genes were significantly up-regulated (see Supplementary Table S4 at `https://academic.oup.com/jxb/article/72/7/2696/6104152#233260137`). We used the susceptibility phenotypes and the transcriptional profiles of the mutant fruit to filter these ripening-associated genes and identify critical preformed defense mechanisms or susceptibility factors. Of the four genotypes, all except *nor* experience an increase in susceptibility in the transition from MG/MG-like to RR/RR-like fruit. Thus, we selected ripening-associated genes that showed the same expression pattern in wild-type, *Cnr*, and/or *rin*, but not *nor*. This filtering resulted in 2,893 down-regulated and 2,003 up-regulated genes, respectively.

We assumed that effective preformed defenses will decrease during ripening. Thus, the set of filtered down-regulated genes, being those that are highly expressed in healthy MG fruit compared with healthy RR fruit, should contain key genes related to preformed defenses. The filtered down-regulated genes contained 251 defense genes, while up-regulated genes included only 171 defense genes, indicating a net loss of about 80 genes in the transition from MG/MG-like to RR/RR-like susceptible fruit. Furthermore, the 251 defense genes from the filtered down-regulated set were over-represented by functional categories involved in reactive oxygen species (ROS) response and detoxification, proteolysis, and the biosynthesis of secondary metabolites (Table 2.1). These down-regulated ROS-related genes spanned several subfamilies including thioredoxins, glutaredoxins, glutathione S-transferases, and peroxidases. Among the down-regulated proteolytic genes were several subtilisin-like proteases, including *SBT3* (*Solyc01g087850*; Meyer et al. (2016)). Lastly, in addition to several genes involved in the methylerythri-

Table 2.1: Defense categories enriched in a subset of significantly down-regulated genes during ripening of healthy tomato fruit.

Defense category	Number of genes	Example functions
Cell redox homeostasis (GO:0045454)	24	Thioredoxins, glutaredoxins
Defense response (GO:0006952)	6	MLO-like proteins, Sn-1 proteins
Proteolysis (GO:0006508)	36	Subtilisin-like proteases (SBT2, SBT3)
Response to oxidative stress (GO:0006979)	16	Peroxidases
Flavonoid biosynthesis (sly00941)	5	Caffeoyl-CoA O-methyltransferase
Glutathione metabolism (sly00480)	18	Glutathione S-transferases
MAPK signaling pathway (sly04016)	17	Protein phosphatase 2C, RBOH proteins
Phosphatidylinositol signaling system (sly04070)	5	Phosphatidylinositol phospholipase C
Plant–pathogen interaction (sly04626)	15	Disease resistance protein RPM1
Terpenoid backbone biosynthesis (sly00900)	8	Geranylgeranyl disphosphate synthase
CAMK	8	Calcium-dependent kinases
RLK	78	Lectin receptor kinases, leucine-rich repeat kinases
ERF	8	ERFA2, ERFC2, ERFC3

The significance cut-off for the enrichments is P_{adj} <0.05. Full enrichment results for both up-regulated and down-regulated defense genes can be found in Supplementary Table S8 at `https://academic.oup.com/jxb/article/72/7/2696/6104152#233260137`.

tol 4-phosphate pathway of terpenoid biosynthesis, two copies of the lignin biosynthesis gene *CCoAOMT* (*Solyc01g107910*, *Solyc04g063210*) were also among the filtered down-regulated class, suggesting that cell wall fortification could be inhibited upon infection. These results indicate that ripening involves a loss of multiple defense genes, and that the pre-existing levels of genes involved in ROS regulation, proteolysis, and secondary metabolite biosynthesis may be critical for resistance.

Finally, we evaluated filtered up-regulated genes that are highly expressed in healthy RR fruit compared with healthy MG fruit, as they may include potential susceptibility factors. Since there is little scientific literature on classes of genes that may constitute susceptibility factors in plants, we focused on the up-regulated genes that were highly expressed in the RR/ RR-like fruit of the susceptible genotypes. Such genes may have disproportionate impacts on susceptibility due to their high expression. To identify these genes, we calculated average normalized read count values for each gene across WT, *Cnr*, and *rin* RR/RR-like fruit. The distribution of these values over the filtered up-regulated

Table 2.2: Highly expressed genes in susceptible RR/RR-like fruit.

Accession	Average RR/RR-like expression	Name	Ripening function
Solyc06g059740	99,772.18	*SlADH2*	Flavor aldehyde biosynthesis
Solyc08g065610	64,989.08	*SlVPE3*	Sugar metabolism
Solyc03g111690	25,643.87	*SlPL*	Pectin degradation
Solyc10g080210	25,044.06	*SlPG2a*	Pectin degradation
Solyc08g014130	21,514.72	*SlIPMS2*	Unknown
Solyc10g076510	20,051.40	—	Unknown
Solyc07g047800	19,462.21	—	Unknown
Solyc12g005860	19,048.01	—	Unknown
Solyc08g080640	17,227.90	*SlNP24*	Unknown
Solyc12g098710	15,070.45	*SlZ*-ISO	Carotenoid biosynthesis
Solyc09g009260	14,572.63	*SlFBA7*	Sugar metabolism
Solyc10g024420	14,103.56	—	Unknown

Names and ripening functions were determined via BLAST and literature searches.

genes is a notably long-tailed one with a range of 2.43 to 179,649.29 and an average of 1,295. We identified genes with abnormally high expression values by selecting outliers (i.e. values above 1.5×the interquartile range) from a $\log_{10}$-transformed distribution of the data. This resulted in a list of 16 genes (Table 2.2). They include several genes previously discovered to be active during tomato fruit ripening, including the flavor volatile biosynthesis gene *ADH2* (*Solyc06g059740*; Speirs et al. (1998)), the carotenoid biosynthesis gene *Z-ISO* (*Solyc12g098710*; Fantini et al. (2013)), the pectin-degrading enzymes *PG2a* (*Solyc10g080210*; Sheehy et al. (1987) and *PL* (*Solyc03g111690*; Uluisik et al. (2016)), and the ethylene receptor *ETR4* (*Solyc06g053710*; Tieman and Klee (1999)), among other genes involved in carbohydrate metabolism.

While any of these genes has the potential to impact susceptibility, genes for cell wall-degrading enzymes, such as *PL* and *PG2a*, which facilitate fruit softening during ripening, represent especially good candidates given both the importance of cell wall integrity in defense against fungal pathogens and previous research on RNAi-developed mutants in

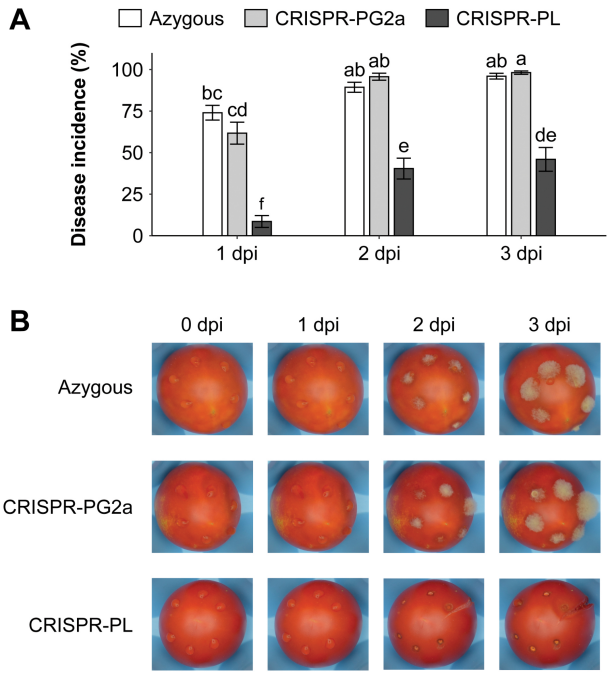

Figure 2.5: Inoculations of CRISPR lines with *Botrytis cinerea*. (A) Disease incidence measurements at 1, 2, and 3 dpi. Letters represent statistical differences between genotypes (P <0.05). (B) Photos of representative inoculated tomatoes from 0 to 3 dpi.

tomato (Cantu et al., 2008; Yang et al., 2017). To validate the impact of *PG2a* and *PL* expression in wild-type RR fruit on susceptibility to *B. cinerea*, we utilized CRISPR-based mutants in each of these genes (Wang et al., 2019a). RR fruit from these lines are similar in regards to soluble solids content, titratable acidity, and juice pH, but CRISPR-PL fruit are nearly 30% firmer than fruit from the CRISPR-PG2a and azygous WT control lines (see Supplementary Table S2 at `https://academic.oup.com/jxb/article/72/7/2696/6104152#233260137`). In conjunction with these firmness differences, RR fruit of the CRISPR-PL line, but not the CRISPR-PG2a line, demonstrated reduced susceptibility to *B. cinerea* compared with the azygous line (Figure 2.5). At 3 dpi, disease incidence in the CRISPR-PL fruit was 56% lower than that in azygous fruit. We conclude that the ripening-associated pectate lyase enzyme is a major susceptibility factor for *B. cinerea* infection in tomato fruit.

2.6 Discussion

During ripening, fruit may gradually lose either the ability to activate or the effectiveness of components of the plant immune system, defensive hormone production and signaling, and downstream transcriptional responses. Alternatively, ripening processes such as cell wall breakdown, simple sugar accumulation, changes in pH and secondary metabolite composition, and, in climacteric fruit, increased levels of ethylene may impact the fruit's capability to resist fungal attack (Alkan and Fortes, 2015; Prusky et al., 2013). The widespread nature of this phenomenon in diverse fruit pathosystems suggests that ripening-associated susceptibility is likely to be mediated by combinations of the above factors.

In tomato, ripening-associated susceptibility has been demonstrated not only for the model necrotrophic pathogen *B. cinerea*, but for other fungal pathogens including *Colletotrichum gloeosporioides* (Alkan et al., 2015), *R. stolonifer*, and *F. acuminatum* (Petrasch et al., 2019b). Here, for the first time, we identified specific host responses in both resistant unripe (MG) and susceptible ripe (RR) fruit that are common to multiple pathogens and thus represent core responses to fungal infection. Most prominently, these core responses featured RLKs, WRKY and ERF transcription factors, JA biosynthesis, and chitin catabolism (Figure 2.2). Some genes that appear in both the MG core and the RR core responses were previously studied components of plant immunity in tomato, including the JA biosynthesis gene *LoxD* (Yan et al., 2013), the subtilisin-like protease *SBT3* (Meyer et al., 2016), the peroxidase *CEVI-1* (Mayda et al., 2000), and the chitinase *CHI9* (Danhash et al., 1993). Though response to inoculation overlaps somewhat with response to wounding in MG fruit (Supplementary Figure 2.S1B), transcriptional profiles (Figuire 2.1B), and ethylene measurements (Supplementary Figure 2.S2B) indicate that the bulk of inoculation responses are a direct result of fungal attack. This is also evident by the presence of a necrotic ring only in inoculated MG fruit and not in the wounded controls or the inoculated RR fruit, indicating that the unripe fruit is capable of inducing an oxidative burst in response to the pathogen presence (Cantu et al., 2009).

However, most defense genes uncovered were found solely in the RR core response.

These included several well-known defense genes that were only expressed in RR fruit, such as *WRKY33* (Liu et al., 2015b), the ERF *PTI5* (Gu et al., 2002; He et al., 2001; Wu et al., 2015), the RLK *TPK1b* (AbuQamar et al., 2008), and the MAP kinase *MPK3* (Kandoth et al., 2007; Stulemeijer et al., 2007; Zhang et al., 2018). While the MG core response did contain some defense genes that were not present in the RR core response (Figure 2.3), expression of most of these genes was also identified in the RR response to one or two pathogens. Many of the genes in the MG core response were either functionally similar to other RR core response genes or were expressed at low levels. Thus, the ability to mount an immune response does not appear to be compromised in RR fruit.

If defense responses do not determine the outcome of the interaction in tomato fruit, developmental features associated with ripening of healthy fruit may instead govern susceptibility. The highly complex transcriptional reprogramming during ripening allows for a large number of potential contributors to the increase in susceptibility. Ripening processes in tomato have been studied using non-ripening mutants such as *Cnr*, *rin*, and *nor*. In addition to being phenotypically distinct, these mutants display differential susceptibility patterns when inoculated with fungal pathogens (Figure 2.4). Previously, susceptibility to *B. cinerea* in tomato fruit was shown to be dependent on *NOR* but not *RIN*, though the role of *CNR* remained uncharacterized (Cantu et al., 2009). Our results with *B. cinerea* as well as *F. acuminatum* and *R. stolonifer* corroborate the roles of *NOR* and *RIN* while also proposing a role for *CNR* in tomato fruit defense against fungal pathogens. In addition to exhibiting hypersusceptibility to *B. cinerea* in RR-like fruit, *Cnr* MG-like fruit were the only fruit of this stage to exhibit any susceptibility. Unlike *rin* and *nor* fruit, *Cnr* fruit have altered cell wall architecture even in MG-like stages (Eriksson et al., 2004; Ordaz-Ortiz et al., 2009), a feature which may be exploited during fungal infection. Moreover, compared with all other fruit, *Cnr* MG-like fruit were deficient in defense responses against *B. cinerea*. Apart from *Cnr* MG-like fruit, the extent of the immune responses appeared to have little impact on susceptibility, as enriched defense categories were similar across both resistant and susceptible mutant fruit.

We took advantage of the susceptibility differences in the ripening mutants to unravel

ripening components that may represent either declining preformed defenses or increasing susceptibility factors. Differential expression analyses carefully filtered based on susceptibility phenotypes revealed that several defense-related genes undergo changes in gene expression during the transition from MG/MG-like to RR/RR-like fruit. Most interestingly, declining preformed defenses appear to be over-represented by gene categories involved in the mediation of ROS levels. Host regulation of ROS levels during early fungal infection is critical for both defense signaling and detoxification of ROS generated by the pathogen (Lehmann et al., 2015; Waszczak et al., 2018), and tomato fruit susceptibility to *B. cinerea* has been shown to be impacted by both of these roles. Improved resistance to *B. cinerea* in the ABA-deficient *sitiens* mutant has been shown to be the result of controlled ROS production, which promotes cell wall fortification (Asselbergh et al., 2007; Curvers et al., 2010), and a similar improved *B. cinerea* resistance is seen in tomato varieties genetically engineered to produce especially high amounts of antioxidant anthocyanins in fruit (Zhang et al., 2015). During ripening, losing control of ROS levels may thus represent the reduction of an important preformed defense.

Some features of ripening have the potential to be either a preformed defense or a susceptibility factor depending on the context. The ethylene burst that accompanies ripening in climacteric fruit is an example. Although ethylene is known for its involvement in defense against necrotrophs (van der Ent and Pieterse, 2012), its induction of the ripening program catalyses downstream events that can be favorable for pathogen infections. Previous research suggests that inhibition of ethylene receptors in MG fruit can either increase or decrease resistance to *B. cinerea* depending on the concentration of inhibitor used (Blanco-Ulate et al., 2013). Thus, ethylene-mediated resistance may be dependent on careful regulation of ethylene levels, and the autocatalytic ethylene biosynthesis that occurs in wild-type fruit ripening may be detrimental. We observed that ethylene production and ethylene-related transcriptional responses were particularly prominent in susceptible fruit, especially *Cnr* MG-like. In addition to ethylene, JA is known to mediate resistance to necrotrophs in plants (Pandey et al., 2016; Wasternack and Hause, 2013). The enrichment of JA biosynthesis genes is seen in the RR core response, as well as the response to

B. cinerea in all mutant fruit at both stages. Basal levels of JA in healthy fruit are highest in *nor* RR-like fruit, where they are nearly twice as high as levels in wild-type RR fruit. Moreover, *nor* fruit are the only fruit at which JA signaling/response genes are enriched in response to *B. cinerea* infection at both stages. The interplay between ethylene and JA and their impact of ripening-associated susceptibility requires further study.

Other features of ripening can increase susceptibility to fungal disease such as the disassembly of plant cell walls leading to fruit softening. Cell wall polysaccharide remodeling, breakdown, and solubilization in ripening fruit occurs as the result of various cell wall-degrading enzymes, particularly those that act on pectin (Brummell, 2006). The cell wall represents an important physical barrier to pathogen attack in plants (Blanco-Ulate et al., 2016a; Malinovsky et al., 2014), and cell wall integrity and fortification improves tomato fruit resistance to *B. cinerea* infection (Cantu et al., 2008; Curvers et al., 2010). The enzymes PL and PG2a feature prominently in tomato fruit ripening and softening (Uluisik et al., 2016; Wang et al., 2019a; Yang et al., 2017) and accumulate in RR/RR-like fruit of susceptible genotypes. However, these enzymes do not have equal impact on fruit softening, as CRISPR-based mutants in *PL*, but not *PG2a*, result in a reduced rate of softening in RR fruit (Wang et al., 2019a). This differential impact on firmness is mirrored in the effect on susceptibility to *B. cinerea*, as the firmer CRISPR-PL mutant was less susceptible than both the CRISPR-PG2a mutant and the azygous control (Figure 2.5). Though RR fruit of the CRISPR-PG2a mutant did not exhibit increased *B. cinerea* resistance, *PG2a* may still contribute to susceptibility, as RNAi-mediated knockdown of *PG2a* together with the expansin gene *Exp1* increases *B. cinerea* resistance while knockdown of either gene alone does not (Cantu et al., 2008). Here we showed that the PL enzyme is a substantial susceptibility factor in tomato fruit, and targeting this enzyme for breeding purposes may improve fungal resistance in addition to lengthening shelf life by slowing the softening process.

Susceptibility and resistance to necrotrophic pathogens is ultimately a complex, multigenic trait in plants. The use of transcriptomic datasets to facilitate a systems-level approach of such pathosystems has increased in recent years (Alkan et al., 2015; Kovalchuk

et al., 2019; Petrasch et al., 2019b; Zhang et al., 2019) and has led to novel insights in both host and pathogen features that impact the outcome of such interactions. Moreover, the additional layer of an enormous developmental change such as ripening only further increases the need for these approaches. We have demonstrated how such an approach can yield critical information on both fruit infection response and broad ripening-associated changes that increase susceptibility, and additionally provide insights into single genes with a disparate impact on susceptibility. From our results, we believe that ripening-associated susceptibility is best explained by a dominant role of susceptibility factors that increase during ripening, which, coupled with a modest loss of preformed defenses, outweighs the efforts of the immune response in ripe fruit (Figure 2.6). Overall, our results have tremendous utility for guiding future study of fruit–pathogen interactions in addition to providing breeders with information on potentially useful genes for targeting in the hopes of ultimately reducing postharvest losses in tomatoes and other fruit crops.

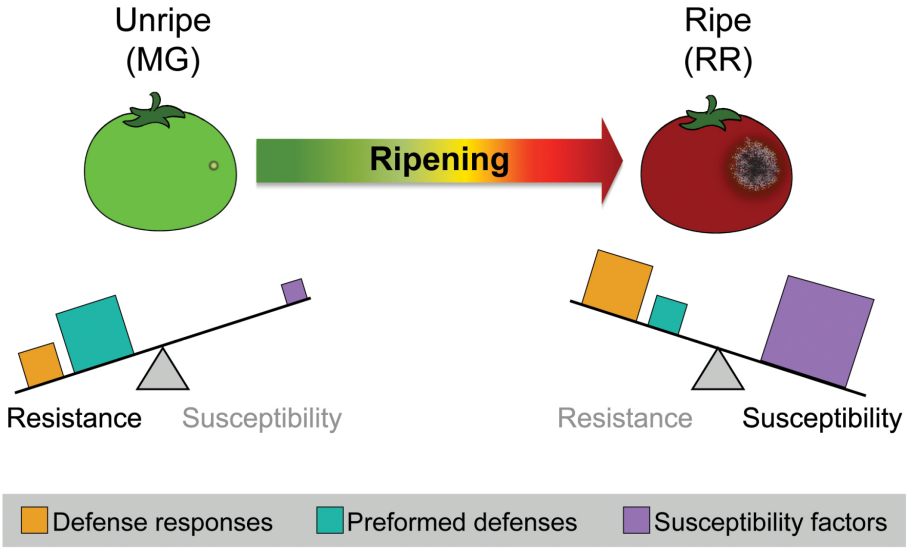

Figure 2.6: Model of contributing factors to ripening-associated susceptibility in tomato fruit. Sizes of squares indicate the relative magnitude of that feature in fruit of that stage. The balance between contributing components determines the ultimate outcome of the infection. MG, mature green; RR, red ripe.

References

AbuQamar, S., Chai, M. F., Luo, H., Song, F., and Mengiste, T. (2008). Tomato protein kinase 1b mediates signaling of plant responses to necrotrophic fungi and insect herbivory. *Plant Cell*, 20(7):1964–1983.

AbuQamar, S., Moustafa, K., and Tran, L. S. (2017). Mechanisms and strategies of plant defense against *Botrytis cinerea*. *Critical Reviews in Biotechnology*, 37(2):262–274.

Ahmadi-Afzadi, M., Orsel, M., Pelletier, S., Bruneau, M., Proux-Wéra, E., Nybom, H., and Renou, J.-P. (2018). Genome-wide expression analysis suggests a role for jasmonates in the resistance to blue mold in apple. *Plant Growth Regulation*, 85(3):375–387.

Alkan, N. and Fortes, A. M. (2015). Insights into molecular and metabolic events associated with fruit response to post-harvest fungal pathogens. *Frontiers in Plant Science*, 6:889.

Alkan, N., Friedlander, G., Ment, D., Prusky, D., and Fluhr, R. (2015). Simultaneous transcriptome analysis of *Colletotrichum gloeosporioides* and tomato fruit pathosystem reveals novel fungal pathogenicity and fruit defense strategies. *New Phytologist*, 205(2):801–815.

Andolfo, G., Jupe, F., Witek, K., Etherington, G. J., Ercolano, M. R., and Jones, J. D. G. (2014). Defining the full tomato NB-LRR resistance gene repertoire using genomic and cDNA RenSeq. *BMC Plant Biology*, 14:120.

Asselbergh, B., Curvers, K., Franca, S. C., Audenaert, K., Vuylsteke, M., Van Breusegem, F., and Höfte, M. (2007). Resistance to *Botrytis cinerea* in *sitiens*, an abscisic acid-deficient tomato mutant, involves timely production of hydrogen peroxide and cell wall modifications in the epidermis. *Plant Physiology*, 144(4):1863–77.

Barral, B., Chillet, M., Léchaudel, M., Lartaud, M., Verdeil, J.-L., Conéjéro, G., and Schorr-Galindo, S. (2019). An Imaging Approach to Identify Mechanisms of Resistance to Pineapple Fruitlet Core Rot. *Frontiers in Plant Science*, 10:1065.

Bautista-Baños, S., Bosquez-Molina, E., and Barrera-Necha, L. L. (2014). *Rhizopus stolonifer* (Soft Rot). In *Postharvest Decay*, pages 1–44. Academic Press.

Benjamini, Y. and Hochberg, Y. (1995). Controlling the false discovery rate: A practical and powerful approach to multiple testing. *Journal of the Royal Statistical Society. Series B (Methodological)*, 57(1):289–300.

Blanco-Ulate, B., Labavitch, J. M., Vincenti, E., Powell, A. L. T., and Cantu, D. (2016a). Hitting the wall: Plant cell walls during *Botrytis cinerea* infections. In *Botrytis - The Fungus, the Pathogen and its Management in Agricultural Systems*, pages 361–386. Springer International Publishing, Cham.

Blanco-Ulate, B., Vincenti, E., Cantu, D., and Powell, A. L. T. (2016b). *Ripening of tomato fruit and susceptibility to Botrytis cinerea.* Springer, Dordrecht, The Netherlands.

Blanco-Ulate, B., Vincenti, E., Powell, A. L. T., and Cantu, D. (2013). Tomato transcriptome and mutant analyses suggest a role for plant stress hormones in the interaction between fruit and *Botrytis cinerea*. *Frontiers in Plant Science*, 4:142.

Bolger, A. M., Lohse, M., and Usadel, B. (2014). Trimmomatic: a flexible trimmer for Illumina sequence data. *Bioinformatics*, 30(15):2114–2120.

Brummell, D. A. (2006). Cell wall disassembly in ripening fruit. *Functional Plant Biology*, 33(2):103–119.

Cantu, D., Blanco-Ulate, B., Yang, L., Labavitch, J. M., Bennett, A. B., and Powell, A. L. T. (2009). Ripening-regulated susceptibility of tomato fruit to *Botrytis cinerea* requires NOR but not RIN or ethylene. *Plant Physiology*, 150(3):1434–1449.

Cantu, D., Vicente, A. R., Greve, L. C., Dewey, F. M., Bennett, A. B., Labavitch, J. M., and Powell, A. L. T. (2008). The intersection between cell wall disassembly, ripening, and fruit susceptibility to *Botrytis cinerea*. *Proceedings of the National Academy of Sciences of the United States of America*, 105(3):859–64.

Casteel, C. L., De Alwis, M., Bak, A., Dong, H., Whitham, S. A., and Jander, G. (2015). Disruption of Ethylene Responses by Turnip mosaic virus Mediates Suppression of Plant Defense against the Green Peach Aphid Vector. *Plant Physiology*, 169(1):209–18.

Centeno, D. C., Osorio, S., Nunes-Nesi, A., Bertolo, A. L., Carneiro, R. T., Araújo, W. L., Steinhauser, M. C., Michalska, J., Rohrmann, J., Geigenberger, P., Oliver, S. N., Stitt, M., Carrari, F., Rose, J. K., and Fernie, A. R. (2011). Malate plays a crucial role in starch metabolism, ripening, and soluble solid content of tomato fruit and affects postharvest softening. *Plant Cell*, 23(1):162–184.

Chiu, C.-M., You, B.-J., Chou, C.-M., Yu, P.-L., Yu, F.-Y., Pan, S.-M., Bostock, R. M., Chung, K.-R., and Lee, M.-H. (2013). Redox status-mediated regulation of gene expression and virulence in the brown rot pathogen Monilinia fructicola. *Plant Pathology*, 62(4):809–819.

Curvers, K., Seifi, H., Mouille, G., de Rycke, R., Asselbergh, B., Van Hecke, A., Vanderschaeghe, D., Höfte, H., Callewaert, N., Van Breusegem, F., and Höfte, M. (2010). Abscisic Acid Deficiency Causes Changes in Cuticle Permeability and Pectin Composition That Influence Tomato Resistance to *Botrytis cinerea*. *Plant Physiology*, 154(2):847–860.

Danhash, N., Wagemakers, C. A., van Kan, J. A., and de Wit, P. J. (1993). Molecular characterization of four chitinase cDNAs obtained from Cladosporium fulvum-infected tomato. *Plant Molecular Biology*, 22(6):1017–29.

Eriksson, E. M., Bovy, A., Manning, K., Harrison, L., Andrews, J., De Silva, J., Tucker, G. A., and Seymour, G. B. (2004). Effect of the Colorless non-ripening mutation on cell wall biochemistry and gene expression during tomato fruit development and ripening. *Plant Physiology*, 136(4):4184–97.

Fantini, E., Falcone, G., Frusciante, S., Giliberto, L., and Giuliano, G. (2013). Dissection of tomato lycopene biosynthesis through virus-induced gene silencing. *Plant Physiology*, 163(2):986–98.

Gao, Y., Wei, W., Fan, Z., Zhao, X., Zhang, Y., Jing, Y., Zhu, B., Zhu, H., Shan, W., Chen, J., Grierson, D., Luo, Y., Jemrić, T., and Fu, D.-Q. (2020). Re-evaluation of the nor mutation and the role of the NAC-NOR transcription factor in tomato fruit ripening. *Journal of Experimental Botany*.

Gao, Y., Zhu, N., Zhu, X., Wu, M., Jiang, C.-Z., Grierson, D., Luo, Y., Shen, W., Zhong, S., Fu, D.-Q., and Qu, G. (2019). Diversity and redundancy of the ripening regulatory networks revealed by the fruitENCODE and the new CRISPR/Cas9 CNR and NOR mutants. *Horticulture Research*, 6(1):39.

Gell, I., De Cal, A., Torres, R., Usall, J., and Melgarejo, P. (2008). Relationship between the incidence of latent infections caused by Monilinia spp. and the incidence of brown rot of peach fruit: factors affecting latent infection. *European Journal of Plant Pathology*, 121(4):487–498.

Giovannoni, J. J., Tanksley, S., Vrebalov, J., and Noensie, F. (2004). NOR gene compositions and methods for use thereof.

Gu, Y. Q., Wildermuth, M. C., Chakravarthy, S., Loh, Y. T., Yang, C., He, X., Han, Y., and Martin, G. B. (2002). Tomato transcription factors Pti4, Pti5, and Pti6 activate defense responses when expressed in Arabidopsis. *Plant Cell*, 14(4):817–831.

Gustavsson, J., Cederberg, C., Sonesson, U., van Otterdijk, R., and Meybeck, A. (2011). Global food losses and food waste: extent, causes and prevention. Technical report.

He, P., Warren, R. F., Zhao, T., Shan, L., Zhu, L., Tang, X., and Zhou, J.-M. (2001). Overexpression of *Pti5* in Tomato Potentiates Pathogen-Induced Defense Gene Expression and Enhances Disease Resistance to *Pseudomonas syringae* pv. *tomato*. *Molecular Plant-Microbe Interactions*, 14(12):1453–1457.

Ito, Y., Nishizawa-Yokoi, A., Endo, M., Mikami, M., Shima, Y., Nakamura, N., Kotake-Nara, E., Kawasaki, S., and Toki, S. (2017). Re-evaluation of the rin mutation and the role of RIN in the induction of tomato ripening. *Nature Plants*, 3(866-874):1.

Kandoth, P. K., Ranf, S., Pancholi, S. S., Jayanty, S., Walla, M. D., Miller, W., Howe, G. A., Lincoln, D. E., and Stratmann, J. W. (2007). Tomato MAPKs LeMPK1, LeMPK2, and LeMPK3 function in the systemin-mediated defense response against herbivorous insects. *Proceedings of the National Academy of Sciences of the United States of America*, 104(29):12205–12210.

Kesanakurti, D., Kolattukudy, P. E., and Kirti, P. B. (2012). Fruit-specific overexpression of wound-induced tap1 under E8 promoter in tomato confers resistance to fungal pathogens at ripening stage. *Physiologia Plantarum*, 146(2):136–148.

Kovalchuk, A., Zeng, Z., Ghimire, R. P., Kivimäenpää, M., Raffaello, T., Liu, M., Mukrimin, M., Kasanen, R., Sun, H., Julkunen-Tiitto, R., Holopainen, J. K., and Asiegbu, F. O. (2019). Dual RNA-seq analysis provides new insights into interactions between Norway spruce and necrotrophic pathogen Heterobasidion annosum s.l. *BMC Plant Biology*, 19(1):2.

Lafuente, M. T., Ballester, A.-R., and González-Candelas, L. (2019). Involvement of abscisic acid in the resistance of citrus fruit to Penicillium digitatum infection. *Postharvest Biology and Technology*, 154:31–40.

Langmead, B. and Salzberg, S. L. (2012). Fast gapped-read alignment with Bowtie 2. *Nature Methods*, 9(4):357–359.

Lassois, L., Haïssam Jijakli, M., and Chillet, M. (2010). Crown rot of bananas: preharvest factors involved in postharvest disease development and integrated control methods. *Plant Disease*, 94(6):648–658.

Lehmann, S., Serrano, M., L'Haridon, F., Tjamos, S. E., and Metraux, J.-P. (2015). Reactive oxygen species and plant resistance to fungal pathogens. *Phytochemistry*, 112(1):54–62.

Liang, X. and Rollins, J. A. (2018). Mechanisms of Broad Host Range Necrotrophic Pathogenesis in Sclerotinia sclerotiorum. *Phytopathology*, 108(10):1128–1140.

Liu, M., Pirrello, J., Chervin, C., Roustan, J.-P., and Bouzayen, M. (2015a). Ethylene Control of Fruit Ripening: Revisiting the Complex Network of Transcriptional Regulation. *Plant Physiology*, 169(4):2380–90.

Liu, S., Kracher, B., Ziegler, J., Birkenbihl, R. P., and Somssich, I. E. (2015b). Negative regulation of ABA Signaling By WRKY33 is critical for Arabidopsis immunity towards *Botrytis cinerea* 2100. *eLife*, 4(JUNE2015):1–27.

Love, M. I., Huber, W., and Anders, S. (2014). Moderated estimation of fold change and dispersion for RNA-seq data with DESeq2. *Genome Biology*, 15(12):550.

Malinovsky, F. G., Fangel, J. U., and Willats, W. G. (2014). The role of the cell wall in plant immunity. *Frontiers in Plant Science*, 5(MAY):1–12.

Manning, K., Tör, M., Poole, M., Hong, Y., Thompson, A. J., King, G. J., Giovannoni, J. J., and Seymour, G. B. (2006). A naturally occurring epigenetic mutation in a gene encoding an SBP-box transcription factor inhibits tomato fruit ripening. *Nature Genetics*, 38(8):948–952.

Mayda, E., Marqués, C., Conejero, V., and Vera, P. (2000). Expression of a Pathogen-Induced Gene Can Be Mimicked by Auxin Insensitivity. *Molecular Plant-Microbe Interactions*, 13(1):23–31.

Mbengue, M., Navaud, O., Peyraud, R., Barascud, M., Badet, T., Vincent, R., Barbacci, A., and Raffaele, S. (2016). Emerging Trends in Molecular Interactions between Plants and the Broad Host Range Fungal Pathogens *Botrytis cinerea* and Sclerotinia sclerotiorum. *Frontiers in Plant Science*, 7(March):1–9.

Meyer, M., Huttenlocher, F., Cedzich, A., Procopio, S., Stroeder, J., Pau-Roblot, C., Lequart-Pillon, M., Pelloux, J., Stintzi, A., and Schaller, A. (2016). The subtilisin-like protease SBT3 contributes to insect resistance in tomato. *Journal of Experimental Botany*, 67(14):4325–4338.

Morales, H., Barros, G., Marín, S., Chulze, S., Ramos, A. J., and Sanchis, V. (2008). Effects of apple and pear varieties and pH on patulin accumulation by Penicillium expansum. *Journal of the Science of Food and Agriculture*, 88(15):2738–2743.

Moriya, Y., Itoh, M., Okuda, S., Yoshizawa, A. C., and Kanehisa, M. (2007). KAAS: an automatic genome annotation and pathway reconstruction server. *Nucleic Acids Research*, 35(Web Server):W182–W185.

Nunes, C. A. (2012). Biological control of postharvest diseases of fruit. *European Journal of Plant Pathology*, 133(1):181–196.

Ordaz-Ortiz, J. J., Marcus, S. E., and Paul Knox, J. (2009). Cell Wall Microstructure Analysis Implicates Hemicellulose Polysaccharides in Cell Adhesion in Tomato Fruit Pericarp Parenchyma. *Molecular Plant*, 2(5):910–921.

Pandey, D., Rajendran, S. R. C. K., Gaur, M., Sajeesh, P. K., and Kumar, A. (2016). Plant Defense Signaling and Responses Against Necrotrophic Fungal Pathogens. *Journal of Plant Growth Regulation*, 35(4):1159–1174.

Patton, M. F., Bak, A., Sayre, J. M., Heck, M. L., and Casteel, C. L. (2020). A polerovirus, Potato leafroll virus, alters plant–vector interactions using three viral proteins. *Plant, Cell & Environment*, 43(2):387–399.

Petrasch, S., Knapp, S. J., van Kan, J. A. L., and Blanco-Ulate, B. (2019a). Grey mould of strawberry, a devastating disease caused by the ubiquitous necrotrophic fungal pathogen *Botrytis cinerea*. *Molecular Plant Pathology*, 20(6):877–892.

Petrasch, S., Silva, C. J., Mesquida-Pesci, S. D., Gallegos, K., van den Abeele, C., Papin, V., Fernandez-Acero, F. J., Knapp, S. J., and Blanco-Ulate, B. (2019b). Infection Strategies Deployed by *Botrytis cinerea*, *Fusarium acuminatum*, and *Rhizopus stolonifer* as a Function of Tomato Fruit Ripening Stage. *Frontiers in Plant Science*, 10:223.

Prusky, D. (1996). Pathogen Quiescence in Postharvest Diseases. *Annual Review of Phytopathology*, 34(1):413–434.

Prusky, D., Alkan, N., Mengiste, T., and Fluhr, R. (2013). Quiescent and Necrotrophic Lifestyle Choice During Postharvest Disease Development. *Annual Review of Phytopathology*, 51(1):155–176.

Roberts, E. and Kolattukudy, P. E. (1989). Molecular cloning, nucleotide sequence, and abscisic acid induction of a suberization-associated highly anionic peroxidase. *Molecular & General Genetics*, 217(2-3):223–32.

Sharma, R. R., Singh, D., and Singh, R. (2009). Biological control of postharvest diseases of fruits and vegetables by microbial antagonists: A review. *Biological Control*, 50(3):205–221.

Sheehy, R. E., Pearson, J., Brady, C. J., and Hiatt, W. R. (1987). Molecular characterization of tomato fruit polygalacturonase. *Molecular & General Genetics*, 208(1-2):30–36.

Speirs, J., Lee, E., Holt, K., Yong-Duk, K., Scott, N. S., Loveys, B., and Schuch, W. (1998). Genetic manipulation of alcohol dehydrogenase levels in ripening tomato fruit affects the balance of some flavor aldehydes and alcohols. *Plant Physiology*, 117(3):1047–1058.

Stulemeijer, I. J. E., Stratmann, J. W., and Joosten, M. H. A. J. (2007). Tomato mitogen-activated protein kinases LeMPK1, LeMPK2, and LeMPK3 are activated during the Cf-4/Avr4-induced hypersensitive response and have distinct phosphorylation specificities. *Plant Physiology*, 144(3):1481–1494.

Tieman, D. M. and Klee, H. J. (1999). Differential expression of two novel members of the tomato ethylene-receptor family. *Plant Physiology*, 120(1):165–172.

Uluisik, S., Chapman, N. H., Smith, R., Poole, M., Adams, G., Gillis, R. B., Besong, T. M. D., Sheldon, J., Stiegelmeyer, S., Perez, L., Samsulrizal, N., Wang, D., Fisk, I. D., Yang, N., Baxter, C., Rickett, D., Fray, R., Blanco-Ulate, B., Powell, A. L. T., Harding, S. E., Craigon, J., Rose, J. K. C., Fich, E. A., Sun, L., Domozych, D. S., Fraser, P. D., Tucker, G. A., Grierson, D., and Seymour, G. B. (2016). Genetic improvement of tomato by targeted control of fruit softening. *Nature Biotechnology*, 34(9):950–952.

van der Ent, S. and Pieterse, C. M. J. (2012). Ethylene: Multi-Tasker in Plant-Attacker Interactions. In *Annual Plant Reviews*, volume 44, pages 343–377. Wiley-Blackwell, Oxford, UK.

van Kan, J. A. L., Shaw, M. W., and Grant-Downton, R. T. (2014). Botrytis species: Relentless necrotrophic thugs or endophytes gone rogue? *Molecular Plant Pathology*, 15(9):957–961.

van Schie, C. C. and Takken, F. L. (2014). Susceptibility Genes 101: How to Be a Good Host. *Annual Review of Phytopathology*, 52(1):551–581.

Veloso, J. and van Kan, J. A. L. (2018). Many Shades of Grey in Botrytis-Host Plant Interactions. *Trends in Plant Science*, 23(7):613–622.

Veronese, P., Ruiz, M. T., Coca, M. A., Hernandez-Lopez, A., Lee, H., Ibeas, J. I., Damsz, B., Pardo, J. M., Hasegawa, P. M., Bressan, R. A., and Narasimhan, M. L. (2003). In defense against pathogens. Both plant sentinels and foot soldiers need to know the enemy. *Plant Physiology*, 131(4):1580–1590.

Vrebalov, J., Ruezinsky, D., Padmanabhan, V., White, R., Medrano, D., Drake, R., Schuch, W., and Giovannoni, J. J. (2002). A MADS-box gene necessary for fruit ripening at the tomato ripening-inhibitor (rin) locus. *Science*, 296(5566):343–6.

Wang, D., Samsulrizal, N., Yan, C., Allcock, N. S., Craigon, J., Blanco-Ulate, B., Ortega-Salazar, I., Marcus, S. E., Bagheri, H. M., Perez-Fons, L., Fraser, P. D., Foster, T., Fray, R. G., Knox, J. P., and Seymour, G. B. (2019a). Characterisation of CRISPR mutants targeting genes modulating pectin degradation in ripening tomato. *Plant Physiology*, 179(2):544–557.

Wang, R., Tavano, E. C. d. R., Lammers, M., Martinelli, A. P., Angenent, G. C., and de Maagd, R. A. (2019b). Re-evaluation of transcription factor function in tomato fruit development and ripening with CRISPR/Cas9-mutagenesis. *Scientific Reports*, 9(1):1696.

Wasternack, C. and Hause, B. (2013). Jasmonates: Biosynthesis, perception, signal transduction and action in plant stress response, growth and development. An update to the 2007 review in Annals of Botany. *Annals of Botany*, 111(6):1021–1058.

Waszczak, C., Carmody, M., and Kangasjärvi, J. (2018). Reactive Oxygen Species in Plant Signaling. *Annual Review of Plant Biology*, 69(1):209–236.

Wittstock, U. and Gershenzon, J. (2002). Constitutive plant toxins and their role in defense against herbivores and pathogens. *Current Opinion in Plant Biology*, 5(4):300–307.

Wu, C., Avila, C. A., and Goggin, F. L. (2015). The ethylene response factor Pti5 contributes to potato aphid resistance in tomato independent of ethylene signalling. *Journal of Experimental Botany*, 66(2):559–570.

Yan, L., Zhai, Q., Wei, J., Li, S., Wang, B., Huang, T., Du, M., Sun, J., Kang, L., Li, C.-B., and Li, C. (2013). Role of Tomato Lipoxygenase D in Wound-Induced Jasmonate Biosynthesis and Plant Immunity to Insect Herbivores. *PLoS Genetics*, 9(12):e1003964.

Yang, L., Huang, W., Xiong, F., Xian, Z., Su, D., Ren, M., and Li, Z. (2017). Silencing of SlPL, which encodes a pectate lyase in tomato, confers enhanced fruit firmness, prolonged shelf-life and reduced susceptibility to grey mould. *Plant Biotechnology Journal*, 15(12):1544–1555.

Young, M. D., Wakefield, M. J., Smyth, G. K., and Oshlack, A. (2010). Gene ontology analysis for RNA-seq: accounting for selection bias. *Genome Biology*, 11(2):R14.

Zhang, J. X., Bruton, B. D., Miller, M. E., and Isakeit, T. (1999). Relationship of Developmental Stage of Cantaloupe Fruit to Black Rot Susceptibility and Enzyme Production by *Didymella bryoniae*. *Plant Disease*, 83(11):1025–1032.

Zhang, S., Wang, L., Zhao, R., Yu, W., Li, R., Li, Y., Sheng, J., and Shen, L. (2018). Knockout of SlMAPK3 Reduced Disease Resistance to *Botrytis cinerea* in Tomato Plants. *Journal of Agricultural and Food Chemistry*, 66(34):8949–8956.

Zhang, W., Corwin, J. A., Copeland, D. H., Feusier, J., Eshbaugh, R., Cook, D. E., Atwell, S., and Kliebenstein, D. J. (2019). Plant–necrotroph co-transcriptome networks illuminate a metabolic battlefield. *eLife*, 8.

Zhang, Y., de Stefano, R., Robine, M., Butelli, E., Bulling, K., Hill, L., Rejzek, M., Martin, C., and Schoonbeek, H.-j. (2015). Different ROS-Scavenging Properties of Flavonoids Determine Their Abilities to Extend Shelf Life of Tomato. *Plant Physiology*, 169(November):pp.00346.2015.

Zheng, Y., Jiao, C., Sun, H., Rosli, H., Pombo, M., Zhang, P., Banf, M., Dai, X., Martin, G., Giovannoni, J., Zhao, P., Rhee, S., and Fei, Z. (2016). iTAK: A Program for Genome-wide Prediction and Classification of Plant Transcription Factors, Transcriptional Regulators, and Protein Kinases. *Molecular Plant*, 9(12):1667–1670.

2.7 Supplemental Material

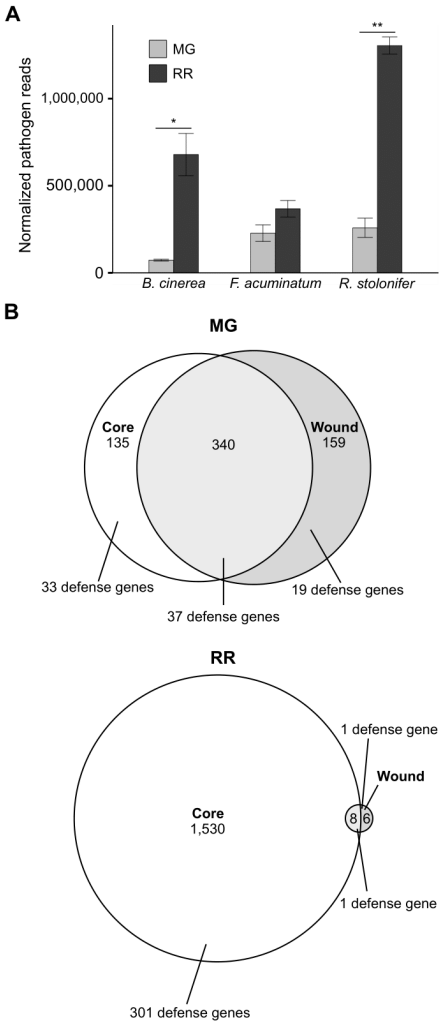

Figure 2.S1: Pathogen measurements and wound responses. (A) Normalized pathogen reads from fruit inoculated with the corresponding pathogen at mature green (MG) and red ripe (RR) stages. Asterisks indicate level of significance of t-test between MG and RR stages for each pathogen. * = P <0.05, ** = P <0.01. (B) Comparison of MG and RR core responses with genes upregulated during wounding response in fruit of the same stage. Number of defense genes are indicated for the subsets.

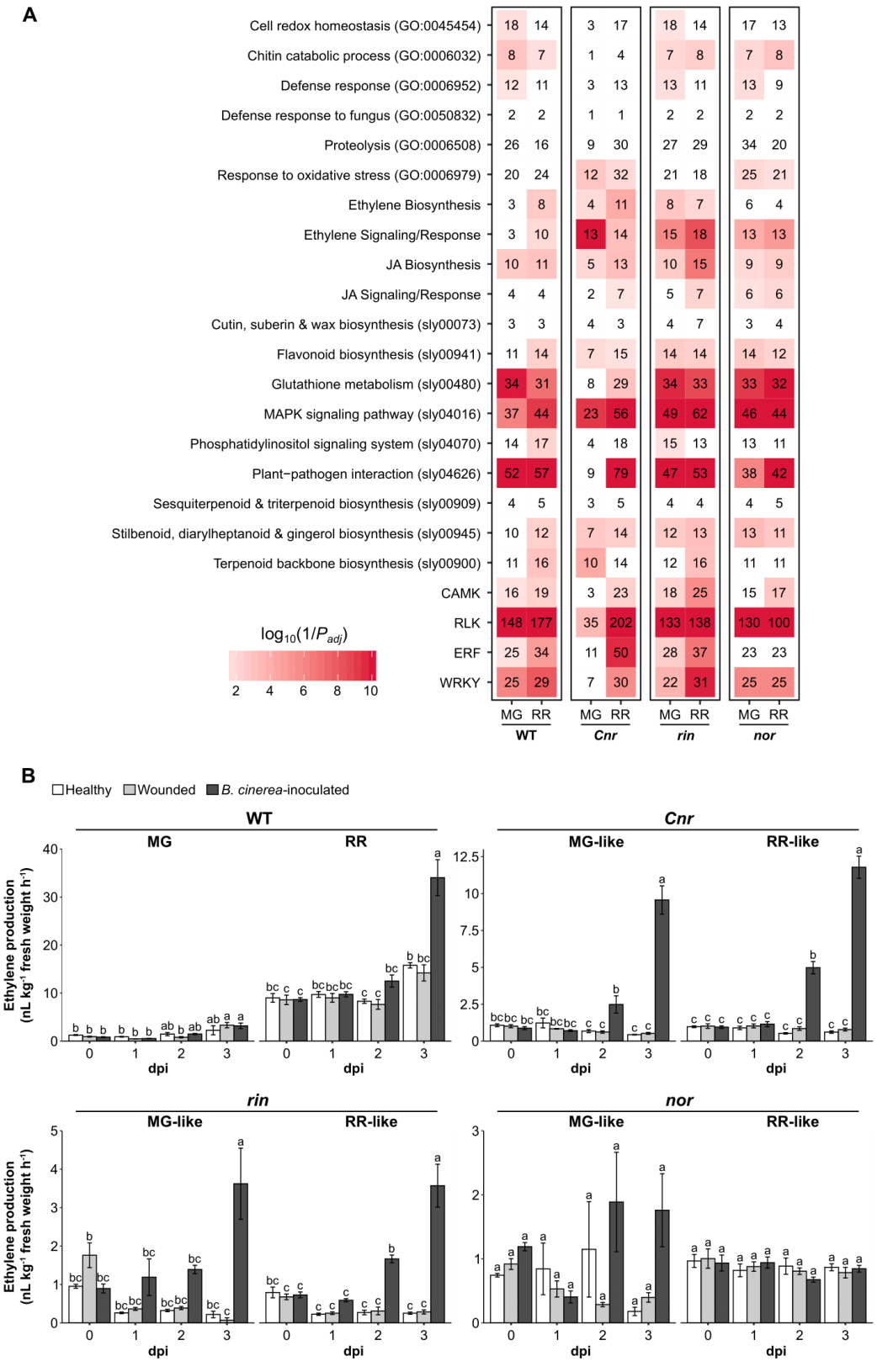

Figure 2.S2: Caption presented on following page.

Figure 2.S2: Defense responses and ethylene levels in wild-type and mutant fruit. (A) Enrichments of various defenserelated classes in the MG/MG-like and RR/RR-like responses. The scale is the $\log_{10}(1/P_{adj})$. Values greater than 10 were converted to 10 for scaling purposes. (B) Levels of ethylene production in healthy, wounded, and *B. cinerea*-inoculated MG/MG-like and RR/RR-like fruit from 0 to 3 days post-inoculation (dpi). Letters represent statistical differences between treatments and time points for each genotype and ripening stage (P <0.05). MG = mature green, RR = red ripe.

Chapter 3

Botrytis cinerea infection accelerates ripening and cell wall disassembly in unripe tomato fruit to promote disease

3.1 Abstract

Postharvest fungal pathogens benefit from the increased host susceptibility that occurs during fruit ripening. In unripe fruit, pathogens often remain quiescent and unable to cause disease until ripening begins, emerging at this point into destructive necrotrophic lifestyles that quickly result in fruit decay. We hypothesized that quiescent infection in an unripe fruit could actively accelerate ripening to facilitate infection and promote disease. Here, we demonstrate that one such pathogen, *Botrytis cinerea*, deploys this strategy. Assessments of ripening progression revealed that *B. cinerea* accelerated external coloration, ethylene production, and softening in unripe fruit, while mRNA sequencing of inoculated unripe fruit confirmed the corresponding upregulation of host genes involved in ripening processes, such as ethylene biosynthesis and cell wall degradation. Furthermore, ELISA-based glycomics profiling of fruit cell wall polysaccharides revealed remarkable similarities in the cell wall polysaccharide changes caused by both unripe fruit inoculation and ripening of healthy fruit, particularly in the increased accessibility of pectin polysaccharides. Virulence and additional ripening assessment experiments with various single and double *B. cinerea* knockout mutants showed that induction of ripening is dependent on the ability to infect the host and break down pectin. The *B. cinerea* double knockout *Δbcpg1Δbcpg2* lacking two critical pectin degrading enzymes was found to be incapable of emerging from

quiescence even long after the fruit had ripened at its own pace, suggesting that the failure to induce ripening severely inhibits fungal survival on unripe fruit. These findings demonstrate that active induction of ripening in unripe tomato fruit is an important infection strategy for *B. cinerea*.

3.2 Introduction

Necrotrophic fungal pathogens often have broad host ranges and are capable of causing disease in multiple tissues within any given plant species. Infections of fruit can display drastically different host-pathogen dynamics than those observed in vegetative tissues. Though both reproductive and vegetative tissues become more susceptible to these types of pathogens during senescence (Häffner et al., 2015), in fruit, a dramatic increase in susceptibility is observed prior to senescence during ripening (Blanco-Ulate et al., 2016a; Prusky, 1996). Because most fruit are economically valuable in their ripe state, while vegetable commodities are consumed prior to senescence, understanding ripening-associated susceptibility to disease is critical to reduce food losses and ensure the high quality of fruit commodities.

Immature and unripe fruit are generally resistant to disease; however, fungal pathogens can establish quiescent infections in these tissues (Prusky et al., 2013). The physiological nature of quiescence, including the level of pathogen colonization and activity, varies widely in different fruit pathosystems. For example, quiescence of the hemibiotrophic pathogen *Colletotrichum* in unripe fruit involves the development of melanized appressoria that penetrate and colonize a limited amount of the fruit cell wall (Alkan et al., 2015; Guidarelli et al., 2011). In contrast, necrotrophic pathogens such as *Botrytis cinerea* are not generally known to produce such structures on fruit, yet they still survive in some capacity on the unripe fruit tissues before emergence from quiescence during fruit ripening (Adaskaveg et al., 2000; Haile et al., 2020; Petrasch et al., 2019a). Regardless of differences in quiescent lifestyles, the onset and progression of fruit ripening trigger a switch to an active necrotrophic lifestyle, resulting in rapid decay of fruit tissues.

Increased susceptibility to necrotrophic pathogens during fruit ripening is widespread

across different fruit species and pathogens (Alkan and Fortes, 2015; Balsells-Llauradó et al., 2020; Cantu et al., 2009; Lassois et al., 2010; Petrasch et al., 2019a). Fruit ripening is a highly complex suite of transcriptional, physiological, and biochemical changes, and many of these are suspected to influence susceptibility to fungal pathogens (Blanco-Ulate et al., 2016a). Multiple ripening changes linked to increased susceptibility have been identified from the tomato-*B. cinerea* pathosystem, which has emerged as a model for fruit-necrotroph interactions (Blanco-Ulate et al., 2016a; Cantu et al., 2009, 2008; Petrasch et al., 2019b; Silva et al., 2021). During ripening in tomato fruit, the pH of the apoplast decreases, providing a more favorable environment for virulence factors including proteases, polygalacturonases, and other cell wall degrading enzymes (Manteau et al., 2003). Ripening in tomato may also be accompanied by a decline in antimicrobial compounds, such as α-tomatine (Akiyama et al., 2021). However, one of the most significant contributors to susceptibility is the disassembly of cell wall polysaccharides during fruit softening, given the importance of plant cell walls as both physical barriers and sources of plant defense signals (Cantu et al., 2008; Prusky et al., 2013).

The cell walls of fruit generally have a higher proportion of pectins than hemicelluloses and cellulose, and fruit walls are usually pectin-rich compared to walls of leaf and stem tissues (Brummell and Harpster, 2001). The major pectin polymers in fruit cell walls are homogalacturonan (HG) and rhamnogalacturonans (RG I and RG II), which contain a variety of complex side-chains (Voragen et al., 2009; Wang et al., 2018). Three types of hemicelluloses are present in the cell walls of fruit, xyloglucans (XyGs), xylans, and mannans; the latter two are less abundant than XyGs (Scheller and Ulvskov, 2010). During ripening, pectins are actively degraded, hemicellulose and cellulose networks are loosened and broken down, and cell wall structural proteins are removed or are no longer synthesized. In addition, the walls around cells in the pericarp and epidermis expand and become hydrated, leading to increased porosity of the cell wall structure and fruit softening (Brummell and Harpster, 2001; Redgwell et al., 1997; Vicente et al., 2007). The importance of this endogenous host cell wall disassembly is highlighted in the reduced susceptibility to *B. cinerea* of tomato mutant lines with suppressed or silenced expression

of various cell wall degrading enzymes (CWDEs) including pectate lyase (*SlPL*; Silva et al. (2021)) and the combination of polygalacturonase 2A (*SlPG2A*) and expansin 1 (*SlExp1*; Cantu et al. (2008)).

The massive benefit of fruit ripening and host cell wall disassembly to postharvest fungal pathogens invites the possibility of active induction of ripening processes as an infection strategy to break quiescence. Some evidence indicates that *B. cinerea* may in fact do this in tomato: the pathogen induces host biosynthesis of the ripening-promoting hormone ethylene (Cantu et al., 2009; Silva et al., 2021) and increases expression of the host CWDEs *SlPG2A* and *SlExp1* in unripe tomato fruit (Cantu et al., 2008). However, induction of ripening and cell wall disassembly by *B. cinerea* in unripe tomato fruit has not yet been demonstrated through physiological measurements. In this paper, we assess and compare the speed of various ripening processes, including color progression, ethylene production, and fruit softening, in *B. cinerea*- and mock-inoculated unripe tomato fruit. As a corollary, we sequenced mRNA in these tissues to detect the induction of metabolic pathways and genes associated with these ripening processes. To examine polysaccharide changes associated with fruit softening, we used an ELISA-based approach to compare changes in the fruit cell wall as a result of unripe fruit inoculation and ripening. Lastly, through virulence studies and additional ripening assessments, we determined that the combination of two *B. cinerea* genes, *BcPG1* and *BcPG2*, is required for both ripening induction and emergence from quiescence in unripe tomato fruit.

3.3 Materials and Methods

3.3.1 Biological material

Tomato (*Solanum lycopersicum*) cv. Ailsa Craig (AC) was obtained from the Tomato Genetics Research Center (UC Davis, CA, USA). The *SlPG2A* antisense line in the AC background (AC-*SlPG2A*) was provided by D. Grierson (University of Nottingham, UK; Smith et al. (1990)). Tomato plants were grown in typical field conditions during the summers of 2010, 2013, and 2020 in Davis, California. Tomato fruit from AC and AC-*SlPG2A* plants were tagged at 3 days post-anthesis (dpa) and harvested at 31 dpa for

mature green (MG) and at 42 dpa for red ripe (RR) stages. The ripening stages were further confirmed by color, size, and texture of the fruit as in Adaskaveg et al. (2021). The *B. cinerea* wild-type strain B05.10, as well as the *Δbcpg1*, *Δbcpg2*, *Δbcpg1Δbcpme1* and *Δbcpme1Δbcpme2* isogenic mutant strains Kars et al. (2005a,b) were grown on 1% potato dextrose agar as described in Petrasch et al. (2019b).

3.3.2 *B. cinerea* inoculation

Tomato fruit were disinfected and inoculated as in Cantu et al. (2008). Briefly, fruit were wounded at six sites (depth of 2 mm and diameter of 1 mm) and inoculated with 10 µL of a water suspension containing 5 x 10^5 conidia/mL suspension of the wild-type strain (B05.10) or each of the mutant strains (*Δbcpg1*, *Δbcpg2*, *Δbcpg1Δbcpg2*, *Δbcpg1Δbcpme1* and *Δbcpme1Δbcpme2*). The viability of the *B. cinerea* conidia across strains was evaluated in parallel to the infection assays by placing the same conidia solutions used for inoculation in 1% potato dextrose agar plates and visually assessing the fungal growth for a week. Tomato fruit used as mock-inoculated material had 10 µL of sterile water placed into the wounded sites. Healthy fruit were not wounded or inoculated. MG and RR tomato fruit (i.e., *B. cinerea*-inoculated, mock-inoculated or healthy) used for the RNAseq analyses and qRT-PCR validation were incubated at 20 °C in high humidity for 3 days. MG tomato fruit used for susceptibility assessment and fungal biomass analyses were incubated for 3 to 6 days at 20 °C in high humidity. Incubation of a subset of the MG fruit inoculated with the *Δbcpg1Δbcpg2* was continued for 10, 15, and 20 days under the same conditions.

Tomato fruit used for fungal biomass measurements, for transcriptomics, and glycomics were deseeded, frozen and ground to fine powder in liquid nitrogen. Three to six biological replicates were produced per treatment and ripening stage; each consisted of independent pools of 8-12 tomato fruit.

3.3.3 Assessments of ripening progression

B. cinerea-inoculated and mock-inoculated fruit were individually labeled and kept stored in high-humidity containers up to 6 dpi and evaluated each day after 3 dpi for color pro-

gression, ethylene production, and firmness loss. A total of 175 *B. cinerea*-inoculated and 181 mock-inoculated fruit were assessed for color progression. Photos were taken of all fruit, and each individual fruit was visually categorized each day into one of five color groups each with a corresponding numerical stage value: mature green (1), breaker (2), orange (3), pink (4), and red ripe (5). Average stage values were calculated from these. For ethylene, 35 *B. cinerea*-inoculated and 37 mock-inoculated fruit were weighed each day and pooled into five sterile 1 liter containers for 30-90 min, after which headspace gas (3 ml) was extracted and analyzed in a Shimadzu CG-8A gas chromatograph (Shimadzu Scientific Instruments, Kyoto, Japan). Sample peaks were measured against an ethylene standard of 1 ppm. Ethylene production was calculated from the peak height, fruit mass, and incubation time. For firmness measurements, 210 *B. cinerea*-inoculated and 217 mock-inoculated were assessed each day, as well as at 0 days, on the TA.XT2i Texture Analyzer (Texture Technologies, United States) using a TA-11 acrylic compression probe, a trigger force of 0.035 kg, and a test speed of 2.00 mm/sec with Exponent software (Texture Technologies Corporation, United States). Firmness loss was calculated as the percentage of firmness at 0 days for each individual fruit. A total of 70 *Δbcpg1Δbcpg2*-inoculated fruit were assessed for color progression, ethylene production, and firmness similarly, and 128 fruit each of *Δbcpg1Δbcpme1* and *Δbcpme1Δbcpme2* were also assessed for color progression. Significant differences in physiological parameters between treatments were determined with analysis of variance (ANOVA) followed by post hoc testing (Tukey's honestly significant difference, HSD) using R (R Foundation for Statistical Computing, Vienna, Austria).

3.3.4 RNA isolation and sequencing

Two grams of *B. cinerea*-inoculated (with wild-type or mutant strains), mock-inoculated, and healthy tomato fruit (pericarp and epidermis) at two ripening stages from each biological replicate were used for RNA extraction, as in the methods described in Blanco-Ulate et al. (2013). RNA concentration and purity were measured using the NanoDrop 2000c Spectrophotometer (Thermo Fisher Scientific, USA). RNA integrity was checked by agarose gel electrophoresis. Eighteen cDNA libraries were prepared using the Illu-

mina TruSeq RNA Sample preparation Kit v.2 according to the low-throughput protocol (Illumina, USA). Each library corresponded to three biological replicates of wild-type tomato fruit (cv. AC) at MG and RR stages, and 3 days after treatment. The cDNA libraries were barcoded individually and analyzed for quantity and quality with the High Sensitivity DNA Analysis Kit in the Agilent 2100 Bioanalyzer (Agilent, USA). cDNA libraries were pooled in equal amounts for sequencing (single end, 50 bp) at the Expression Analysis Core Facility (UC Davis, CA, USA) in an Illumina HiSeq 2000 sequencer.

3.3.5 RNAseq data processing

Raw sequencing reads trimmed for quality and adapter sequences using Trimmomatic v0.33 (Bolger et al., 2014) with the following parameters: maximum seed mismatches=2, palindrome clip threshold=30, simple clip threshold=10, minimum leading quality=3, minimum trailing quality=3, window size=4, required quality=15, and minimum length=36. Trimmed reads were mapped using Bowtie2 (Langmead and Salzberg, 2012) to a combined transcriptome of tomato (SL4.0 release; `http://solgenomics.net`) and *B. cinerea* (`http://fungi.ensembl.org/Botrytis_cinerea/Info/Index`). Count matrices were made from the Bowtie2 results using sam2counts.py v0.91 (`https://github.com/vsbuffalo/sam2counts/`). Only reads that mapped to the tomato transcriptome were used in the following analyses. The Bioconductor package DESeq2 (Love et al., 2014) was used to normalize raw read counts and to determine differential expression (P_{adj} <0.05) among treatments. Differential expression results for 1 dpi data were obtained directly from Silva et al. (2021) (GSE148217). For ripening gene expression, raw sequencing reads were downloaded from the fruitENCODE website (`http://www.epigenome.cuhk.edu.hk/encode.html`) and processed as above, with the exception that these reads were mapped only to the tomato transcriptome.

3.3.6 Functional annotation and enrichments

Annotations for biochemical pathways including terpenoid and carotenoid biosynthesis as well as ethylene biosynthesis were obtained using the Kyoto Encyclopedia of Genes and Genomes (KEGG) Automatic Annotation Server (Moriya et al., 2007). Additional an-

notations for ethylene biosynthesis genes were obtained from Liu et al. (2015). CAZyme annotations were obtained via HMMER alignments of the full SL4.0 proteome to HMM profiles obtained from dbCAN (`http://bcb.unl.edu/dbCAN2/`) with a an e-value threshold of 1 x 10^{-23} and a coverage threshold of 0.2. Information on the functionality of each CAZyme family was obtained from `http://www.cazy.org/`. All functional enrichments were performed using Fisher's test with resulting P-values adjusted via the Benjamini–Hochberg method (Benjamini and Hochberg, 1995).

3.3.7 Quantitative reverse transcription PCR (qRT-PCR)

cDNA was prepared from the isolated RNA using M-MLV Reverse Transcriptase (Promega, USA). qRT-PCR was performed on a StepOnePlus PCR System using Fast SYBR Green Master Mix (Applied Biosystems, USA). All qRT-PCR reactions were performed as follows: 95 °C for 10 min, followed by 40 cycles of 95 °C for 3 s and 60 °C for 30 s. Based on a correlation analysis between the total raw reads for tomato present in the RNAseq samples and the reads for each individual gene in those samples, two genes with high and significant Pearson coefficients were chosen as references for the qRT-PCR experiments. These genes correspond to the tomato UBIQUITIN LIKE-1 (*SlUbq-like1*, *Solyc12g04474*; $r = 0.90$, $P = 5.18$ x 10^{-7}) and the *B. cinerea RIBOSOMAL PROTEIN-LIKE5* (*BcRPL5*, *Bcin14g04230*; $r = 0.94$, $P = 5.92$ x 10^{-3}) and were processed in parallel with the genes of interest. Primer efficiencies were confirmed to be above 90% using 4-fold cDNA dilutions (1:1, 1:4, 1:16, 1:64 and 1:256) in duplicate as well as checking for amplification in a negative control without DNA. Specificity of the primers was checked by analyzing dissociation curves ranging from 60 °C to 95 °C. The primer sequences to amplify *SlPME1-2* and *SlPMEU1* were extracted from Reca et al. (2012), while sequences for *BcRPL5*, *BcPG1-6*, and *BcPME1-2* genes were obtained from Zhang and van Kan (2013). Transcript levels for all genes were linearized using the formula $2^{(\text{REFERENCE CT - TARGET CT})}$. Data presented are for 3-6 biological replicates. Differences in relative expression levels were assessed by ANOVA followed by Tukey's HSD using R.

3.3.8 Cell wall extraction and fractionation

Total cell walls were prepared from combined outer pericarp and epidermis (15 g) from healthy and *B. cinerea*-inoculated fruit (with the B05.10 strain) at 3 dpi, as described by Vicente et al. (2007), with the following modifications: samples were ground to a fine powder in liquid nitrogen rather than homogenized, boiled in 100% ethanol for 45 min, and the insoluble material was filtered through glass microfiber filters (Ahlstrom, Finland) rather than Miracloth. Three preparations of extracted walls were obtained per experimental class; each extraction was from an independent pool of fruit (6-10 fruit) from three different harvests. Sequential chemical extractions of the total cell wall material (alcohol insoluble residue, AIR) were performed as specified in Vicente et al. (2007). All the extractions were done at room temperature and the 4% KOH-soluble fraction was omitted, because the cell wall analyses were not focused on separating hemicellulose classes. Two independent sets of extraction series were prepared from each AIR sample, resulting in six replications per sample class. Four classes of soluble fractions were obtained: WSF (water-soluble fraction), CSF (CDTA-soluble fraction), NSF (Na_2CO_3-soluble fraction) and KSF (24% KOH-soluble fraction).

3.3.9 Glycomic analysis of cell wall fractions

Total sugar content of the cell wall fractions was calculated by adding the content of uronic acids and of neutral sugars present in each of the samples. The uronic acid content was measured according to Blumenkrantz and Asboe-Hansen (1973), and neutral sugar content was determined by the anthrone method (Yemm and Willis, 1954); both protocols were scaled down to a 96-well plate format. Galacturonic and glucose standard curves were established in order to respectively determine the uronic acid and neutral sugar concentrations. Measurements for each fraction were done in triplicate using a Synergy H1 Hybrid Multi-Mode Microplate Reader (Biotek, USA). Based on the neutral sugar and uronic acid content, all cell wall fractions were diluted to the same total sugar concentration for the glycomic experiments. Glycome profiling of the cell wall fractions was performed by high-throughput ELISAs with a toolkit of plant cell wall glycan-directed monoclonal antibodies as designed and validated by Pattathil et al. (2010) and described

by Zhu et al. (2010). Monoclonal antibodies were obtained as hybridoma cell culture supernatants from stocks of the Complex Carbohydrate Research Center (CCRC, JIM and MAC series), available from CarboSource Services (`www.carbosource.net`). For the scatterplot analysis of treatments, a linear regression model was fitted to the data and was tested for statistical significance ($P_{adj}<.05$) in R. Enrichments were performed using Fisher's test with resulting P-values adjusted via the Benjamini–Hochberg method (Benjamini and Hochberg, 1995).

3.3.10 Disease development assays

Wild-type or AC-*SlPG2A* MG tomato fruit inoculated with the wild-type strain (B05.10) or one of the double mutant strains (*Δbcpg1Δbcpg2*, *Δbcpg1Δbcpme1* and *Δbcpme1Δbcpme2*) and were assessed for disease symptoms during four consecutive days starting at 3 days post-inoculation (dpi). Disease development was recorded as disease incidence (percentage of inoculation sites showing symptoms) and disease severity (diameter of the soft rot lesions). These susceptibility evaluations were repeated over the course of eight separate harvest dates using 10-15 fruit per experimental treatment. Differences in disease incidence and severity between tomato genotypes and *B. cinerea* strains at each dpi were assessed by ANOVA followed by Tukey's HSD using R.

B. cinerea biomass was quantified using the QuickStix Kit (EnviroLogix, USA), which utilizes the monoclonal antibody BC12.CA4 (Meyer et al., 2000) as described by Blanco-Ulate et al. (2015). Three to six biological replicates of the distinct *B. cinerea*-inoculated tissues were created. One gram of ground tissue (pericarp and epidermis) from each biological replication was suspended in the kit buffer, 2:1 m/v for samples that did not display obvious symptoms of fungal infection, 1:5 m/v for MG samples and 1:120 m/v for RR samples. The intensity of the monoclonal antibody reaction was determined using the QuickStix Reader (EnviroLogix, USA) and converted into fungal biomass (µg g^{-1} fresh weight of fruit extracts) according to Blanco-Ulate et al. (2015).

3.4 Results

3.4.1 *Botrytis cinerea* infections accelerate ripening processes in unripe fruit

We hypothesized that inoculating mature green (MG) fruit with *Botrytis cinerea* would lead to accelerated ripening progression. To test this, we compared *B. cinerea*-inoculated and mock-inoculated MG fruit (cv. Alisa Craig, AC) after several days post-inoculation (dpi). We first selected fruit at the MG stage based on size, color, and firmness (see Materials and Methods), then divided these fruit randomly into two groups. Fruit from both groups were wounded six times. Then, fruit from the first group were inoculated with a *B. cinerea* spore suspension, while fruit from the second group were inoculated with sterile water (i.e., mock-inoculated). We chose mock-inoculated MG fruit rather than healthy MG fruit to control for the effects of the wounding response. All fruit were then stored in high humidity and evaluated from 3 dpi to 6 dpi. These specific times of evaluation were chosen because up until 3 dpi inoculated MG fruit remain resistant to disease and do not typically show signs of ripening (Silva et al., 2021).

Using non-destructive methods, we assessed the ripening rate in *B. cinerea*-inoculated and mock-inoculated MG fruit based on three characteristic physiological processes: external color progression, ethylene production, and loss of fruit firmness (i.e., softening). At 3 dpi, the first day of evaluation, inoculated and mock-inoculated fruit were not significantly ($P > 0.05$) different for any of the ripening parameters evaluated, which confirmed that the fruit from both treatments were collected at an similar ripening stage. Additionally, no symptoms of fungal disease (e.g., water-soaked lesions or mycelial growth) were evident in any of the fruit at this initial time point (Figure 3.1).

After 3 dpi, ripening processes accelerated in inoculated MG fruit. This coincided with a rise in the percentage of symptomatic inoculated fruit, reaching 26% at 6 dpi (Figure 3.1A). While fruit from both treatments experienced color progression based on their climacteric ripening behavior, *B. cinerea*-inoculated fruit turned red significantly faster ($P < 0.05$) than mock-inoculated fruit, which remained green longer (Figure 3.1B). For example, by 6 dpi, 44% of *B. cinerea*-inoculated fruit were at either the orange or red stage,

compared to just 28% of mock-inoculated fruit. In contrast to color progression, a rapid increase in ethylene production was observed only in the *B. cinerea*-inoculated fruit, where levels increased dramatically from 3 dpi onwards (P <0.05), while ethylene levels remained constant in mock-inoculated fruit, indicating the normal climacteric ethylene burst had not yet occurred in most of these fruit (Figure 3.1C). Lastly, while both *B. cinerea*-inoculated and mock-inoculated fruit experienced a steady loss of firmness, inoculated fruit lost firmness at a significantly (P <0.05) faster rate, reaching an average of 56% loss compared to 49% in mock-inoculated fruit at 6 dpi (Figure 3.1D). Altogether, these results indicate that *B. cinerea* inoculations accelerate ripening processes, even when the majority of these fruits do not display any disease symptoms (i.e., water-soaked lesions) yet.

3.4.2 *B. cinerea* infections induce premature expression of ripening-related genes in unripe fruit

We performed an RNAseq analysis to identify ripening-related genes or pathways that are induced by *B. cinerea* infections and that could explain the accelerated physiological changes observed in the *B. cinerea*-inoculated MG fruit. We sequenced mRNA from *B. cinerea*-inoculated and mock-inoculated MG fruit at 3 dpi, just before the acceleration of ripening progression was evident due to *B. cinerea* inoculation. Healthy MG fruit (i.e., not wounded) subjected to the same conditions as the other treatments and sequenced after 3 days post-harvest (dph) were also included and used as a baseline; compared to healthy fruit, we expected to see induction of ripening-related transcriptional activity by *B. cinerea*, but not mock-inoculation. In addition to these samples, we incorporated two other existing transcriptomic datasets: (i) healthy (H), *B. cinerea*-inoculated (I), and mock-inoculated (M) samples created identically to the 3 dpi samples but sequenced at 1 dpi (Silva et al., 2021) to account for the possibility that genes were triggered earlier during the inoculation, and (ii) publicly available samples of healthy fruit at five developmental stages from MG to RR from the fruitENCODE database (Lü et al., 2018) to capture ripening-related genes. All transcriptomic dataset were generated from fruit samples of the tomato variety, Ailsa Craig (AC). For differential expression analysis, inoculated and

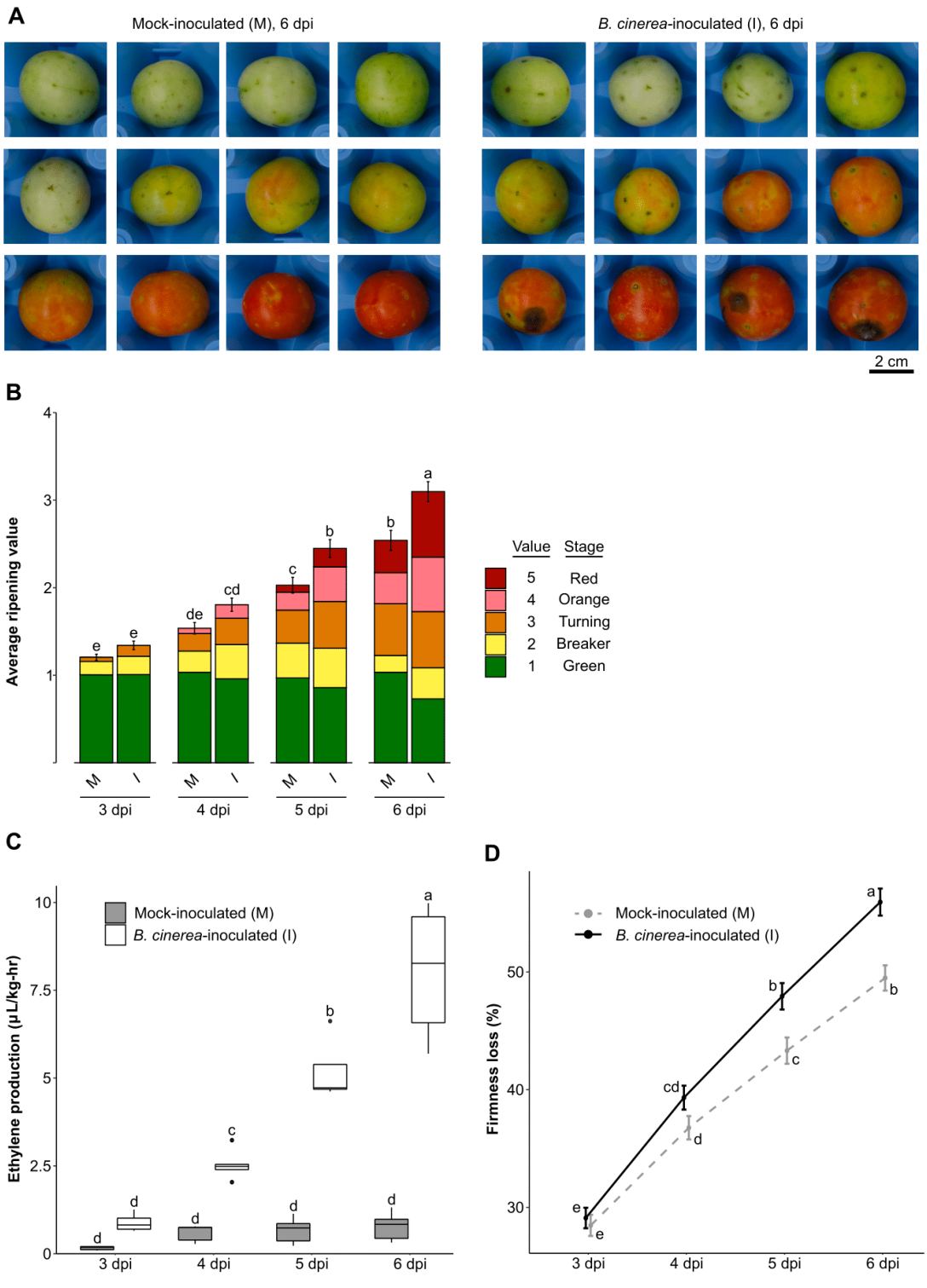

Figure 3.1: Caption presented on following page.

Figure 3.1: Acceleration of ripening in *Botrytis cinerea*-inoculated unripe fruit. All panels contain data taken each day between 3 and 6 days post-inoculation (dpi). (A) Representative photos of mock-inoculated and *B. cinerea*-inoculated mature green (MG) fruit at 6 dpi. (B) Average ripening stage value as assessed by color in mock-inoculated and *B. cinerea*-inoculated MG fruit (n=172-181). Colored blocks within each column represent the proportion of fruit at the matching stage in the color key. (C) Production of ethylene in mock- and *B. cinerea*-inoculated MG fruit (n=5). (D) Firmness loss in mock- and *B. cinerea*-inoculated MG fruit measured as a percentage of initial firmness at 0 dpi (n= 210-216). Letters in B-D indicate the statistical differences (P <0.05) between each treatment across all dpi as calculated by ANOVA and Tukey's HSD test. M, mock-inoculated; I, inoculated.

mock-inoculated samples were compared to healthy MG fruit of the corresponding dpi, while the fruitENCODE samples from breaker (B), B + 5 days (B+5), B + 7 days (B+7), and B + 10 days (red ripe, RR) were compared to the MG fruitENCODE samples. A table of the differential expression results, including relevant gene annotations, can be found in Supplemental Table S1 at `https://ucdavis.box.com/s/yp72rney9f6sl5nqfdz17lagmsjt2f86`.

Of the 34,075 known protein-coding genes in the tomato genome, 5,512 were found to be differentially expressed (P_{adj} <0.05) as a result of *B. cinerea* inoculation in MG fruit (MG I / MG H) at either 1 or 3 dpi (Table 3.1). In contrast, a much smaller number of genes (582) were differentially expressed due to mock inoculation (MG M / MG H), and most of these (482 or 82.8%) had the same expression pattern as they had in *B. cinerea*-inoculated fruit. These results indicate that *B. cinerea* inoculation, but not mock inoculation, has a substantial impact on gene expression in MG fruit, and that wounding responses in MG fruit represent a small subset of fungal inoculation responses. From the fruitENCODE data, a total of 10,795 genes were found to be differentially expressed at one or more of the four ripening stages when compared to MG.

We first focused on the expression of genes with functional annotations belonging to three different categories: lycopene biosynthesis, ethylene biosynthesis, and cell wall de-

Table 3.1: Differentially expressed genes as a result of mock inoculation, *Botrytis cinerea* inoculation of unripe fruit, and healthy fruit ripening.

Category	Subcategory	Upregulated	Downregulated	Total
Inoculation	1 dpi	2,823	1,734	4,577
	3 dpi	1,934	1,004	2,938
	Total	3,249	2,252	5,512*
Mock-Inoculation	1 dpi	499	31	530
	3 dpi	139	24	163
	Total	533	49	582
Ripening	B	2,341	2,761	5,102
	B + 5	2,292	3,277	5,569
	B + 7	3,543	4,491	8,034
	RR	3,383	4,644	8,027
	Total	4,617	5,377	10,795

*Total values in these cells include genes with mixed expression patterns (i.e. upregulated in one subcategory and down in another subcategory) within that category.

grading enzymes (CWDEs), due to their link to the accelerated ripening processes demonstrated before (Figure 3.1). We curated annotations for these pathways from the Kyoto Encyclopedia of Genes and Genome (KEGG) database, the dbCAN CAZyme annotation server (Zhang et al., 2018), and additional literature on tomato ethylene biosynthesis genes (Liu et al., 2015). During ripening, several genes in the lycopene biosynthesis pathway, including *phytoene synthase 1* (*SlPSY1*, *Solyc03g031860*), *zeta-carotene isomerase* (*SlZ-ISO*, *Solyc12g098710*), *zeta-carotene desaturase* (*SlZDS*, *Solyc01g097810*), and *carotene isomerase* (*SlCrtISO*, *Solyc03g007960*), were all significantly (P_{adj} <0.05) upregulated (Supplemental Table S1 at https://ucdavis.box.com/s/yp72rney9f6sl5nqfdz17lagmsjt2f86). Simultaneously, *lycopene beta-cyclase* (*SlLCY-B*, *Solyc12g008980*), and *lycopene epsilon-cyclase* (*SlLCY-E*, *Solyc04g040190* and *Solyc10g079480*), which convert lycopene to beta-carotene and epsilon-carotene, respectively, were downregulated. Curiously, none of these same changes in gene expression were observed as a result of *B. cinerea* inoculation at

either 1 or 3 dpi, though baseline expression of *SlPSY1* in MG fruit at 3 dpi was fairly high (average normalized read count = 46,519). This suggests that the induction of color progression may occur through an indirect effect on the metabolic flux through manipulation of a neighboring pathway, or simply occurs at a different timepoint than those evaluated.

B. cinerea inoculation resulted in clear upregulation of ethylene biosynthesis genes (Figure 3.2). Interestingly, while *B. cinerea* sometimes upregulated the same genes involved in ripening, it often upregulated additional paralogs that are not normally induced during ripening. For example, *B. cinerea* inoculation caused an upregulation of the ripening-related ethylene biosynthesis genes *SlACS4* (*Solyc05g050010*) and *SlACO1*, (*Solyc07g049530*), but also *SlACS8* (*Solyc03g043890*), *SlACO2* (*Solyc12g005940*), and *SlACO3* (*Solyc07g049550*), which do not appear ripening-related. As ethylene is a strong promoter of fruit ripening in tomato, induced ethylene biosynthesis in *B. cinerea*-inoculated MG fruit may lead to activation of downstream ripening genes, thus accelerating the ripening process even further.

Likewise, CWDE genes from nine separate families known to be involved in fruit softening were induced by *B. cinerea*. A total of 30 genes across these families were found to be upregulated during ripening, with eight of these genes also being upregulated by *B. cinerea* inoculation. However, *B. cinerea* inoculation induced an additional 26 CWDEs beyond the eight ripening-related ones, demonstrating substantial recruitment of host CWDEs after MG inoculation. These included nine pectin methylesterases (PMEs), many of which appeared to be also induced by mock-inoculation at 1 dpi, though by 3 dpi upregulation was sustained by only *B. cinerea* inoculation for all but one gene. Also upregulated by *B. cinerea* were six polygalacturonases (PGs) and three pectate lyases (PLs), enzymes responsible for pectin backbone degradation. Notably, *B. cinerea* only weakly upregulated two xyloglucanases at 1 dpi, suggesting that hemicellulose may not be a critical target for degradation. Additional glycosyl hydrolases with mixed activity on pectin, hemicellulose, cellulose, and other sugars (GH1, GH3, and GH35) were also found to be upregulated during ripening and *B. cinerea* infection. We selected 16 tomato genes

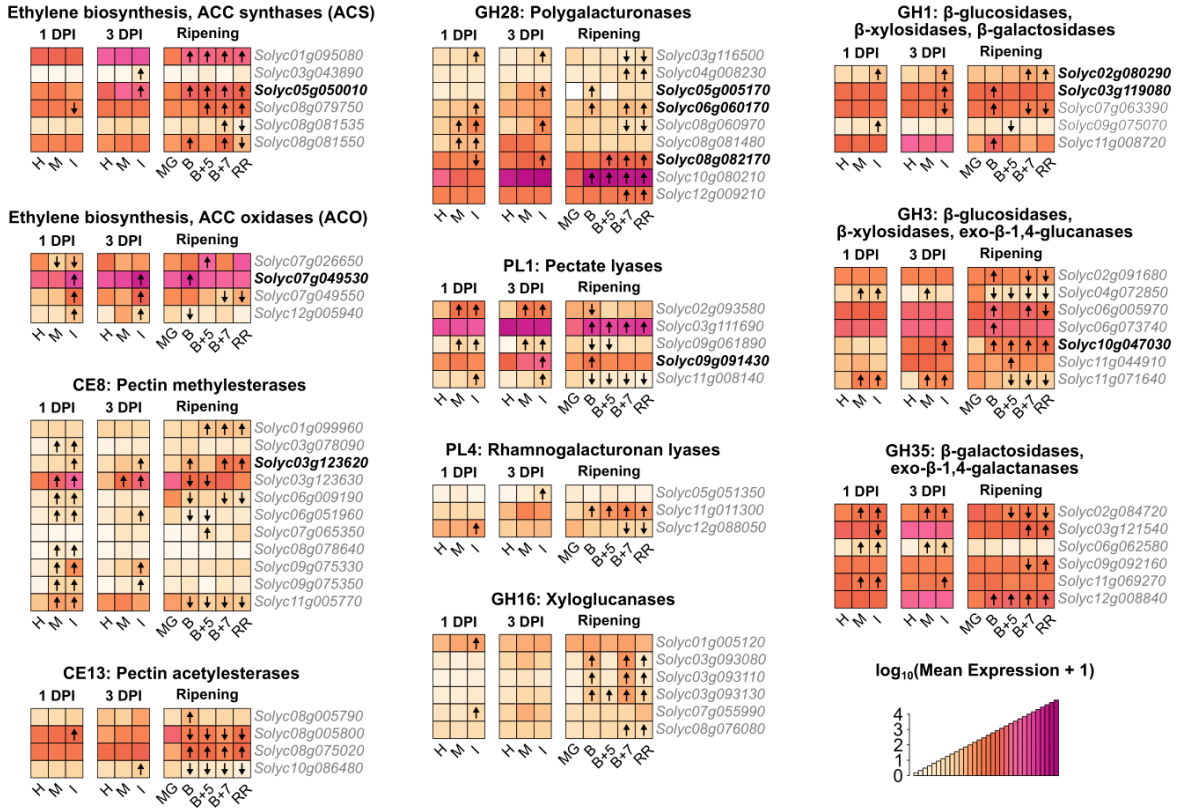

Figure 3.2: Expression patterns of ethylene biosynthesis and cell wall degrading enzyme genes in *Botrytis cinerea*-inoculated unripe fruit and healthy fruit ripening. Heatmaps of normalized expression values in healthy, mock-inoculated, and *B. cinerea*-inoculated mature green (MG) fruit at 1 and 3 days post-inoculation, as well as healthy ripening obtained from the fruitENCODE (Lü et al., 2018). Normalized expression values have undergone a $\log_{10}$(mean expression + 1) transformation. Arrows within heatmap tiles indicate statistically significant (P_{adj} <0.05) upregulated or downregulated genes when compared to expression values in healthy MG fruit at that timepoint. Boldtype font indicates genes that were upregulated by both *B. cinerea* inoculation and ripening. H, healthy; M, mock-inoculated; I, inoculated; B, breaker; RR, red ripe; dpi, days post-inoculation.

encoding different CWDEs for qRT-PCR validation of the RNASeq data (Supplemental Table S2 at `https://ucdavis.box.com/s/9mr3xvvx4766nl25kk80fxhdgtrkpx1f`). A strong correlation ($r = 0.88$) was obtained between the $\log_2$ fold change values from the RNASeq data and the qPCR data. Altogether, these results suggest that *B. cinerea* infections lead to the activation of host CWDE expression, particularly pectin-related enzymes, which then facilitate the disassembly of the fruit cell walls.

Beyond the lycopene biosynthesis, ethylene biosynthesis, and CWDE categories, we were interested in the overall overlap between genes induced by MG inoculation and the ripening-related genes. A total of 629 genes were upregulated during both MG inoculation (1 and/or 3 dpi) and ripening, and 1,031 genes were downregulated in these comparisons. To assess the functionality of these genes, we performed enrichment analyses ($P_{adj} <0.05$) of KEGG pathway annotations (Table 3.2). Among the commonly upregulated genes, the most significantly enriched pathways were "plant-pathogen interaction" (sly04626) and "proteasome" (sly03050). The K04626 genes, upon closer inspection, were found to mostly consist of various calmodulins and calcium-dependent protein kinases. Additionally, the "alpha-linolenic acid metabolism" (sly00592) pathway was enriched, and the corresponding genes were found to be those responsible for the biosynthesis of jasmonic acid, a hormone that, similarly to ethylene, positively regulates both ripening and pathogen response (Peña-Cortés et al., 2004). Enrichment analyses of the commonly downregulated genes revealed an abundance of various photosynthesis-related pathways. The decreased photosynthetic capacity as a result of ripening fruit is well-known, and the occurrence of this as the result of *B. cinerea* inoculation can also help explain the accelerated color progression in the inoculated MG fruit. Ultimately this overlap between MG inoculation responsive genes and ripening-related genes indicates that *B. cinerea* may activate a variety of ripening pathways.

Table 3.2: Pathway enrichment among genes commonly upregulated or downregulated by both *Botrytis cinerea* inoculation of unripe fruit and ripening.

Category	KEGG Pathway	Number of Genes	P_{adj}
Upregulated	Plant-pathogen interaction (sly04626)	18	2.9×10^{-7}
	Proteasome (sly03050)	10	2.0×10^{-6}
	Glutathione metabolism (sly00480)	10	2.7×10^{-3}
	alpha-Linolenic acid metabolism (sly00592)	6	2.0×10^{-2}
	Citrate cycle (sly00020)	6	3.8×10^{-2}
	Sulfur metabolism (sly00920)	5	4.7×10^{-2}
Downregulated	Photosynthesis (sly00195)	30	7.5×10^{-21}
	Carbon fixation (sly00710)	25	5.8×10^{-18}
	Photosynthesis – antenna proteins (sly00196)	16	9.7×10^{-12}
	Pentose phosphate pathway (sly00030)	13	4.4×10^{-7}
	Glyoxylate and dicarboxylate metabolism (sly00630)	12	1.2×10^{-4}
	Fructose and mannose metabolism (sly00051)	11	7.1×10^{-4}
	Porphyrin and chlorophyll metabolism (sly00860)	9	1.3×10^{-3}
	Glycolysis / gluconeogenesis (sly00010)	13	1.0×10^{-2}

Formal KEGG codes are given within parentheses. Only significantly enriched pathways ($P_{adj} < .05$) are shown.

3.4.3 Tomato fruit inoculation with *B. cinerea* and healthy ripening result in similar changes to cell wall polysaccharide composition

Of the three ripening processes analyzed above, induction of cell wall degradation is likely to have the largest impact on the disease outcome by facilitating fungal colonization. We profiled the cell wall glycome of fruit to characterize the prevalence of specific polysaccharides which indicate the extent of cell wall degradation. To compare the cell wall changes induced by MG fruit inoculation and those that occur during healthy fruit ripening, we selected three types of fruit: (i) *B. cinerea*-inoculated MG fruit at 3 dpi, (ii) healthy MG fruit at 3 dph, and (iii) healthy RR fruit at 3 dph. Because mock-inoculated fruit showed very limited induction of CWDE expression, most of which overlapped with the CWDEs induced by *B. cinerea*, we did not include them in these analyses. As with the

transcriptomic data, we chose 3 dpi or 3 dph as our assessment time point because it is the last day before symptoms of the disease appear in MG inoculated fruit, and thus cell wall structure at this time may indicate important changes required to establish infection.

First, we extracted the total cell wall polysaccharides and then generated four different soluble fractions each differing in their polysaccharide composition. The water-soluble fraction (WSF) contained small molecules and pectin polysaccharide species that are soluble in un-buffered water. The CDTA-soluble fraction (CSF) included calcium-bound pectins. The Na_2CO_3-soluble fraction (NSF) was composed of pectins linked to the cell wall matrix via covalent ester linkages. The KOH-soluble fraction (KSF) was enriched for hemicellulose polysaccharides (xyloglucans and xylans). The WSF, CSF, NSF, and KSF fractions were subjected to glycome profiling with 150 cell wall polysaccharide-directed monoclonal antibodies (mABs) to detect diverse epitopes present in pectin, hemicelluloses, or mixed polysaccharide substrates (Figure 3.3A). We calculated $\log_2$ fold changes for the MG fruit inoculation (MG I / MG H) and ripening (RR H / MG H) comparisons for each mAB in each fraction. A total of 116 mABs assayed across the different fractions demonstrated significant ($P < 0.05$) $\log_2$ fold changes for MG fruit inoculation and ripening (boldtype in Figure 3.3A, Figure 3.3B). Log_2 fold changes correlated strongly between comparisons (adjusted $r^2 = 0.82$), suggesting a high degree of similarity in polysaccharide changes in the cell wall brought on by both *B. cinerea* inoculation in MG fruit and healthy fruit ripening. Nearly all (103/116) of these mABs showed increased binding (i.e., positive $\log_2$ fold changes) in both comparisons, indicating that both the MG fruit inoculation responses and ripening processes resulted in increased access to pectin polysaccharides reflective of cell wall disassembly.

We performed Fisher's exact test to calculate statistically ($P_{adj} < 0.05$) overrepresented polysaccharide classes among the mABs with significant $\log_2$ fold changes in each fraction (Figure 3.3C). Enrichment patterns were remarkably similar between MG fruit inoculation (MG I / MG H) and ripening (RR H / MG H). In particular, multiple mABs associated with RG I backbone and arabinogalactan polysaccharides experienced increased binding strength in the CSF and NSF fractions as a result of both comparisons. In contrast,

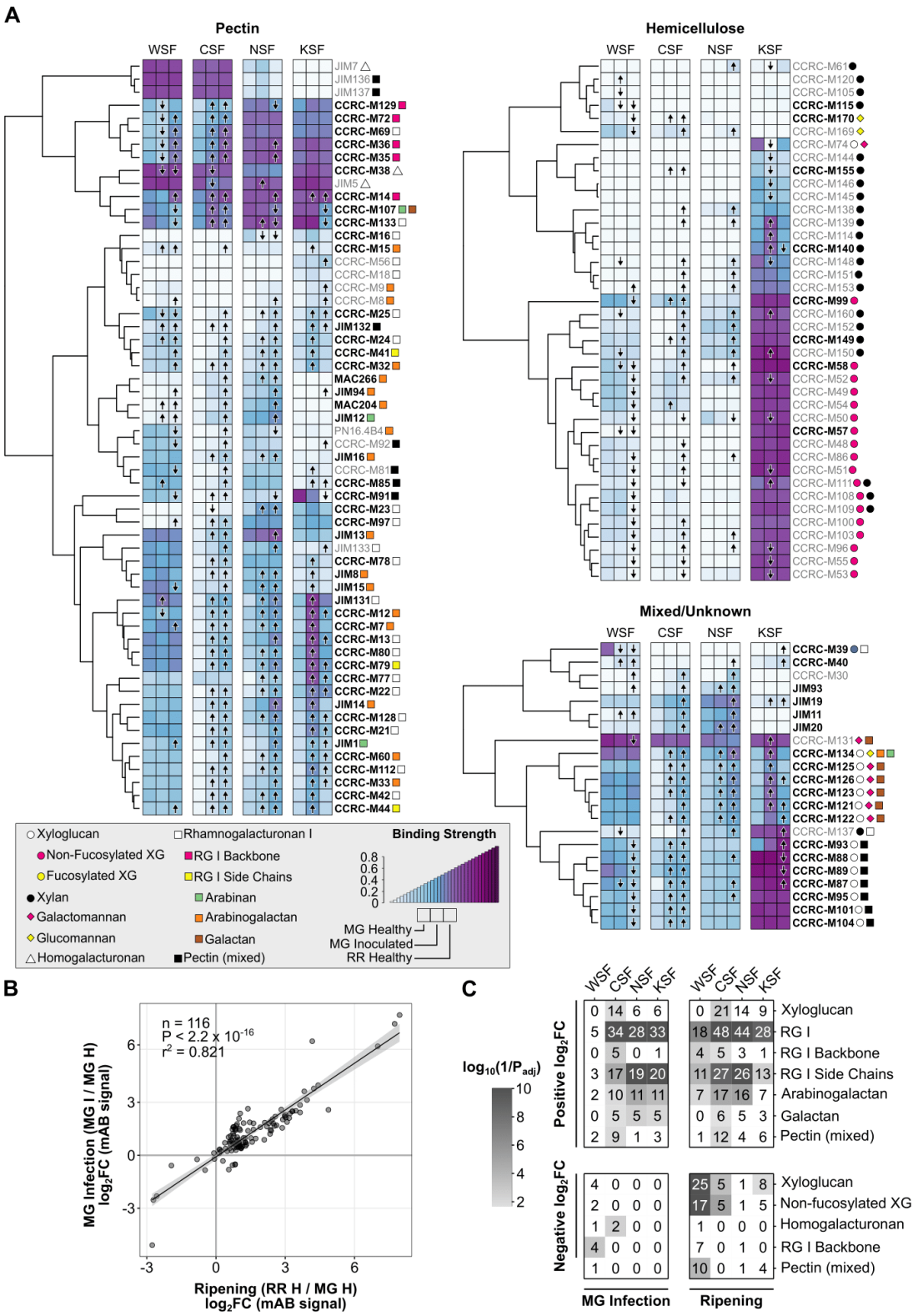

Figure 3.3: Caption presented on following page.

Figure 3.3: Glycomics profiling of *Botrytis cinerea*-inoculated unripe fruit. (A) Heatmaps of binding strength of polysaccharide-binding monoclonal antibodies (mAB) in healthy mature green (MG), *B. cinerea*-inoculated MG fruit, and healthy red ripe (RR) at 3 days post-inoculation or days post-harvest. mAB codes are given to the right of each heatmap row, with the recognized classes of cell wall polysaccharides indicated by colored shapes according to the given key. mAB listed in boldtype are those included in the scatterplot in panel B. Arrows within heatmap tiles indicate statistically significant (P_{adj} <0.05) increasing or decreasing antibody strength when compared via *t*-test to values in healthy MG fruit (n=6). (B) Scatterplot and linear regression model of $\log_2$ fold change ($\log_2$FC) values of mAB signals in MG inoculation (*B.cinerea*-inoculated MG / healthy MG) and ripening (healthy RR / healthy MG) comparisons. (C) Enrichment of polysaccharide classes with statistically significant positive or negative $\log_2$ fold changes in each cell wall fraction for the ripening and MG inoculation comparisons. Numbers within each tile indicate the number of mABs with a statistically significant $\log_2$ fold change in that respective fraction and polysaccharide class. WSF, water-soluble fraction; CSF, CDTA-soluble fraction; NSF, Na_2CO_3-soluble fraction; KSF, KOH-soluble fraction.

changes in binding strength of hemicellulose-specific mABs were largely restricted to the ripening process, consistent with the relative lack of hemicellulose-specific CWDEs activated during infection (Figure 3.2D). For instance, although multiple mABs associated with non-fucosylated xyloglucans exhibited decreased binding strength in the WSF and CSF fractions as a result of ripening, these changes were absent from MG inoculation.

Additionally, to test if the ripening-like polysaccharide changes due to *B. cinerea* inoculation were specific to MG fruit, we performed the same glycomics analyses with inoculated RR fruit (RR I / RR H; Supplemental Figure 3.S1A). Unlike the MG inoculation, the changes due to RR inoculation correlated poorly with the ripening changes (adjusted r^2 = 0.106, Supplemental Figure 3.S1B). Accordingly, enrichment in positive $\log_2$ fold changes of RG-related categories as a result of RR inoculation was weak in contrast to MG inoculation and ripening enrichment results. With the exception that RR inoculation did result in enrichment of negative $\log_2$ fold changes in xyloglucan-related

categories, similar to ripening (Supplemental Figure 3.S1C).

3.4.4 *B. cinerea* requires two pectin degrading enzymes to promote fruit susceptibility in unripe fruit

Transcriptomic and glycomic analyses indicate that pectin degradation is triggered by *B. cinerea* infections of MG fruit as well as fruit ripening, and that expression of a diversity of host CWDEs might be responsible. However, *B. cinerea* is known to employ its own cell wall degrading enzymes during infection to facilitate host tissue breakdown. We have previously demonstrated that *B. cinerea* expression of pectin-degrading enzymes, such as PGs (GH28 family), PL/PELs (PL1, PL3 families), and PMEs (CE8 family), is especially prominent during infections of unripe tomato fruit (Petrasch et al., 2019b). To pinpoint individual genes from these families whose expression is prominent after MG inoculation and can contribute to the cell wall breakdown, we measured the expression of 17 genes known to encode *B. cinerea* pectin-degrading enzymes by quantitative PCR (qPCR) in MG fruit, RR fruit, and leaves at both 1 and 3 dpi (Figure 3.4). We included both 1 and 3 dpi timepoints as *B. cinerea* has been shown to express CWDE genes early during infection, and that the profile of expressed genes can shift by 3 dpi as the infection progresses. Furthermore, RR fruit and leaves were included to compare the expression levels of these genes in MG fruit against other tomato tissues.

Overall, the expression of these pectin-degrading genes was particularly prominent in MG fruit compared to leaves and RR fruit, emphasizing the importance of pectin degradation as an infection strategy in MG fruit (Figure 3.4). Of the 17 genes tested, four stood out as having the highest relative gene expression values in MG fruit: *BcPG1*, *BcPG2*, *BcPME1*, and *BcPME2* (Figure 3.4A-B). *BcPG1* and *BcPG2* were also higher expressed in MG fruit at 1 and/or 3 dpi compared to RR fruit or leaves. *BcPG1* and *BcPME1* are known virulence factors (ten Have et al., 1998; Valette-Collet et al., 2003), while *BcPG2* and *BcPME2* are comparatively understudied. Of these four, *BcPG2* appeared to have the most MG-specific gene expression, particularly at 3 dpi. Expression of PL/PEL genes, in contrast, were lower on average, though some (e.g. *BcPEL2*, *BcPEL3*) exhibited MG fruit-specific expression (Figure 3.4C).

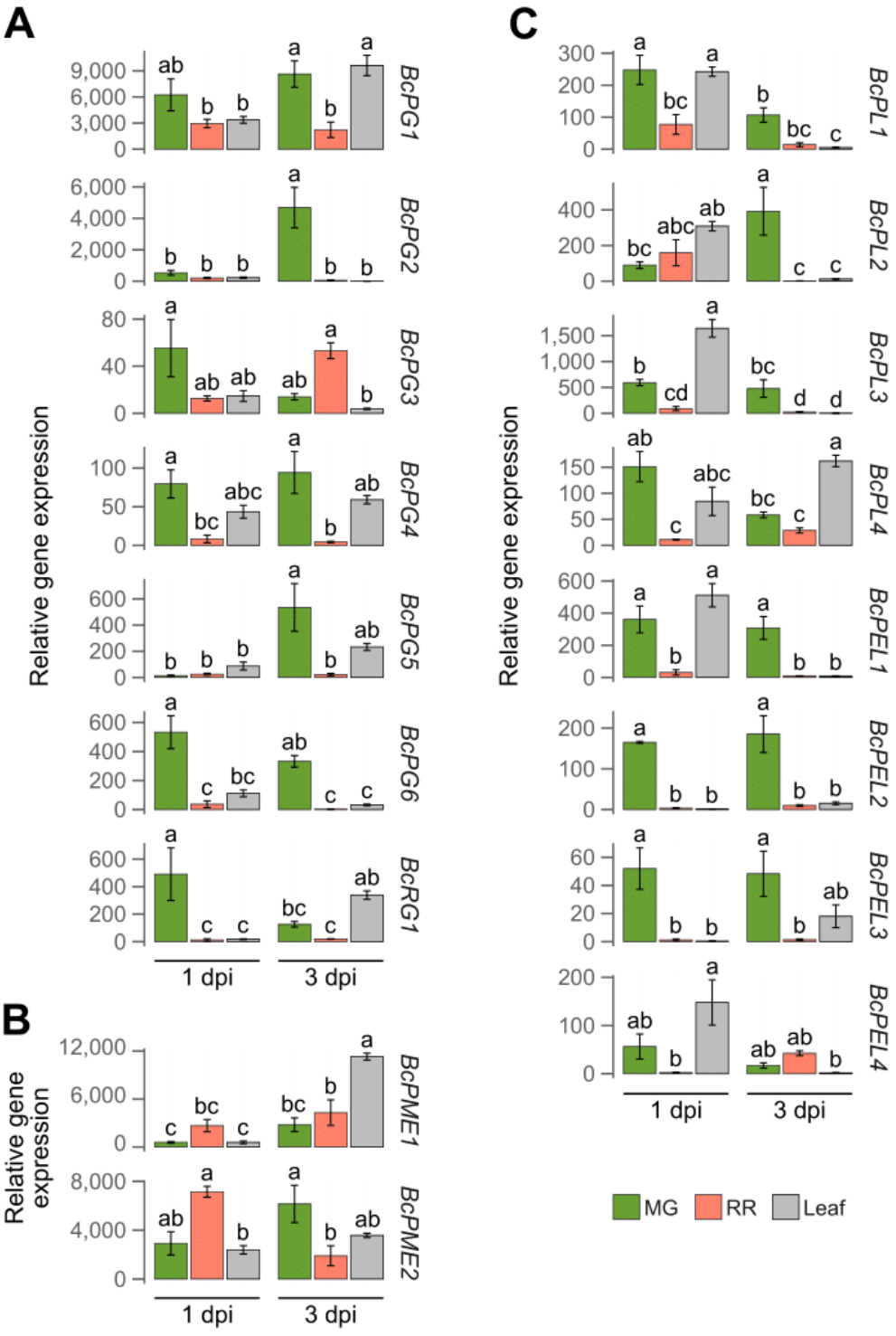

Figure 3.4: Caption presented on following page.

Figure 3.4: qPCR-based expression of selected cell wall degrading enzymes expressed by *Botrytis cinerea* during tomato infections. Names of each gene are given to the right of each graph. Letters indicate statistical differences (P <0.05) between tissues across both 1 and 3 days post-inoculation as calculated by ANOVA and Tukey's HSD test (n=4-6). (A) *Botrytis cinerea* polygacturonase (*BcPG*) and rhamnogalacturonase (*BcRG*) genes. (B) *Botrytis cinerea* pectin methylesterase (*BcPME*) genes. (C) *Botrytis cinerea* pectin lyase (*BcPL*) and pectate lyase (*BcPEL*) genes. MG, mature green; RR, red ripe; dpi, days post-inoculation.

To test the importance of *BcPG1*, *BcPG2*, *BcPME1*, and *BcPME2* after MG inoculation, we utilized two previously reported double mutant lines: *Δbcpme1Δbcpme2* and *Δbcpg1Δbcpme1*, and a newly generated *Δbcpg1Δbcpg2* line. We decided to study the double mutants instead of single ones because it is known that these CWDEs work interdependently to break down pectin and some may present functional redundancy (Kars and van Kan, 2007). We evaluated their virulence in MG fruit by measuring both disease incidence and severity each day from 3 to 6 dpi. All mutant strains except for *Δbcpg1Δbcpg2* were equally virulent as the wild-type B05.10 strain on MG fruit (Figure 3.5A). However, *Δbcpg1Δbcpg2* was completely avirulent on MG fruit, suggesting that the double knockout of these two PG genes was sufficient to prevent colonization on MG fruit. The importance of the cell wall integrity in unripe fruit to limit fungal infection is further evidenced by the fact that *Δbcpg1Δbcpg2*, as well as the other mutants, are completely capable of infecting RR fruit, which have disassembled cell walls (Figure 3.5B).

In addition to wild-type (AC) fruit, we also tested AC-*SlPG2A*, a tomato line with suppressed expression of the main ripening-associated PG (Smith et al., 1990) and the highest expressed CWDE in RR fruit (average normalized read count = 16,328.9), in order to evaluate how the loss of this host enzyme would impact pathogen establishment and growth in MG fruit. Silencing of *SlPG2A* on its own does not improve resistance to *B. cinerea* in RR fruit (Cantu et al., 2008; Silva et al., 2021), but the importance of inducing pectin degradation for MG fruit infections may reveal a greater impact for this enzyme in these tissues. Except for *Δbcpg1Δbcpg2*, which was completely avirulent on AC-*SlPG2A*

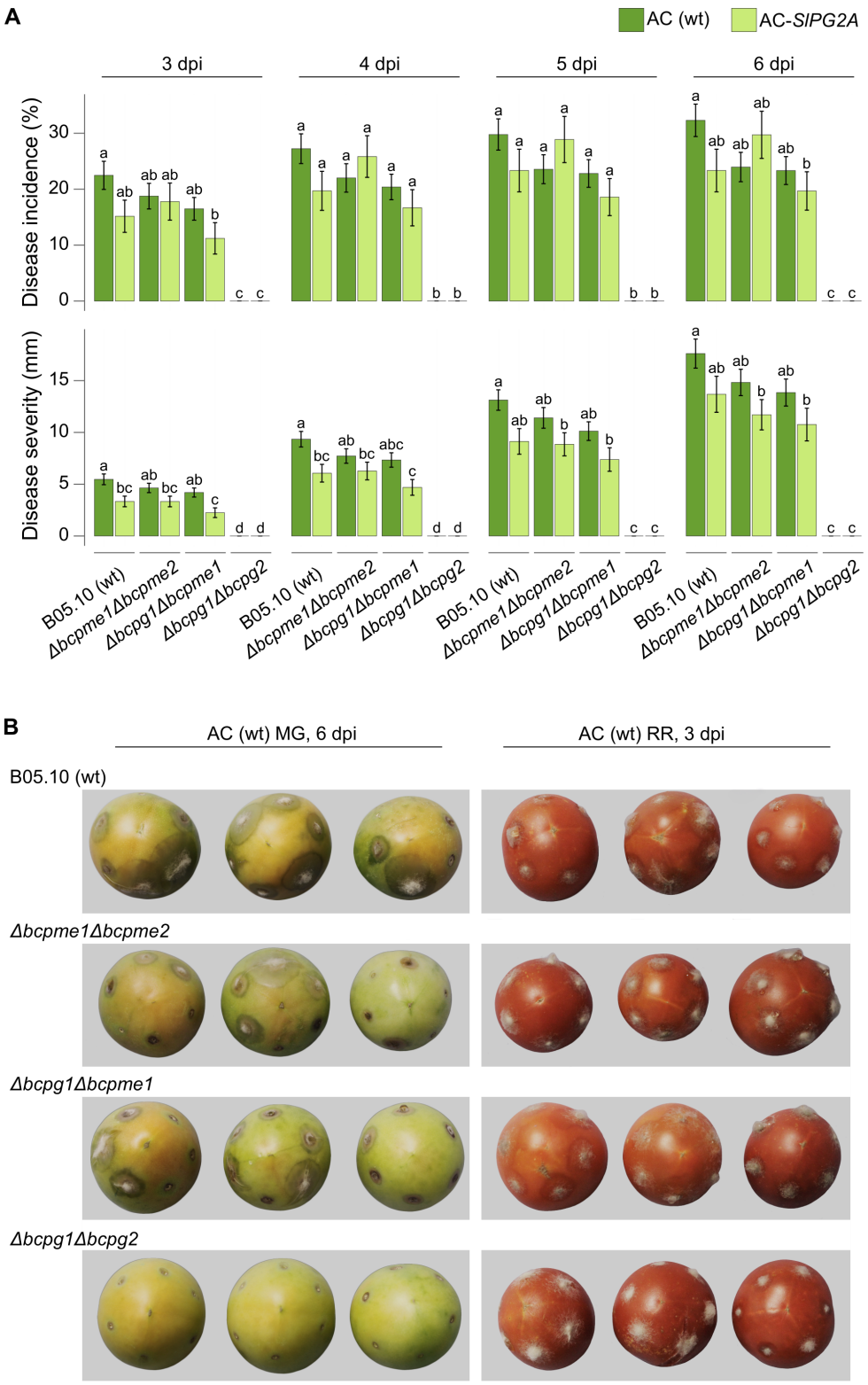

Figure 3.5: Caption presented on following page.

Figure 3.5: Disease incidence and severity of *Botrytis cinerea* double mutants in unripe fruit. (A) Measurements of disease incidence and severity in wild-type (B05.10) and double mutants on wild-type (AC) and AC-*SlPG2A* mature green (MG) fruit from 3 to 6 days post-inoculation (dpi). Letters indicate statistical differences ($P < 0.05$) between *B. cinerea* and tomato genotypes at each dpi as calculated by ANOVA and Tukey's HSD test. (B) Representative photos of inoculated wild-type MG fruit at 6 dpi (left) and wild-type red ripe (RR) fruit at 3 dpi (right).

fruit, all *B. cinerea* strains showed both reduced disease incidence and disease severity on AC-*SlPG2A* fruit compared to wild-type fruit (Figure 3.5A). This underscores that cell wall breakdown in inoculated MG fruit is the result of both host and pathogen CAZyme activity and further highlights the importance of inducing host ripening processes during infection of unripe fruit.

3.4.5 Induction of ripening by *B. cinerea* in MG fruit is dependent on *BcPG1* and *BcPG2*

If the *Δbcpg1Δbcpg2* mutant is completely avirulent on MG fruit, we expected that inoculation of MG fruit with this strain would not accelerate ripening to the same degree that the wild-type strain (B05.10) did. To test this hypothesis, we performed the same phenotypic analyses of ripening progression as above in *Δbcpg1Δbcpg2*-inoculated MG fruit and compared these to both B05.10-inoculated and mock-inoculated MG fruit (Figure 3.6). All three measurements indicate that although *Δbcpg1Δbcpg2* inoculation can accelerate ripening, it is not to the same degree as the wild-type strain. Measurements in *Δbcpg1Δbcpg2*-inoculated fruit were found to be closer to mock-inoculated than B05.10-inoculated fruit. Furthermore, the other double mutants had a similar impact on color progression compared to B05.10 (Supplemental Figure 3.S2), indicating that the loss of virulence in the *Δbcpg1Δbcpg2* mutant is responsible for the weakened ability to promote ripening.

The failure of the *Δbcpg1Δbcpg2* mutant to substantially induce ripening by 6 dpi suggests that it loses critical virulence factors for establishment and survival in MG fruit.

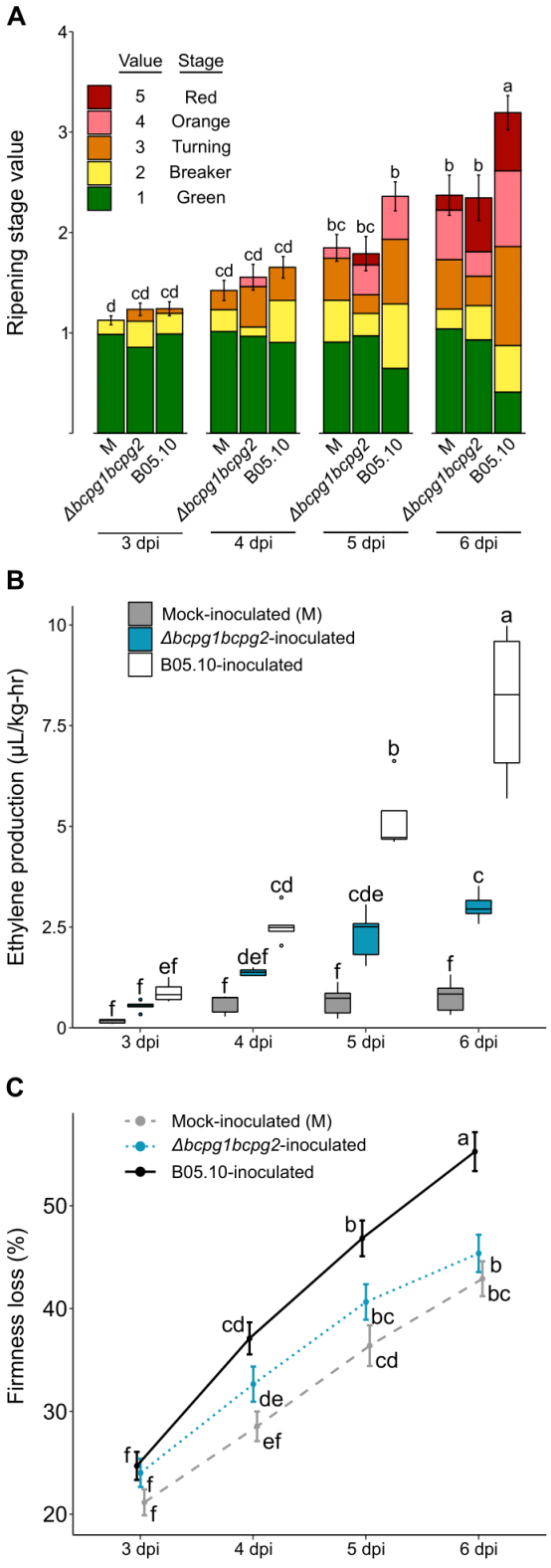

Figure 3.6: Caption presented on following page.

Figure 3.6: Ripening progression of unripe fruit inoculated with the *Botrytis cinerea* *Δbcpg1Δbcpg2* double mutant. (A) Average ripening stage value as assessed by color in mock-inoculated (M), B05.10-inoculated, and *Δbcpg1Δbcpg2*-inoculated mature green (MG) fruit (n=43-55) from 3 to 6 days post-inoculation (dpi). Colored blocks within each column represent the proportion of fruit at that respective stage. (B) Production of ethylene in M, B05.10-inoculated, and *Δbcpg1Δbcpg2*-inoculated MG fruit (n=35-37). (C) Firmness loss in M, B05.10-inoculated, and *Δbcpg1Δbcpg2*-inoculated MG fruit measured as a percentage of initial firmness at 0 dpi (n=70-216). Letters in B-D indicate the statistical differences (P <0.05) between each treatment across all dpi as calculated by ANOVA and Tukey's HSD test.

However, it is unclear whether this loss is fatal or detrimental to the pathogen, or if it is able to remain quiescent until the fruit ripens at its normal rate, and then causes disease. To identify the ultimate fate of *Δbcpg1Δbcpg2* mutants on MG fruit, we assessed disease incidence and measured fungal biomass in *Δbcpg1Δbcpg2*-inoculated fruit up to 20 dpi, well after the fruit reached the RR stage through normal ripening. These measurements revealed that *Δbcpg1Δbcpg2* never fully recovered from its failure to substantially accelerate ripening, reaching a biomass at 20 dpi approximately only twice as great as its biomass at 3 dpi (Table 3.3) and there was no lesion development in any of the inoculated tomatoes. In contrast, when RR fruit were inoculated with *Δbcpg1Δbcpg2* directly, the pathogen grew rapidly, and biomass at 3 dpi was nearly 350 times greater than the biomass at 20 dpi from inoculated MG fruit. Altogether, these results suggest that induction of ripening in MG fruit is a critical survival and infection strategy of *B. cinerea*, and the *BcPG1* and *BcPG2* are necessary for this strategy.

3.5 Discussion

3.5.1 Acceleration of tomato fruit ripening as a fungal infection strategy

Postharvest fruit-pathogen interactions are a unique and economically important field of research for combatting food loss. A complete picture of ripening-associated susceptibility

is only just developing, but the tomato-*B. cinerea* pathosystem has been used successfully as a model system for the identification of infection strategies, host responses, and specific features of ripening that lead to increased susceptibility (Blanco-Ulate et al., 2016a; Cantu et al., 2009, 2008; Petrasch et al., 2019b; Silva et al., 2021). Most recently, we provided evidence for the importance of the accumulation of host susceptibility factors during ripening that shifts the fruit towards a more favorable environment for disease (Silva et al., 2021). The enormous benefit of ripening to infection success presents the opportunity for the evolution of an infection strategy that actively accelerates this process during quiescent infections of unripe fruit.

Such an infection strategy would suggest manipulation of host gene expression by the pathogen. *B. cinerea* has been shown to be capable of this in both vegetative and fruit tissues. To promote senescence, *B. cinerea* infection induces expression of genes associated with programmed cell death in both tomato (Hoeberichts et al., 2003) and Arabidopsis leaves (Swartzberg et al., 2008). *B. cinerea* also actively suppresses host defense genes in both tomato and Arabidopsis through the production of small RNAs (Weiberg et al., 2013). In *B. cinerea*-inoculated unripe tomato fruit, previous microarray experiments have revealed upregulation of a small selection of ripening genes, including the ethylene biosynthesis genes *SlACS2* and *SlACS4*, the CWDEs *SlPG2A* and *SlEXP1*, and several others (Cantu et al., 2008). Thus, induction of ripening processes by *B. cinerea* to promote

Table 3.3: Fungal biomass of *Δbcpg1Δbcpg2*-inoculated fruit.

Stage at Inoculation	dpi	Biomass
MG	3	22.1 (b)
	6	29.4 (ab)
	10	50.6 (a)
	15	30.1 (ab)
	20	43.3 (ab)
RR	3	14,951.6

Letters indicate statistical differences (P <0.05) between each dpi among the MG fruit as calculated by ANOVA and Tukey's HSD test.

susceptibility is plausible.

Physiological measurements of color progression, ethylene production, and fruit softening, all hallmarks of climacteric fruit ripening, confirm the ability of *B. cinerea* to accelerate ripening in unripe tomato fruit (Figure 3.1). While unripe fruit are resistant up to 3 dpi, the ripening acceleration that occurs after this point coincides with the onset of disease symptoms as *B. cinerea* emerges from quiescence and into its necrotrophic phase on these increasingly susceptible fruit. Additionally, RNA data at 1 and 3 dpi support the activation of both ethylene biosynthesis and cell wall degradation, but not lycopene biosynthesis as a result of *B. cinerea* inoculation. The lack of carotenoid biosynthesis upregulation by *B. cinerea* is puzzling, but it is possible that *B. cinerea*-triggered downregulation of photosynthesis prompts chloroplast-to-chromoplast conversion, which, together with the already fairly high baseline expression of *SlPSY1* in MG fruit at 3 dpi may allow for increased carotenoid biosynthesis in the absence of upregulation of carotenoid biosynthesis genes.

B. cinerea inoculation of MG fruit at 1 and 3 dpi does not accelerate the expression of all known ripening-related genes. This is supported by the fact that we did not detect the upregulation of *SlACS2* (*Solyc02g068490*; Supplemental Table S1 at `https://ucdavis.box.com/s/yp72rney9f6sl5nqfdz17lagmsjt2f86`), *SlPG2A* (*Solyc10g080210*), and *SlPL* (*Solyc03g111690*; Figure 3.2), which are well-known for their involvement in ripening. Additionally, *B. cinerea* inoculation did not result in upregulation of the ripening-promoting transcription factors *SlRIN* (*Solyc05g012020*), *SlNOR* (*Solyc10g006880*), *SlCNR* (*Solyc02g077920*), or *SlTAGL1* (*Solyc07g055920*; Supplemental Table S1 at `https://ucdavis.box.com/s/yp72rney9f6sl5nqfdz17lagmsjt2f86`). However, it is possible that these genes as well as other ripening-related processes are triggered by inoculation at a different timepoint than those evaluated, as the accelerated ethylene biosynthesis will inevitably activate most ripening processes.

Ethylene is the most important hormone involved in the ripening of climacteric fruit. Ethylene biosynthesis during fruit ripening is classically described as featuring two systems. In System 1, unripe fruit exhibit auto-inhibitory biosynthesis that maintains the

hormone at low levels. At the onset of ripening, fruit experience a burst of ethylene production and transition to autocatalytic biosynthesis, or System 2 (Pech et al., 2012). In addition, ethylene also plays a role in plant defense against pathogens, though it can promote either resistance or disease depending on the pathosystem (van der Ent and Pieterse, 2012). In unripe tomato fruit, System 1 ethylene biosynthesis may facilitate resistance to *B. cinerea* up to 3 dpi, while System 2 biosynthesis accelerates ripening and promotes disease (Blanco-Ulate et al., 2013). The rate of increased ethylene biosynthesis observed in *B. cinerea*-inoculated unripe fruit after 3 dpi suggests that *B. cinerea* pushes the fruit into System 2 prematurely (Figure 3.1C). This is supported by the upregulation of two System 2 genes, *SlACS2* and *SlACO4*, in response to *B. cinerea* inoculation of unripe fruit.

3.5.2 *B. cinerea* hijacks the host cell wall degrading machinery to facilitate fruit colonization

B. cinerea inoculation of MG fruit also results in upregulation of 34 different host CWDEs, which together with enzymes secreted by *B. cinerea* are likely responsible for the accelerated rate of softening in these fruit. In particular, the mass upregulation of host PMEs may be critical, as these enzymes are thought to facilitate further degradation by other enzyme classes (Jolie et al., 2010). Cell wall breakdown during fruit ripening facilitates disease, as loss of cell wall integrity allows for easy colonization by fungi and removes important signaling components for pathogen defense (Blanco-Ulate et al., 2016b; Cantu et al., 2008; Prusky et al., 2013). Silencing of host CWDEs, particularly *SlPL*, reduces susceptibility to *B. cinerea* in ripe fruit (Cantu et al., 2008; Silva et al., 2021). Thus, *B. cinerea* relies on host CWDEs to promote infection. This is further evidenced here by the reduced virulence of wild-type and mutant *B. cinerea* strains in MG fruit of the AC-*SlPG2A* mutant, which has silenced expression of *SlPG2A*, an important CWDE with extremely high expression levels in ripening fruit (Silva et al., 2021).

In addition to physiological and gene expression evidence, we provide novel insight into cell wall composition during unripe fruit infection through an ELISA-based glycomics analysis (Pattathil et al., 2010). This approach provides a high-resolution view of

the effects of both ripening and infection on cell wall composition. Fruit cell walls are rich in pectin, a heterogeneous polysaccharide that can be further categorized into homogalacturonan (HG), rhamnogalacturonan I (RG I), and rhamnogalacturonan II (RG II). HG and RG II are characterized by a backbone of galacturonic acid (GalA) residues, while RG I backbones contain a disaccharide repeat of GalA and rhamnose. In HG, the GalA residues may be acetylated, methylesterified, or xylosated, affecting its binding properties as well as accessibility to CWDEs. RG I backbones are decorated with arabinan, arabinogalactan, galactan, and xylan side chains, while RG II features complex side chains that form cross-linked dimers through borate diesters (Höfte and Voxeur, 2017). Fruit softening is the result of the activity of various classes of enzymes which actively break down these pectin structures as well as hemicellulose structures (Brummell, 2006; Wang et al., 2018). PMEs remove the methylester groups from HG GalA residues, loosening the pectin network and increasing accessibility of HG to PGs and PLs, which hydrolyze the GalA backbone (Jolie et al., 2010). The side chains of RG I can be broken down by galactosidases, arabinosidases, and xylosidases (Brummell, 2006). In the hemicellulose network, the XyG-cellulose connections are weakened by expansins, and XyG molecules are depolymerized by xyloglucanases (Brummell, 2006).

The changes in the cell wall structure as a result of MG inoculation were remarkably similar to those that occur during ripening, particularly among the pectin polysaccharides (Figure 3.3). Increased binding signals of RG I and its subcomponents in several fractions in both MG inoculation and ripening indicate increased accessibility to these molecules, perhaps due to loosening of the network through PMEs and/or degradation of side chains by various enzymes. The lack of substantial hemicellulose remodeling as a result of MG inoculation underscores the special importance of the pectin network in mediating protection against *B. cinerea*. Interestingly, though the changes in cell wall structure as a result of RR infection were much less similar to the ripening changes, they were more similar in regards to the decreased signals of xyloglucans (Supplemental Figure 3.S1). This may suggest that the hemicellulose network is a secondary target for degradation by *B. cinerea* that receives focus after pectin has already been broken down. Previous research has also

shown that expression of xyloglucanases by *B. cinerea* as well as two other pathogens, *Rhizopus stolonifer* and *Fusarium acuminatum*, appears more prevalent in infections of RR fruit than MG fruit (Petrasch et al., 2019b).

3.5.3 Successful establishment of *B. cinerea* in unripe fruit is dependent on its ability to degrade pectin

The importance of pectin degradation in MG fruit infections is a critical narrative emerging from the *B. cinerea*-tomato pathosystem. Multiple pectin-degrading enzymes are expressed at high levels in MG fruit, and expression of these genes as a whole is greater in MG fruit compared to RR fruit and leaves (Figure 3.4). While *BcPG1* and *BcPME1* are known to be important virulence factors, only the combination of *BcPG1* and *BcPG2* being silenced resulted in complete avirulence on MG fruit (Figure 3.5), even up to 20 dpi after the fruit has fully ripened, despite the fact that *Δbcpg1Δbcpg2* mutants are capable of causing disease on ripe fruit (Table 3.2). Critically, infections of MG fruit by *Δbcpg1Δbcpg2* do not appear to accelerate ripening processes to nearly the same degree as wild-type *B. cinerea* (Figure 3.6). These findings lead to two possible hypotheses. In the first possibility, this establishment is required before *B. cinerea* can actively accelerate ripening through the secretion of unknown virulence factors. In the second possibility, the host does not detect the pathogen in the absence of a quiescent infection, and the lack of a defense response, perhaps mediated by ethylene, results in no trigger for early ripening. In both cases, *BcPG1* and *BcPG2* are necessary for early establishment of a quiescent infection in MG fruit. Though these hypotheses are not mutually exclusive, they differ in the amount of agency assigned to *B. cinerea* and its infection strategy. Given previous demonstrations of *B. cinerea* actively manipulating host gene expression (Weiberg et al., 2013), we believe the first hypothesis to be quite plausible.

These physiological, gene expression, and glycomics data all demonstrate the ability for *B. cinerea* to induce ripening in MG fruit as a strategy to emerge from quiescence and cause disease. The similarities in the changes in cell wall composition between MG inoculation and ripening is likely due to the activity of both pathogen and host enzymes. Lastly, the induction of ripening is dependent on the ability of *B. cinerea* to establish

in unripe tissues even before causing lesion development. The pectin degrading enzymes *BcPG1* and *BcPG2* are key virulence factors as they are both critical for successful infection of MG fruit. This research expands the understanding of pectin degradation in the *B. cinerea*-tomato pathosystem by suggesting that its importance goes beyond simply opening cell walls for colonization but also might trigger a cascade of ripening activity that causes the host to make itself more susceptible. This new dynamic may further guide identification of possible ripening-promoting virulence factors in *B. cinerea* and perhaps other postharvest fruit pathogens and ultimately improve our understanding of ripening-related susceptibility.

References

Adaskaveg, J. A., Silva, C. J., Huang, P., and Blanco-Ulate, B. (2021). Single and Double Mutations in Tomato Ripening Transcription Factors Have Distinct Effects on Fruit Development and Quality Traits. *Frontiers in Plant Science*, 12:647035.

Adaskaveg, J. E., Förster, H., and Thompson, D. F. (2000). Identification and Etiology of Visible Quiescent Infections of *Monilinia fructicola* and *Botrytis cinerea* in Sweet Cherry Fruit. *Plant Disease*, 84(3):328–333.

Akiyama, R., Nakayasu, M., Umemoto, N., Kato, J., Kobayashi, M., Lee, H. J., Sugimoto, Y., Iijima, Y., Saito, K., Muranaka, T., and Mizutani, M. (2021). Tomato E8 Encodes a C-27 Hydroxylase in Metabolic Detoxification of α-Tomatine during Fruit Ripening. *Plant and Cell Physiology*.

Alkan, N. and Fortes, A. M. (2015). Insights into molecular and metabolic events associated with fruit response to post-harvest fungal pathogens. *Frontiers in Plant Science*, 6:889.

Alkan, N., Friedlander, G., Ment, D., Prusky, D., and Fluhr, R. (2015). Simultaneous transcriptome analysis of *Colletotrichum gloeosporioides* and tomato fruit pathosystem reveals novel fungal pathogenicity and fruit defense strategies. *New Phytologist*, 205(2):801–815.

Balsells-Llauradó, M., Silva, C. J., Usall, J., Vall-llaura, N., Serrano-Prieto, S., Teixidó, N., Mesquida-Pesci, S. D., de Cal, A., Blanco-Ulate, B., and Torres, R. (2020). Depicting the battle between nectarine and *Monilinia laxa*: the fruit developmental stage dictates the effectiveness of the host defenses and the pathogen's infection strategies. *Horticulture Research*, 7(1).

Benjamini, Y. and Hochberg, Y. (1995). Controlling the false discovery rate: A practical and powerful approach to multiple testing. *Journal of the Royal Statistical Society. Series B (Methodological)*, 57(1):289–300.

Blanco-Ulate, B., Amrine, K. C. H., Collins, T. S., Rivero, R. M., Vicente, A. R., Morales-Cruz, A., Doyle, C. L., Ye, Z., Allen, G., Heymann, H., Ebeler, S. E., and Cantu, D. (2015). Developmental and Metabolic Plasticity of White-Skinned Grape Berries in Response to *Botrytis cinerea* during Noble Rot. *Plant Physiology*, 169(4):2422–43.

Blanco-Ulate, B., Labavitch, J. M., Vincenti, E., Powell, A. L. T., and Cantu, D. (2016a). Hitting the wall: Plant cell walls during *Botrytis cinerea* infections. In *Botrytis - The Fungus, the Pathogen and its Management in Agricultural Systems*, pages 361–386. Springer International Publishing, Cham.

Blanco-Ulate, B., Vincenti, E., Cantu, D., and Powell, A. L. T. (2016b). *Ripening of tomato fruit and susceptibility to Botrytis cinerea.* Springer, Dordrecht, The Netherlands.

Blanco-Ulate, B., Vincenti, E., Powell, A. L. T., and Cantu, D. (2013). Tomato transcriptome and mutant analyses suggest a role for plant stress hormones in the interaction between fruit and *Botrytis cinerea*. *Frontiers in Plant Science*, 4:142.

Blumenkrantz, N. and Asboe-Hansen, G. (1973). New method for quantitative determination of uronic acids. *Analytical Biochemistry*, 54(2):484–489.

Bolger, A. M., Lohse, M., and Usadel, B. (2014). Trimmomatic: a flexible trimmer for Illumina sequence data. *Bioinformatics*, 30(15):2114–2120.

Brummell, D. A. (2006). Cell wall disassembly in ripening fruit. *Functional Plant Biology*, 33(2):103–119.

Brummell, D. A. and Harpster, M. H. (2001). Cell wall metabolism in fruit softening and quality and its manipulation in transgenic plants. *Plant Molecular Biology*, 47(1):311–339.

Cantu, D., Blanco-Ulate, B., Yang, L., Labavitch, J. M., Bennett, A. B., and Powell, A. L. T. (2009). Ripening-regulated susceptibility of tomato fruit to *Botrytis cinerea* requires NOR but not RIN or ethylene. *Plant Physiology*, 150(3):1434–1449.

Cantu, D., Vicente, A. R., Greve, L. C., Dewey, F. M., Bennett, A. B., Labavitch, J. M., and Powell, A. L. T. (2008). The intersection between cell wall disassembly, ripening, and fruit susceptibility to *Botrytis cinerea*. *Proceedings of the National Academy of Sciences of the United States of America*, 105(3):859–64.

Guidarelli, M., Carbone, F., Mourgues, F., Perrotta, G., Rosati, C., Bertolini, P., and Baraldi, E. (2011). Colletotrichum acutatum interactions with unripe and ripe strawberry fruits and differential responses at histological and transcriptional levels. *Plant Pathology*, 60(4):685–697.

Häffner, E., Konietzki, S., and Diederichsen, E. (2015). *Keeping control: The role of senescence and development in plant pathogenesis and defense*, volume 4.

Haile, Z. M., Malacarne, G., Pilati, S., Sonego, P., Moretto, M., Masuero, D., Vrhovsek, U., Engelen, K., Baraldi, E., and Moser, C. (2020). Dual Transcriptome and Metabolic Analysis of Vitis vinifera cv. Pinot Noir Berry and *Botrytis cinerea* During Quiescence and Egressed Infection. *Frontiers in Plant Science*, 10:1704.

Hoeberichts, F. A., ten Have, A., and Woltering, E. J. (2003). A tomato metacaspase gene is upregulated during programmed cell death in *Botrytis cinerea*-infected leaves. *Planta*, 217(3):517–522.

Höfte, H. and Voxeur, A. (2017). Plant cell walls. *Current Biology*, 27(17):R865–R870.

Jolie, R. P., Duvetter, T., Van Loey, A. M., and Hendrickx, M. E. (2010). Pectin methylesterase and its proteinaceous inhibitor: a review. *Carbohydrate Research*, 345(18):2583–2595.

Kars, I., Krooshof, G. H., Wagemakers, L., Joosten, R., Benen, J. A. E., and Van Kan, J. A. L. (2005a). Necrotizing activity of five *Botrytis cinerea* endopolygalacturonases produced in Pichia pastoris. *The Plant Journal*, 43(2):213–225.

Kars, I., McCalman, M., Wagemakers, L., and van Kan, J. A. L. (2005b). Functional analysis of *Botrytis cinerea* pectin methylesterase genes by PCR-based targeted mutagenesis: Bcpme1 and Bcpme2 are dispensable for virulence of strain B05.10. *Molecular Plant Pathology*, 6(6):641–652.

Kars, I. and van Kan, J. A. L. (2007). Extracellular Enzymes and Metabolites Involved in Pathogenesis of Botrytis BT - Botrytis: Biology, Pathology and Control. pages 99–118. Springer Netherlands, Dordrecht.

Langmead, B. and Salzberg, S. L. (2012). Fast gapped-read alignment with Bowtie 2. *Nature Methods*, 9(4):357–359.

Lassois, L., Haïssam Jijakli, M., and Chillet, M. (2010). Crown rot of bananas: preharvest factors involved in postharvest disease development and integrated control methods. *Plant Disease*, 94(6):648–658.

Liu, M., Pirrello, J., Chervin, C., Roustan, J.-P., and Bouzayen, M. (2015). Ethylene Control of Fruit Ripening: Revisiting the Complex Network of Transcriptional Regulation. *Plant Physiology*, 169(4):2380–90.

Love, M. I., Huber, W., and Anders, S. (2014). Moderated estimation of fold change and dispersion for RNA-seq data with DESeq2. *Genome Biology*, 15:550.

Lü, P., Yu, S., Zhu, N., Chen, Y.-R., Zhou, B., Pan, Y., Tzeng, D., Fabi, J. P., Argyris, J., Garcia-Mas, J., Ye, N., Zhang, J., Grierson, D., Xiang, J., Fei, Z., Giovannoni, J. J.,

and Zhong, S. (2018). Genome encode analyses reveal the basis of convergent evolution of fleshy fruit ripening. *Nature Plants*, 4(10):784–791.

Manteau, S., Abouna, S., Lambert, B., and Legendre, L. (2003). Differential regulation by ambient pH of putative virulence factor secretion by the phytopathogenic fungus *Botrytis cinerea*. *FEMS Microbiology Ecology*, 43(3):359–366.

Meyer, U. M., Spotts, R. A., and Dewey, F. M. (2000). Detection and Quantification of *Botrytis cinerea* by ELISA in Pear Stems During Cold Storage. *Plant Disease*, 84(10):1099–1103.

Moriya, Y., Itoh, M., Okuda, S., Yoshizawa, A. C., and Kanehisa, M. (2007). KAAS: an automatic genome annotation and pathway reconstruction server. *Nucleic Acids Research*, 35(Web Server):W182–W185.

Pattathil, S., Avci, U., Baldwin, D., Swennes, A. G., McGill, J. A., Popper, Z., Bootten, T., Albert, A., Davis, R. H., Chennareddy, C., Dong, R., O'Shea, B., Rossi, R., Leoff, C., Freshour, G., Narra, R., O'Neil, M., York, W. S., and Hahn, M. G. (2010). A comprehensive toolkit of plant cell wall glycan-directed monoclonal antibodies. *Plant Physiology*, 153(2):514–25.

Pech, J.-C., Purgatto, E., Bouzayen, M., and Latché, A. (2012). Ethylene and Fruit Ripening. *Annual Plant Reviews*, 44:275–304.

Peña-Cortés, H., Barrios, P., Dorta, F., Polanco, V., Sánchez, C., Sánchez, E., and Ramírez, I. (2004). Involvement of Jasmonic Acid and Derivatives in Plant Response to Pathogen and Insects and in Fruit Ripening. *Journal of Plant Growth Regulation*, 23(3):246–260.

Petrasch, S., Knapp, S. J., van Kan, J. A. L., and Blanco-Ulate, B. (2019a). Grey mould of strawberry, a devastating disease caused by the ubiquitous necrotrophic fungal pathogen *Botrytis cinerea*. *Molecular Plant Pathology*, 20(6):877–892.

Petrasch, S., Silva, C. J., Mesquida-Pesci, S. D., Gallegos, K., van den Abeele, C., Papin, V., Fernandez-Acero, F. J., Knapp, S. J., and Blanco-Ulate, B. (2019b). Infection Strategies Deployed by *Botrytis cinerea*, *Fusarium acuminatum*, and *Rhizopus stolonifer* as a Function of Tomato Fruit Ripening Stage. *Frontiers in Plant Science*, 10:223.

Prusky, D. (1996). Pathogen Quiescence in Postharvest Diseases. *Annual Review of Phytopathology*, 34(1):413–434.

Prusky, D., Alkan, N., Mengiste, T., and Fluhr, R. (2013). Quiescent and Necrotrophic Lifestyle Choice During Postharvest Disease Development. *Annual Review of Phytopathology*, 51(1):155–176.

Reca, I. B., Lionetti, V., Camardella, L., D'Avino, R., Giardina, T., Cervone, F., and Bellincampi, D. (2012). A functional pectin methylesterase inhibitor protein (SolyPMEI) is expressed during tomato fruit ripening and interacts with PME-1. *Plant Molecular Biology*, 79(4):429–442.

Redgwell, R. J., Fischer, M., Kendal, E., and MacRae, E. A. (1997). Galactose loss and fruit ripening: high-molecular-weight arabinogalactans in the pectic polysaccharides of fruit cell walls. *Planta*, 203(2):174–181.

Scheller, H. V. and Ulvskov, P. (2010). Hemicelluloses. *Annual Review of Plant Biology*, 61(1):263–289.

Silva, C. J., van den Abeele, C., Ortega-Salazar, I., Papin, V., Adaskaveg, J. A., Wang, D., Casteel, C. L., Seymour, G. B., and Blanco-Ulate, B. (2021). Host susceptibility factors render ripe tomato fruit vulnerable to fungal disease despite active immune responses. *Journal of Experimental Botany*, 72(7):2696–2709.

Smith, C. J., Watson, C. F., Morris, P. C., Bird, C. R., Seymour, G. B., Gray, J. E., Arnold, C., Tucker, G. A., Schuch, W., and Harding, S. (1990). Inheritance and effect on ripening of antisense polygalacturonase genes in transgenic tomatoes. *Plant Molecular Biology*, 14(3):369–79.

Swartzberg, D., Kirshner, B., Rav-David, D., Elad, Y., and Granot, D. (2008). *Botrytis cinerea* induces senescence and is inhibited by autoregulated expression of the IPT gene. *European Journal of Plant Pathology*, 120(3):289–297.

ten Have, A., Mulder, W., Visser, J., and van Kan, J. A. (1998). The endopolygalacturonase gene Bcpg1 is required for full virulence of *Botrytis cinerea*. *Molecular Plant-Microbe Interactions*, 11(10):1009–1016.

Valette-Collet, O., Cimerman, A., Reignault, P., Levis, C., and Boccara, M. (2003). Disruption of *Botrytis cinerea* pectin methylesterase gene Bcpme1 reduces virulence on several host plants. *Molecular plant-microbe interactions : MPMI*, 16(4):360–367.

van der Ent, S. and Pieterse, C. M. J. (2012). Ethylene: Multi-Tasker in Plant-Attacker Interactions. In *Annual Plant Reviews*, volume 44, pages 343–377. Wiley-Blackwell, Oxford, UK.

Vicente, A. R., Saladié, M., Rose, J. K. C., and Labavitch, J. M. (2007). The linkage between cell wall metabolism and fruit softening: looking to the future. *Journal of the Science of Food and Agriculture*, 87:1435–1448.

Voragen, A. G. J., Coenen, G.-J., Verhoef, R. P., and Schols, H. A. (2009). Pectin, a versatile polysaccharide present in plant cell walls. *Structural Chemistry*, 20(2):263.

Wang, D., Yeats, T. H., Uluisik, S., Rose, J. K. C., and Seymour, G. B. (2018). Fruit Softening: Revisiting the Role of Pectin. *Trends in Plant Science*, 23(4):302–310.

Weiberg, A., Wang, M., Lin, F.-M., Zhao, H., Zhang, Z., Kaloshian, I., Huang, H.-D., and Jin, H. (2013). Fungal Small RNAs Suppress Plant Immunity by Hijacking Host RNA Interference Pathways. *Science*, 342(6154):118–123.

Yemm, E. W. and Willis, A. J. (1954). The estimation of carbohydrates in plant extracts by anthrone. *The Biochemical Journal*, 57(3):508–514.

Zhang, H., Yohe, T., Huang, L., Entwistle, S., Wu, P., Yang, Z., Busk, P. K., Xu, Y., and Yin, Y. (2018). dbCAN2: a meta server for automated carbohydrate-active enzyme annotation. *Nucleic Acids Research*, 46(W1):W95–W101.

Zhang, L. and van Kan, J. A. L. (2013). *Botrytis cinerea* mutants deficient in d-galacturonic acid catabolism have a perturbed virulence on Nicotiana benthamiana and Arabidopsis, but not on tomato. *Molecular Plant Pathology*, 14(1):19–29.

Zhu, X., Pattathil, S., Mazumder, K., Brehm, A., Hahn, M. G., Dinesh-Kumar, S. P., and Joshi, C. P. (2010). Virus-Induced Gene Silencing Offers a Functional Genomics Platform for Studying Plant Cell Wall Formation. *Molecular Plant*, 3(5):818–833.

3.6 Supplemental Material

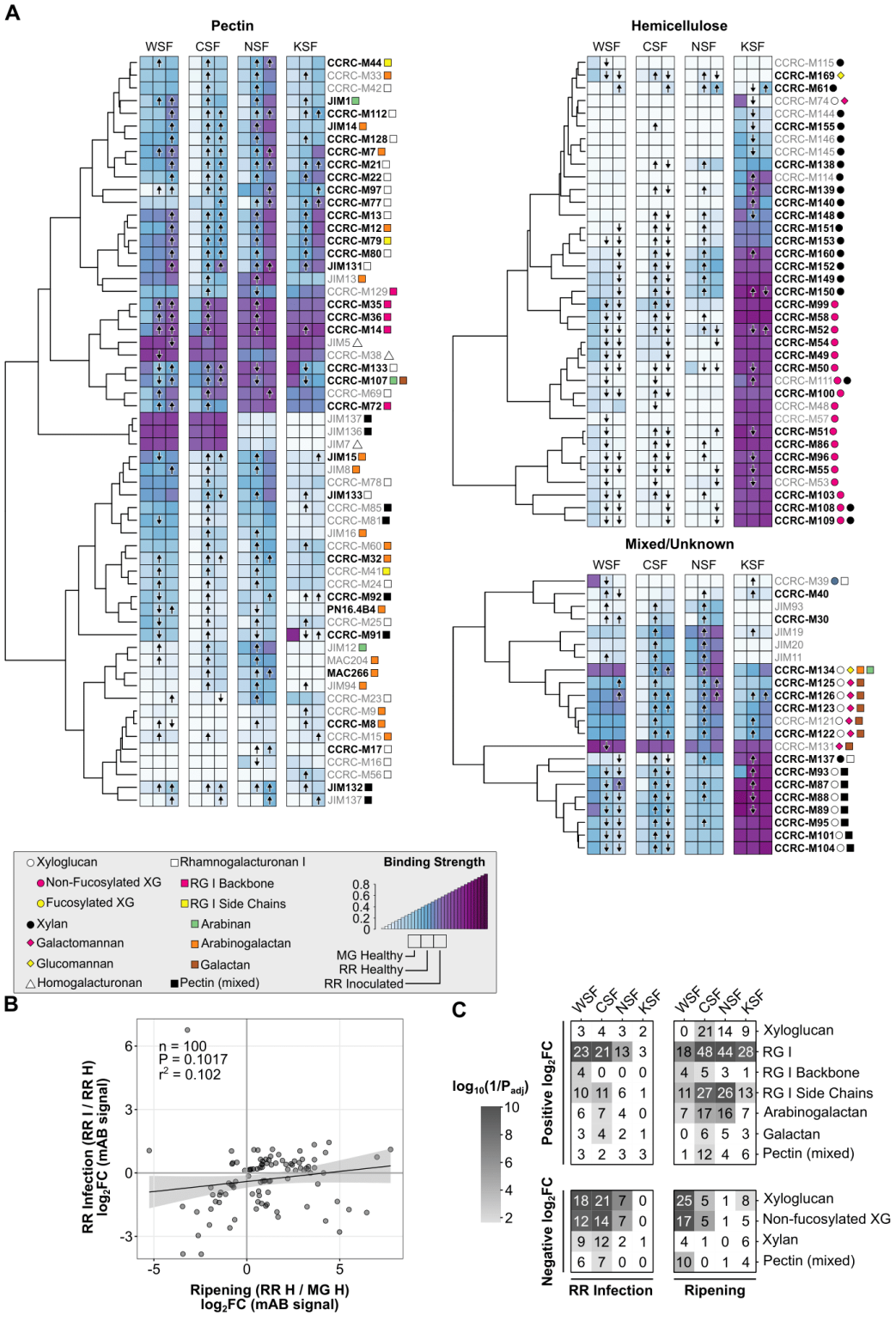

Figure 3.S1: Caption presented on following page.

Figure 3.S1: Heatmaps of monoclonal antibody (mAB) binding strength in healthy MG, healthy RR, and *B. cinerea*-inoculated RR fruit for polysaccharide-binding antibodies. mAB codes are given to the right of each heatmap row, with the recognized classes of cell wall polysaccharides indicated by colored shapes according to the given key. mAB listed in boldtype are those included in the scatterplot in panel B. Arrows within heatmap tiles indicate statistically significant (P_{adj} <0.05) increasing or decreasing antibody strength when compared via t-test to values in healthy RR fruit. (B) Scatterplot and linear regression model of $\log_2$ fold change ($\log_2$FC) values of mAB signals in the ripening (healthy RR / healthy MG) and RR infection (*B.cinerea*-inoculated RR / healthy RR) comparisons. (C) Enrichment of polysaccharide classes with statistically significant positive or negative $\log_2$ fold changes in each cell wall fraction for the ripening and RR infection comparisons. Numbers within each tile indicate the number of mABs with a statistically significant $\log_2$ fold change in that respective fraction and polysaccharide class. WSF, water-soluble fraction; CSF, CDTA-soluble fraction; NSF, Na_2CO_3-soluble fraction; KSF, KOH-soluble fraction.

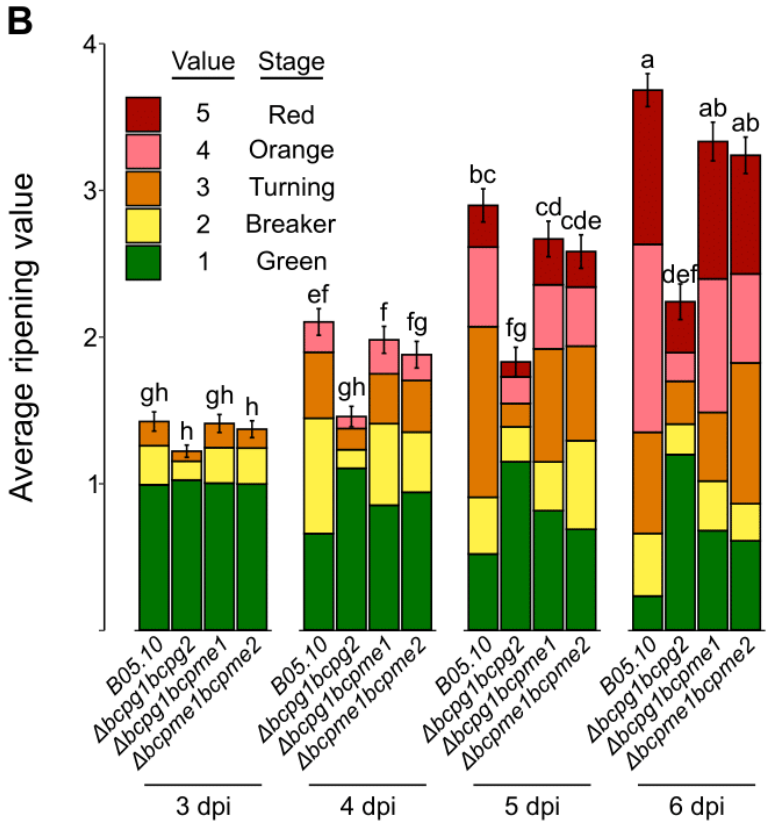

Figure 3.S2: Color progression in *Botrytis cinerea* mutant-inoculated MG fruit. Average ripening stage value as assessed by color in B05.10-, *Δbcpg1Δbcpg2*-, *Δbcpg1bcpme1*-, and *Δbcpme1bcpme2*-inoculated MG fruit (n=70-128). Colored blocks within each column represent the proportion of fruit at that respective stage. Letters indicate statistical differences (P <0.05) between each treatment across all dpi as calculated by ANOVA and Tukey's HSD test.

Chapter 4

Depicting the battle between nectarine and *Monilinia laxa*: the fruit developmental stage dictates the effectiveness of the host defenses and the pathogen's infection strategies

4.1 Publication Statement

The content of this chapter was peer-reviewed and published as follows:

Balsells-Llauradó, M., Silva, C. J., Usall, J., Vall-llaura, N., Serrano-Prieto, S., Teixidó, N., Mesquida-Pesci, S. D., de Cal, A., Blanco-Ulate, B., and Torres, R. (2020). Depicting the battle between nectarine and *Monilinia laxa*: the fruit developmental stage dictates the effectiveness of the host defenses and the pathogen's infection strategies. *Horticulture Research*, 7(1).

For this publication, I performed all bioinformatics and statistical analyses and contributed substantially to the writing of the manuscript, including the construction and interpretation of Figures 3, 4a-b, and 5.

4.2 Abstract

Infections by the fungus *Monilinia laxa*, the main cause of brown rot in Europe, result in considerable losses of stone fruit. Herein, we present a comprehensive transcriptomic approach to unravel strategies deployed by nectarine fruit and *M. laxa* during their interaction. We used *M. laxa*-inoculated immature and mature fruit, which was resistant and susceptible to brown rot, respectively, to perform a dual RNA-Seq analysis. In im-

mature fruit, host responses, pathogen biomass, and pathogen transcriptional activity peaked at 14–24 h post inoculation (hpi), at which point *M. laxa* appeared to switch its transcriptional response to either quiescence or death. Mature fruit experienced an exponential increase in host and pathogen activity beginning at 6 hpi. Functional analyses in both host and pathogen highlighted differences in stage-dependent strategies. For example, in immature fruit, *M. laxa* unsuccessfully employed carbohydrate-active enzymes (CAZymes) for penetration, which the fruit was able to combat with tightly regulated hormone responses and an oxidative burst that challenged the pathogen's survival at later time points. In contrast, in mature fruit, *M. laxa* was more dependent on proteolytic effectors than CAZymes, and was able to invest in filamentous growth early during the interaction. Hormone analyses of mature fruit infected with *M. laxa* indicated that, while jasmonic acid activity was likely useful for defense, high ethylene activity may have promoted susceptibility through the induction of ripening processes. Lastly, we identified *M. laxa* genes that were highly induced in both quiescent and active infections and may serve as targets for control of brown rot.

4.3 Introduction

Monilinia laxa is the main causal agent of brown rot in Europe, leading to important losses of stone fruit in the field and postharvest (Rungjindamai et al., 2014). The worldwide yearly losses are estimated to be 1.7M euros for peach and nectarine (Martini and Mari, 2014) and 170M USD for peach, cherry, and plum production (RosBreed, 2020). The disease is controlled using several cultural practices (e.g., removing the overwintering inoculum), chemical fungicides in the orchard, treatments onto mummified fruit, and postharvest storage at low temperatures(Rungjindamai et al., 2014; Usall et al., 2015). However, the gradual withdrawal of some fungicides driven by concerns about their negative impact on the environment and human health, the constant threat of the emergence of fungicide resistance, and the appearance of novel virulence alleles demonstrate the need for alternative methods for managing brown rot (Badenes and Byrne, 2012; Ma et al., 2005; Usall et al., 2015). Prior to infection, *M. laxa* can remain latent or quiescent on

flowers and fruit surfaces until favorable host factors (i.e., fruit developmental stage (Mari et al., 2003)), and environmental factors and other characteristics intrinsic to the stone fruit variety (Gununu et al., 2019), trigger the disease cycle (Luo et al., 2005).

During fruit infection, *M. laxa* can overcome the need for wounds to infect and penetrate the plant cell. As a necrotrophic pathogen, *M. laxa* relies on the secretion of cell wall-degrading enzymes (CWDEs), such as pectin methyl esterases (De Miccolis Angelini et al., 2018), and possibly phytotoxins, although these compounds have not been fully identified yet (Garcia-Benitez et al., 2019). After penetration, *M. laxa* colonizes the epidermis of the fruit with hyphae (Lee and Bostock, 2007a) causing the collapse and disruption of cells, lysogenic cavities, and total degradation of the cuticle and epidermis, similar to the lesions caused by *M. fructicola* (Garcia-Benitez et al., 2016).

Overall, fruit can be infected at any growth stage, but their susceptibility to brown rot increases with maturation, which results in a short postharvest life (Mari, 2019). Hence, the activation of immune responses alongside the physicochemical properties of the fruit may determine the pathogen's ability to infect and spread. Although these underlying mechanisms have not been fully elucidated, possible explanations could depend on changes in cell wall composition, volatiles, organic acids, and phenolic compounds (Lee and Bostock, 2007b; Villarino et al., 2011).

We hypothesize that *M. laxa* is able to adapt its infection strategies according to the nectarine developmental stage, resulting in either quiescent or disease progression, while the plant host can only establish effective defenses to restrict pathogen growth in fruit tissues that have not yet reached full maturity. Here, the fruit responses and pathogenicity mechanisms in the nectarine–*M. laxa* interaction were investigated as a function of the host developmental stage and time. Nectarine fruit was harvested at two different developmental stages (immature and mature) and inoculated with *M. laxa*. Disease development and ethylene production were assessed for 3 days. Thanks to the recent availability of the *M. laxa* 8L genome (Naranjo-Ortíz, 2018), a comparative transcriptomics study was conducted on the nectarine–*M. laxa* pathosystem across four time points. This approach allowed us to identify not only host defense responses that were uniquely or highly in-

duced in immature fruit during early infections, which may partially explain why these tissues are resistant to brown rot, but also key strategies employed by the fungus to either become established in tissues or colonize them, which may be targeted to control brown rot.

4.4 Materials and Methods

4.4.1 Plant material and fungal culture

"Venus" nectarines (*P. persica* var. *nucipersica* (Borkh.) Schneider) were obtained from an organic orchard located in Raïmat (Lleida, Spain). Fruit was bagged 6 weeks before the last harvest and then harvested at two different fruit developmental stages, "mature" (211 Julian days) and "immature" (184 Julian days), and used immediately after harvest. Injured or deformed fruit was discarded, and fruit for analysis was further homogenized by using a portable DA-Meter (TR-Turoni, Forli, Italy), based on the single index of absorbance difference (I_{AD} = 1.99–2.26 for immature fruit and I_{AD} = 0.25–1.60 for mature fruit). Other assessments of quality parameters were performed on 20 randomly selected fruit (weight, cheek diameter, flesh firmness, soluble solids content, and titratable acidity), according to the method of Baró-Montel (2018).

The *M. laxa* single-spore strain 8L (ML8L, Spanish Culture Type Collection number CECT 21100) was used for all experiments. Fungal conidial suspensions were maintained and prepared, as described by Baró-Montel et al. (2019).

4.4.2 Fruit inoculations

Each fruit was inoculated with the application of six 30-µL drops of a conidial suspension at a concentration of 106 conidia mL^{-1} on the fruit surface. Mock-inoculated fruits were equally treated with sterile water containing 0.01% (w/v) Tween-80. Fruit were placed in closed containers with a relative humidity of 97 ±3% at 20 ±1 °C. Four replicates consisting of five fruit per treatment were obtained at each sampling point (6, 14, 24, 48, and 72 hpi). Six cylinders of peel and pulp tissue (1-cm diameter and depth) encompassing the inoculation sites were sampled from each fruit and pooled for each replicate. Samples were immediately flash-frozen in liquid nitrogen and stored at -80 °C until extraction. For

symptom analysis, inoculated fruit was imaged at the set time points. Ethylene production of both mock and *M. laxa* inoculated immature and mature fruit was determined, as described by Baró-Montel (2019).

4.4.3 Fruit and fungal RNA extraction

Frozen samples were ground using a mortar and pestle. The total RNA was extracted following the protocol described previously (Baró-Montel et al., 2019). Contaminant DNA was removed by treating RNA extracts with Turbo DNA-free DNase (Ambion, TX, USA). RNA concentration and purity were assessed with the Qubit® 3.0 Fluorometer (Invitrogen, USA). Gel electrophoresis on an agarose gel stained with GelRed™ Nucleic Acid Gel Stain (Biotium, Hayward, CA, USA) was used to confirm the RNA was free of DNA and not degraded.

4.4.4 cDNA libraries preparation and RNA sequencing

A total of 48 samples were analyzed by RNA sequencing, using three replicates of each treatment and stage at four of the sampled time points (6, 14, 24, and 48 hpi). cDNA libraries were prepared using the Illumina TruSeq RNA Sample Preparation Kit v2 (Illumina, USA). Quality control of the cDNA libraries was performed with the High Sensitivity DNA Analysis Kit in the Agilent 2100 Bioanalyzer (Agilent Technologies, USA). Paired-end libraries of 150-bp were sequenced on the Illumina HiSeq 4000 platform in IDSEQ INC (Davis, CA, USA).

4.4.5 RNA-Seq bioinformatics pipeline and data processing

Quality and adapter trimming on raw reads were performed with Trimmomatic v0.33 (Bolger et al., 2014) with the following parameters: maximum seed mismatches = 2, palindrome clip threshold = 30, simple clip threshold = 10, minimum leading quality = 3, minimum trailing quality = 3, window size = 4, required quality = 15, and minimum length = 36. Basic quality measurements were assessed with FastQC (`https://www.bioinformatics.babraham.ac.uk/projects/fastqc/`) before and after quality trimming. Mapping of parsed reads to a combined transcriptome of nectarine and *M. laxa* was performed using Bowtie2 (Langmead and Salzberg, 2012). The nectarine transcriptome was obtained for

peach (*Prunus persica* v2.0.a1) from the Genome Database for Rosaceae (Verde, 2013, 2017) (https://www.rosaceae.org/species/prunus_persica/genome_v2.0.a1) as no nectarine genome was available. The transcriptome of *M. laxa* was previously obtained by our group (Naranjo-Ortíz, 2018). Count matrices were made from the Bowtie2 results using sam2counts.py v0.919 (https://github.com/vsbuffalo/sam2counts) and are available in Supplementary Tables S6 and S7 at https://www.nature.com/articles/s41438-020-00387-w#Sec19 for nectarine and *M. laxa*, respectively. Differential expression (DE) analyses were conducted with the Bioconductor package DESeq2 (Love et al., 2014) in R. Reads were first normalized for library size. Differentially expressed genes (DEGs) were considered to be those with an adjusted P-value less than or equal to 0.05. Two principal component analyses (PCA) were constructed with DESeq2 using the "plotPCA" function after normalized data sets were transformed with the "vst" function separately for nectarine and *M. laxa*.

4.4.6 Functional analysis of nectarine genes

Functional annotations for the nectarine transcriptome were downloaded and processed from the Genome Database for Rosaceae version Peach v2.0.a1 (v2.1) (Verde, 2013, 2017). Once differential expression analysis was combined with the functional annotations, enrichment analysis of KEGG (Kyoto Encyclopedia of Genes and Genomes) pathways was performed using Fisher's exact test (P <0.05).

4.4.7 Functional annotation and analysis of *M. laxa* genes

Transcripts were annotated with multiple databases. Gene ontology (GO) terms were obtained via Blast2GO (https://www.blast2go.com/). Additional BLAST searches were carried out to the transporter classification database (TCDB, http://www.tcdb.org/) and the pathogen–host interactions database (PHI, http://www.phi-base.org/). Custom HMMER alignment results for HMM profiles from the protein families database (Pfam), the carbohydrate-active enzyme annotation database (dbCAN, http://csbl.bmb.uga.edu/dbCAN/), and the fungal peroxidases database (fPox, http://peroxidase.riceblast.snu.ac.kr/) were similarly included. The presence of secretion signal peptides

was evaluated for all genes in the transcriptome using SignalP v.4.0 (Petersen et al., 2011). An e-value of 10^{-3} was used as the cutoff value across all methods described. All enrichments carried out for *M. laxa* were performed as previously described for nectarine.

4.4.8 Gene expression analysis with RT-qPCR and primer design

To determinate the fungal biomass in all samples and to validate RNA-Seq results, gene expression analyses with RT-qPCR were carried out. First-strand cDNA was synthesized on 1 µg of RNA using the M-MLV Reverse Transcriptase (Promega, USA) in the SimpliAmp Thermal Cycler (Applied Biosystems, USA). Expression of the reference genes was quantified through real-time quantitative PCR (RT-qPCR) using KAPA SYBR® Fast qPCR Master Mix (Kapa Biosystems, Inc., Wilmington, USA) in the 7500 Real Time PCR System (Applied Biosystems, USA) with 2 µL of cDNA. Relative expression levels for fungal biomass determination were calculated according to the relative gene expression of the *M. laxa* reference gene *ACT* normalized to the nectarine reference gene expression *TEF2*. Primers for genes of interest were obtained from literature or designed de novo and are available in Supplementary Table S8 at `https://www.nature.com/articles/s41438-020-00387-w#Sec19`. Primer efficiency was determined by the serial dilution method, using a mix of all cDNA samples as a template.

4.4.9 Data availability

The raw sequencing reads and the read mapping count matrices have been deposited in the National Center for Biotechnology Information Gene Expression Omnibus database under the accession GSE146293.

4.5 Results

4.5.1 Nectarine susceptibility to brown rot is developmentally controlled

We visually assessed the development of brown rot over time at two maturity stages of nectarine (Figure 4.1a). Quality parameters were measured and summarized in Supplementary Table S1 at `https://www.nature.com/articles/s41438-020-00387-w#Sec19`.

Overall, the disease progressed in mature tissues, while only surface discoloration was observed in immature tissues. At the mature stage, tissue maceration was observed on the surface of the fruit at 14 hpi followed by the pathogen penetration of the pericarp tissues between 14 and 24 hpi, and increasing lesion spread at 48 and 72 hpi. Fungal biomass was also estimated in both inoculated and control (mock-inoculated) fruit to complement the visual assessments (Figure 4.1b). Although no symptoms of brown rot disease were visible on the immature fruit surface at any time point, the *M. laxa* biomass increased from 6 to 14 hpi, when the highest quantity was detected, and then significantly decreased until 72 hpi. Although at early stages of infection (6–14 hpi), the fungal biomass was not significantly different between immature and mature tissues, it increased exponentially ($y = 0.2119e^{0.0596t}$, $R^2 = 0.9075$) in the mature fruit at later time points, reaching levels approximately twenty times more than the maximum observed in immature fruit. In control tissues, a negligent quantity of the fungal biomass was detected across all time points in both stages.

A dual RNA-Seq study revealed the dynamics of the fruit–pathogen interaction at early (6 hpi and 14 hpi) and late (24 hpi and 48 hpi) infection time points. The expression of 21,334 nectarine genes (79.39% of total transcriptome) and 8,364 *M. laxa* genes (87.30% of total transcriptome) was detected across all developmental stages and time points (Supplementary Table S2 at `https://www.nature.com/articles/s41438-020-00387-w#Sec19`). The proportion of the total (i.e., from both host and pathogen) mapped reads for each sample that corresponded to *M. laxa* (Figure 4.1c) strongly correlated ($r = 0.996$) with the measurements of fungal biomass. Remarkably, more than 6,000 genes were found to be expressed in inoculated immature fruit at 14 hpi and 24 hpi, indicating that the pathogen was active in these tissues but yet it could not cause disease. More genes were detected in mature fruit, increasing across time, from 6,565 at 6 hpi up to 8,287 at 48 hpi, reflecting the progression of pathogen growth and host tissue colonization.

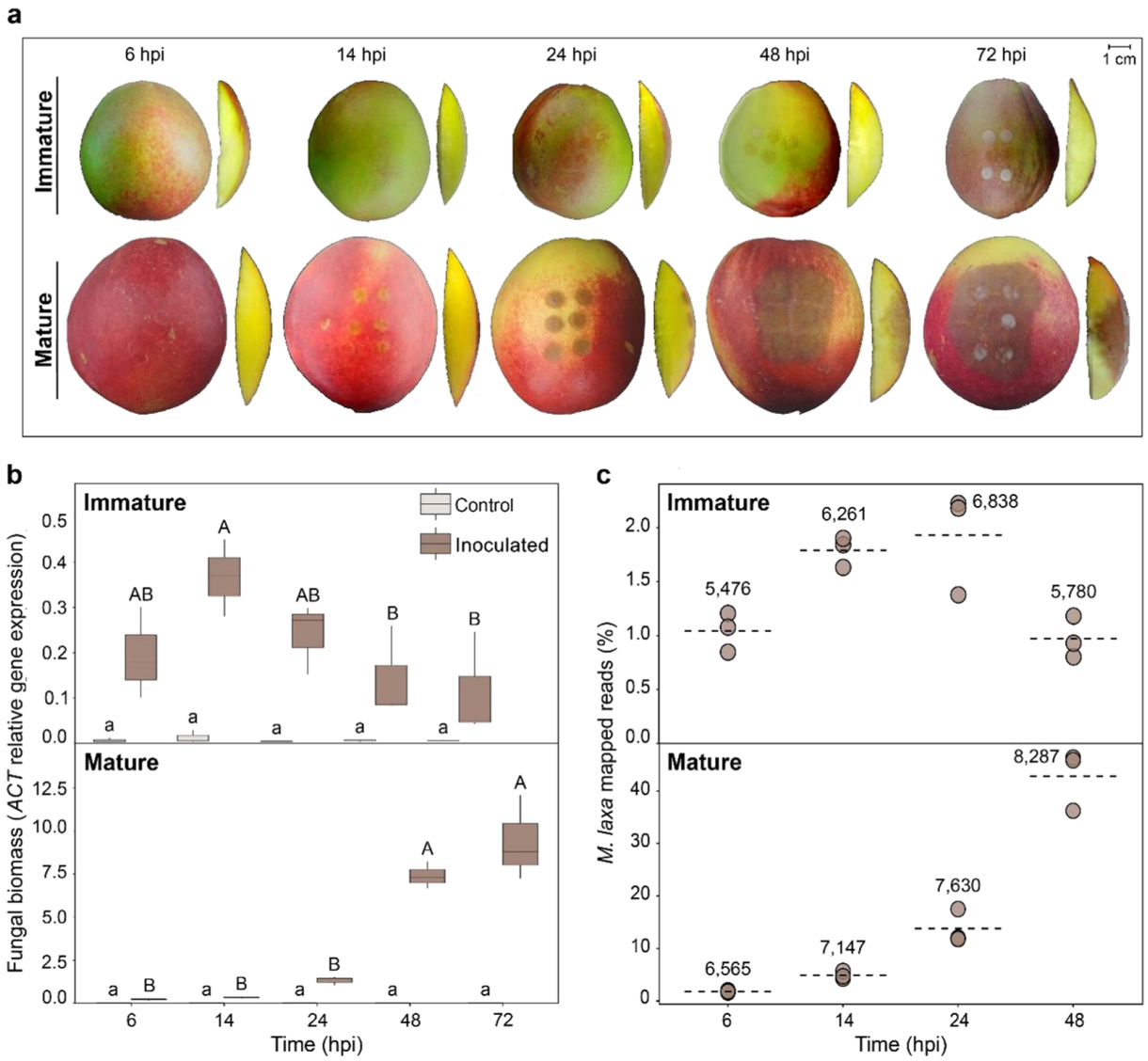

Figure 4.1: Fungal behavior development in "Venus" nectarines. (a) Brown rot spread development in immature and mature tissues at different time points after inoculation (6, 14, 24, 48, and 72 hpi). Two different viewpoints are shown (left image—entire fruit showing 6 drops; right image— perpendicular section of the fruit to discern fungus penetration if observable). (b) Determination of pathogen biomass by relative gene expression of the *M. laxa* reference gene (*ACT*), normalized to the expression of the nectarine reference gene (*TEF2*) in both stages (immature and mature) of both control (light brown) and inoculated (dark brown) tissues. The box plot represents the mean of three biological replicates with its interquartile range. Caption continued on following page.

Figure 4.1: Lowercase and uppercase letters indicate significance differences (P <0.05, Student's T test) in control and inoculated tissues, respectively. (c) Abundance (%) of *M. laxa* mapped reads in inoculated tissue out of the total amount of reads at each time point in both tissues. Each dot represents the number of mapped reads for each of the three biological replicates. The dashed line represents the average of the mapped reads in each group. Numbers represent the average of genes that were obtained at each time point in both tissues

4.5.2 Nectarine and *M. laxa* synchronize their transcriptional responses during their interaction

The principal component analyses (PCA) revealed that in nectarine, PC1 and PC2 (89% cumulative variance) clearly separated the samples based on their developmental stage and infection status (Figure 4.2A). Notably, at both development stages, 14 hpi was the time point when the inoculated samples appeared to experience a significant change in their expression profiles compared to the controls. These results demonstrate that early time points are critical for dictating the outcome of the interaction. For *M. laxa*, PC1 (53%) distinguished the samples based on the fruit developmental stage, while PC2 (16%) mainly divided the samples between early- and late-inoculation time points (Figure 4.2b). In immature fruit, there was an evident switch in the pathogen's transcriptional profile after 14 hpi, coinciding with the decrease in fungal biomass, and then continued to change up to 48 hpi. In mature fruit, *M. laxa* showed a change in gene expression between 6 and 14 hpi, when disease symptoms were first noticed on the fruit surface. Then, between 14 and 24 hpi, the pathogen altered its gene expression in mature fruit once again and retained most of these changes up to 48 hpi. Remarkably, the expression patterns of *M. laxa* at late time points of infection were highly divergent when infecting immature and mature tissues, suggesting that the pathogen utilizes different survival or infection mechanisms depending on the host developmental stage.

A differential gene expression (DE) analysis was performed to determine the responses of immature and mature fruit to *M. laxa*, and to identify specific strategies used by the pathogen at specific times of infection. Nectarine DE genes (DEGs) (P_{adj} <0.05)

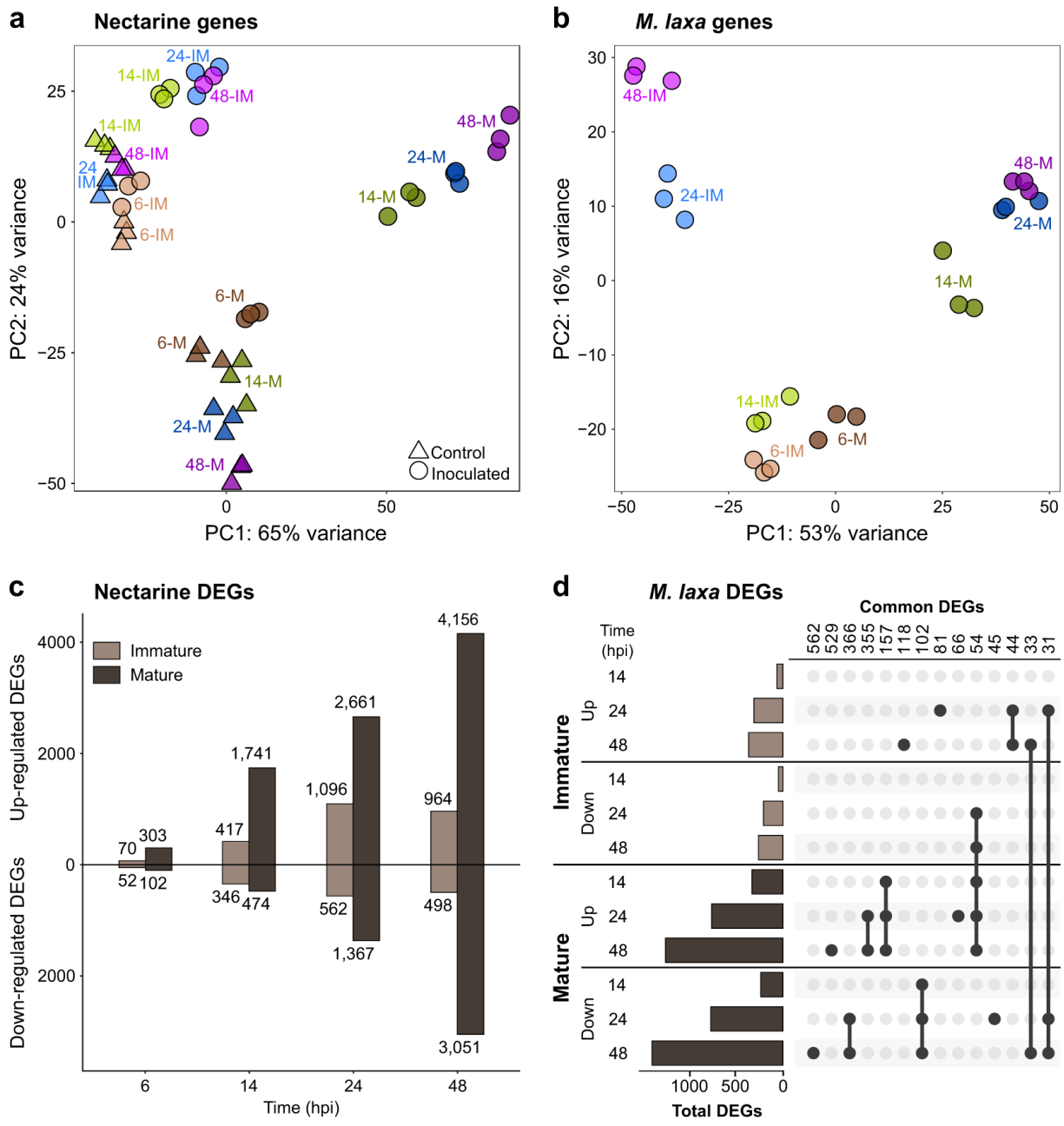

Figure 4.2: Nectarine and *M. laxa* gene expression profiles. (a, b) Patterns of gene expression represented by principal component analysis (PCA) plots of normalized count matrices for nectarine (a) and *M. laxa* (b), generated by DESeq2 through differential expression analysis for both control (△) and inoculated tissue (◯) Labels indicate the time point (6, 14, 24, and 48 hpi) in both immature (IM) and mature (M) stage. Caption continued on following page.

Figure 4.2: (c) Amount of nectarine differentially expressed genes (DEGs) as a result of the pairwise comparison of inoculated vs control tissue obtained in DESeq2 (P_{adj} <0.05). The upper part shows the upregulated DEGs and the lower, the downregulated ones, of all the four time points analyzed for the immature (light brown) and the mature (dark brown). The number of DEGs in each set are shown. (d) Amount of *M. laxa* DEGs obtained through pairwise comparisons between 14, 24, and 48 hpi compared to 6 hpi in both immature (light brown) and mature (dark brown) tissue. The highest groups of DEGs number in each set are indicated. Dots and lines represent the common DEGs that were found between time points in each stage.

were identified in comparisons between inoculated and control fruit for each maturity stage and time point (Figure 4.2c and Supplementary Table S3 at `https://www.nature.com/articles/s41438-020-00387-w#Sec19`). A total of 4,005 DEGs were detected in immature fruit across all time points, and of these the majority (63.60%) were upregulated in inoculated tissues. In immature fruit, the number of DEGs (up- and downregulated) progressively increased over time and peaked at 24 hpi; then, the changes in gene expression appeared to reach a slightly lower plateau at 48 hpi. Mature fruit displayed a stronger transcriptional response to *M. laxa* infection since a total of 13,855 DEGs (3.5-fold that from immature fruit) were detected at early and late time points. The number of DEGs in mature fruit continuously increased from 6 hpi to 48 hpi, indicating that the host tissues were undergoing a large transcriptional reprograming as the disease progressed.

Monilinia laxa DEGs were detected by comparing the expression profiles of the fungus at each time point against 6 hpi for immature and mature fruit, respectively (Figure 4.2d and Supplementary Table S4 at `https://www.nature.com/articles/s41438-020-00387-w#Sec19`). These comparisons allowed us to depict how the pathogen modified its transcriptional response based on the initial time point of the interaction when gene expression profiles of *M. laxa* were similar between immature and mature fruit (Figure 4.2b). A total of 3,160 DEGs (P_{adj} <0.05) were detected, with 895 DEGs identified in immature fruit and 2,842 in mature fruit. A closer inspection of these DEGs corroborated

the divergence observed in the PCA at later time points (Figure 4.2d). For example, the largest group of *M. laxa* unique DEGs consisted of downregulated genes in mature tissue at 48 hpi, followed by the upregulated ones in the same conditions. The DE data were further validated by RT-qPCR using eight nectarine (r = 0.892, P = 2.2 x 10^{-16}) and eight *M. laxa* (r = 0.915, P = 2.2 x 10^{-16}) DEGs, as shown in Supplementary Table S5 at `https://www.nature.com/articles/s41438-020-00387-w#Sec19`.

4.5.3 Susceptible mature fruit display a stronger transcriptional response to *M. laxa* infection than resistant immature fruit

To study host metabolic pathways altered during *M. laxa* progression, we performed a functional enrichment analysis for KEGG terms in the upregulated nectarine DEGs at each time point for immature and mature fruit (Supplementary Table S3 at `https://www.nature.com/articles/s41438-020-00387-w#Sec19`). Figure 4.3a depicts KEGG terms that were significantly enriched (P_{adj} <0.05) in at least four out of the eight comparisons (i.e., between mature and immature tissues and the four time points). In immature fruit, enriched pathways were more evident at or after 24 hpi. In contrast, multiple pathways were enriched in mature fruit, as shown by early time points, which suggests an overall activation of stress responses associated with the biotic challenge and tissue breakdown. These time-dependent responses to *M. laxa* were also evident when quantifying the number of DEGs for enriched categories related to plant defense (Figure 4.3b), which confirmed that immature fruit had the highest gene expression induction at 24 hpi, and that mature fruit had a larger number of genes induced than immature fruit as early as 6 hpi. DEGs related to the plant–pathogen interaction pathway (e.g., *CERK1*, *PTI1*, *MAP2K1*, *WRKY33*) were largely absent from the immature fruit response, with the exception of 24 hpi, but were quite abundant in the mature fruit response starting at 14 hpi (Supplementary Table S3 at `https://www.nature.com/articles/s41438-020-00387-w#Sec19`). Hormone signaling was enriched early in fruit at both developmental stages, though it appeared to become less relevant in immature fruit at 48 hpi. Cysteine and methionine metabolism and α-linolenic acid metabolism pathways, associated with ethylene (ET) biosynthesis and jasmonic acid (JA) biosynthesis, respectively, were enriched in both im-

mature and mature fruit, though more prominently in the latter. Pathways related to the biosynthesis of terpenoids were also found to be enriched at early time points in immature (14 hpi) and mature fruit (6 hpi), but their enrichment was higher in immature than mature tissue. Other pathways that appeared to be relevant for nectarine responses against *M. laxa* included the phenylpropanoid and glutathione metabolism, which were highly induced in the mature fruit, likely utilized as antioxidants.

4.5.4 Ethylene and jasmonic acid pathways are activated in response to *M. laxa* inoculations of nectarine

Given the enrichment of genes involved in plant hormone signaling transduction during early infection and the activation of methionine and α-linolenic metabolism in both fruit tissues across time, a targeted analysis of ET and JA pathways was conducted. The transcriptional activation of JA biosynthesis was evident in immature and mature fruit, with special emphasis in the induction of multiple genes encoding the initial biosynthetic steps (Figure 4.4a), from lipoxygenase (*LOX*) to 12-oxophytodienoic acid reductase (*OPR3*). Later steps of the biosynthesis pathway were only moderately activated in both tissues. In mature tissues at 48 hpi, a downregulation of the JA-amino synthetase (*JAR*1) gene was observed, involved in the production of the active form of JA, and of the homolog of the JA receptor coronatine-insensitive protein 1 (*COI1*). Two out of the five paralogs of the signaling repressor JA ZIM domain (*JAZ*) appeared to be activated in immature and mature tissues at multiple time points. The three paralogs encoding the transcriptional activator of JA responses, *MYC2*, were strongly induced in mature fruit after 14 hpi and upregulated in immature fruit only at 14 hpi and 24 hpi. In fact, the *MYC2* gene expression level of the third paralog (*Prupe.5G130700.1*) was significantly higher in inoculated immature than mature tissue, but then, its expression was significantly higher in mature than immature tissue at both 24 and 48 hpi (Supplementary Table S3 at `https://www.nature.com/articles/s41438-020-00387-w#Sec19`).

The steps committed to ET biosynthesis catalyzed by the 1-aminocyclopropane-1-carboxylate synthase (*ACS*) and the 1-aminocyclopropane- 1-carboxylate oxidase (*ACO*) genes were highly induced in response to *M. laxa* inoculations, particularly in mature

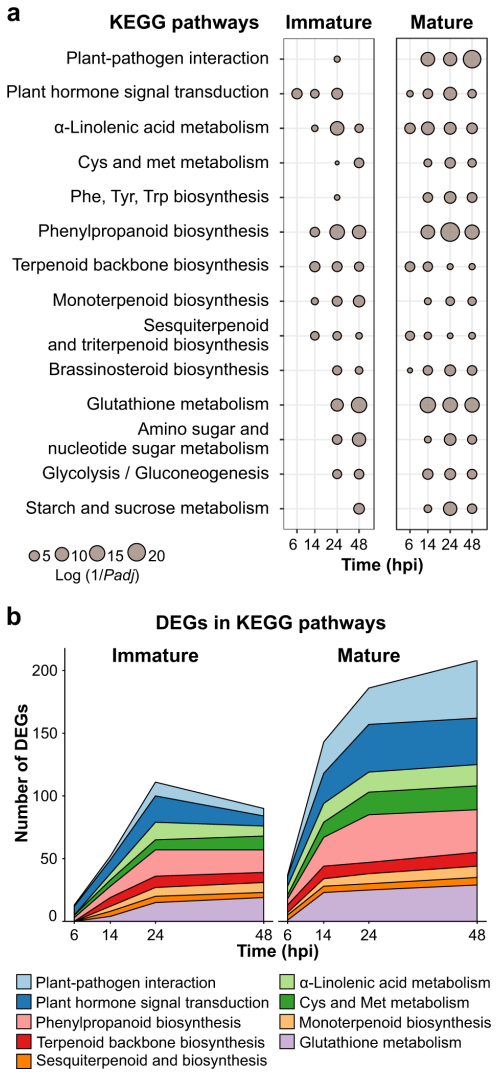

Figure 4.3: KEGG enrichments of upregulated genes in nectarine. (a) Metabolic pathways from the KEGG database that were found in at least half of the eight comparisons obtained in the differential expression analyses (inoculated vs control). The dot size represents the log of the inverted P_{adj} value obtained in the KEGG enrichment analyses along with all the time points in both stages (P_{adj} <0.05) (Supplementary Table S3 at `https://www.nature.com/articles/s41438-020-00387-w#Sec19`). (b) The magnitude of the fruit response in terms of the number of DEGs that have KEGG annotations for the selected metabolic pathways in both stages through time. Each color represents one different KEGG pathway.

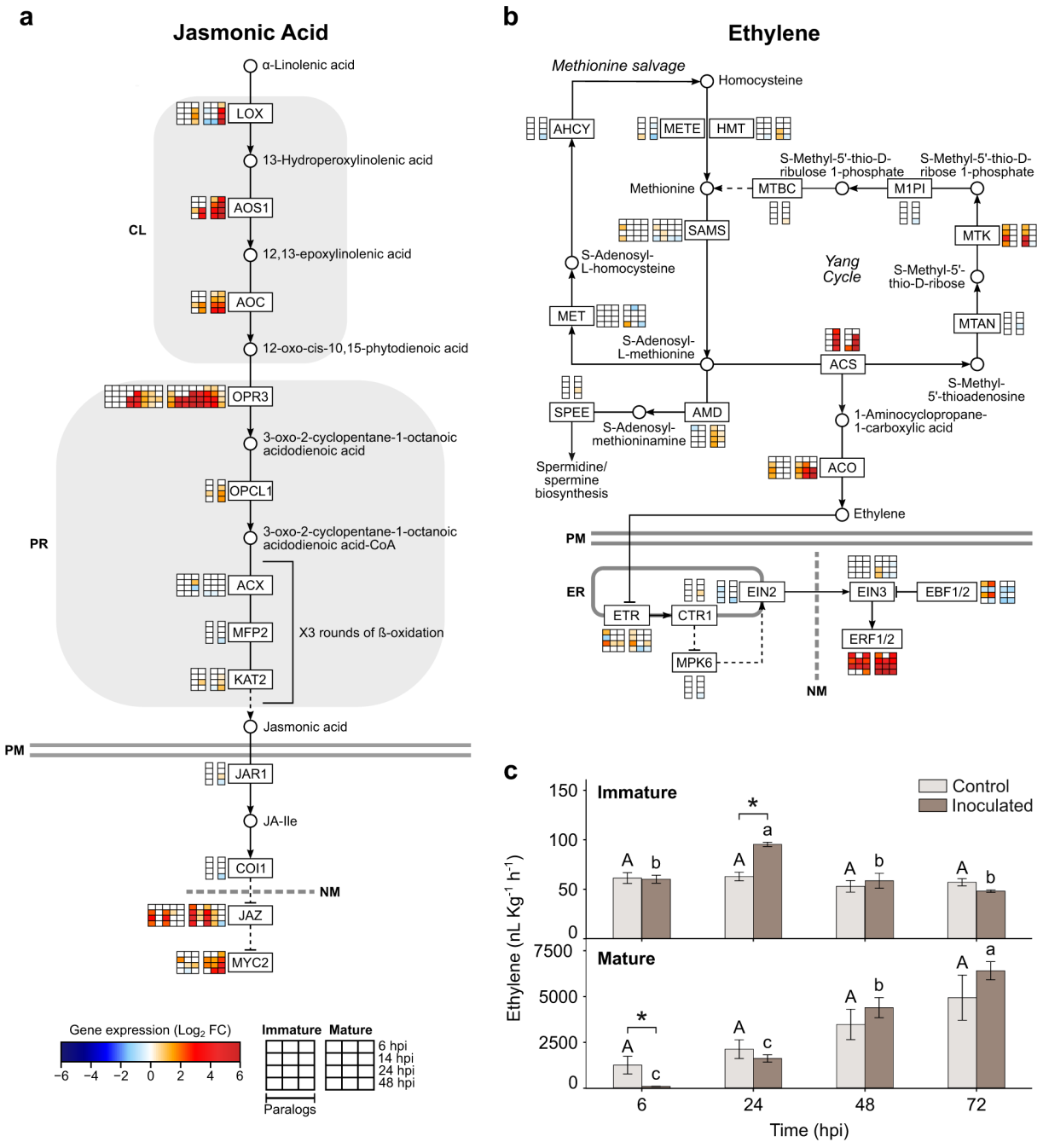

Figure 4.4: Caption presented on following page.

Figure 4.4: Activation of jasmonic and ethylene pathways in nectarine fruit after inoculations with *M. laxa*. (a, b) Jasmonic acid and ethylene pathways are shown with substrates (◯ and enzymes (boxes) and include 32 and 41 DEGs for JA and ET, respectively. The scale color of the heat maps represents the intensity of the significant expression changes (Log_2FC), which resulted from the pairwise comparison of inoculated vs control samples (P_{adj} <0.05). Paralogs of each analyzed enzyme are represented in columns and grouped by their expression in immature (left boxes) and mature (right boxes) at each time point (hpi). Dashed lines indicated that some steps had been omitted. PM plasmatic membrane, NM nucleus membrane, ER endoplasmic reticulum, CL chloroplast, PR peroxisome. Enzyme abbreviations and lists of paralogs genes for each protein are provided (Supplementary Table S3 at). (c) Ethylene measurements of the nectarine–*M. laxa* pathosystem through time. Values represent the mean (n=4) and the vertical bars, the standard error. Symbols (*) indicate significant differences according to Student's T test (P <0.05). Uppercase and lowercase letters indicate significant differences (P <0.05, Tukey's test) in control and inoculated tissues, respectively.

fruit (Figure 4.4b). The *ACS2* (*Prupe.5G106200.1*) and the *ACO3* (*Prupe. 7G212000.1*) genes showed the highest upregulation (*ACS2* in both tissues and *ACO3* in mature tissue). Ethylene signal transduction elements (*ETR*, *CTR*, *EIN2*, and *EIN3*) showed only moderate changes in gene expression in response to the pathogen. Interestingly, although the negative regulator *EBF1/2* was downregulated at 14 and 48 hpi in both tissues, it was highly upregulated in immature tissue at 6 and 24 hpi. However, all three paralogs of the ET response factor 1/2 (*ERF1/2*), which control multiple ET responses and are a point of signal integration for JA and ET signal transduction, were highly upregulated in both tissues. The *ERF1/2* gene expression level of the second paralog (*Prupe. 6G348700.1*) was significantly higher in mature inoculated than immature inoculated fruit at 14 hpi (data not shown).

In addition, the ET produced by *M. laxa*-inoculated and control fruit was measured to complement the transcriptional data (Figure 4.4c). Control nectarines followed the ET pattern of a climacteric fruit; low and steady levels of ET in immature fruit and high

and significantly increased levels in mature fruit until ripening. However, in inoculated immature fruit, ET production significantly peaked at 24 hpi, corresponding to the peak of transcriptional responses in this tissue, before returning to levels equivalent to the control fruit. In inoculated mature fruit, the ET production was significantly lower than control fruit at 6 hpi, but then significantly increased. These results suggest that nectarine was performing a tightly regulated response of ET.

4.5.5 *Monilinia laxa* adapts its infection strategies according to the host environment conditions

To determine which fungal genes and functions are biologically relevant during *M. laxa* interactions with nectarine, we performed a functional analysis of the pathogen transcriptome. First, a total of 9,581 transcripts were de novo annotated for multiple functional categories, including carbohydrate-active enzymes (CAZymes), fungal peroxidases (fPox), genes involved in pathogen–host interactions (PHI), membrane transport proteins (TCBD), and proteins with signal peptides (SignalP), among others (Figure 4.5a and Supplementary Table S4 at `https://www.nature.com/articles/s41438-020-00387-w#Sec19`). Then, an enrichment analysis (Fisher, P_{adj} <0.05) of these large functional categories in the upregulated DEGs across infection was performed to obtain a general picture of specific gene categories induced by the pathogen in immature and mature fruit (Figure 4.5b). In immature fruit, these large categories were enriched in *M. laxa* upregulated DEGs at least at one time point when compared to 6 hpi. Particularly at 24 hpi, a significant abundance of CAZymes and PHI genes was observed. Fungal peroxidases were only significantly enriched in immature fruit at 48 hpi. In contrast, enrichment of CAZymes and fungal peroxidases was not observed at any time point in mature tissues. Genes in involved in pathogen–host interactions and membrane transport remained enriched at relatively even levels from 14 to 48 hpi in mature fruit.

We identified GO terms related to pathogenicity, virulence, and fungal growth among the upregulated DEGs for each host developmental stage (Figure 4.5c). Among this subset of biologically relevant GO terms, threefold more upregulated DEGs were detected when *M. laxa* was inoculated in mature fruit compared to immature fruit. Particularly, the

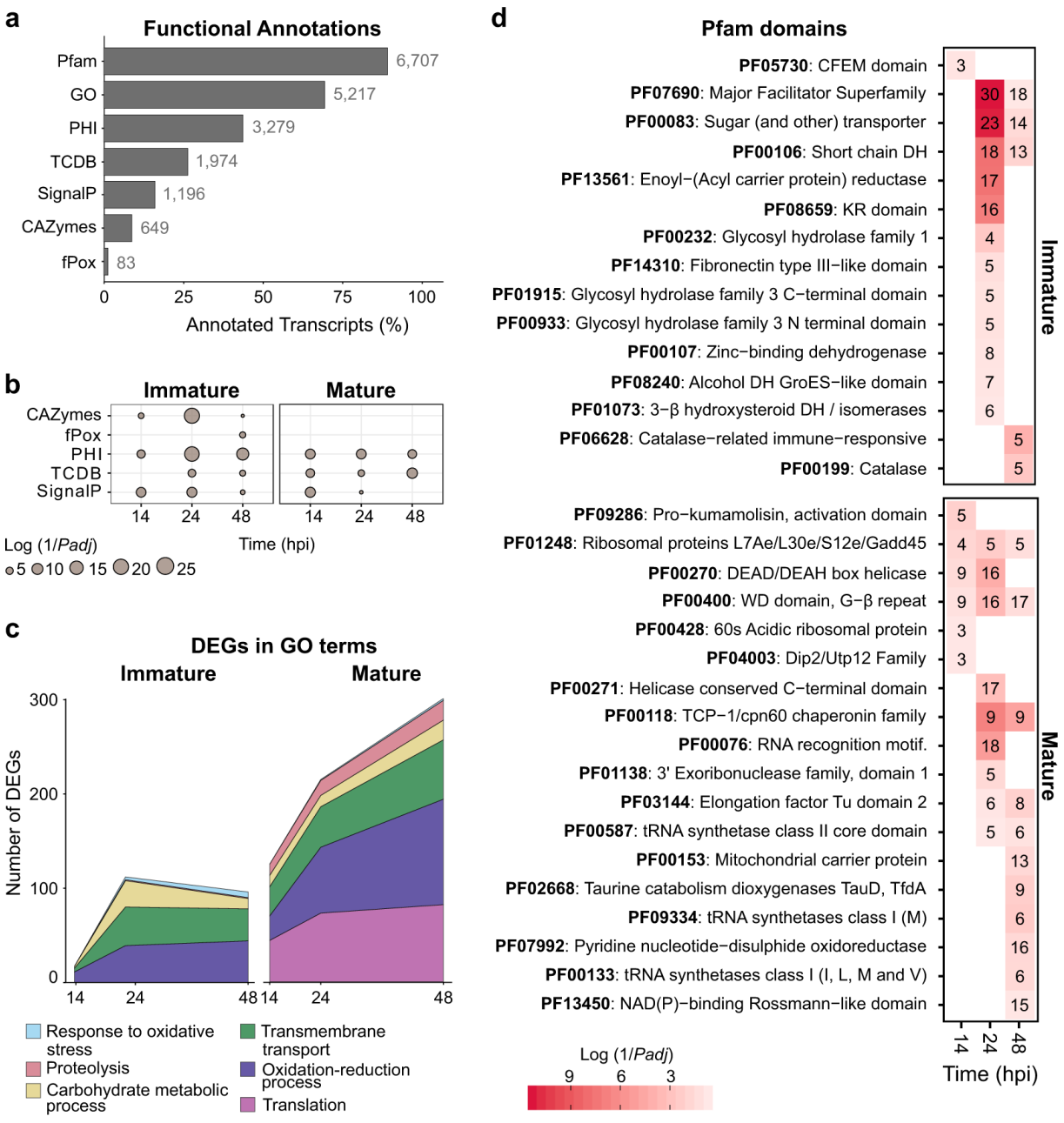

Figure 4.5: Caption presented on following page.

Figure 4.5: Summary of functional annotations and functional enrichments of *M. laxa*. (a) De novo functional annotations in all *M. laxa* transcripts obtained (9,581) (Supplementary Table S4 at `https://www.nature.com/articles/s41438-020-00387-w#Sec19`). Each category is represented by the proportion (%) of annotated transcripts across *M. laxa* transcriptome and the specific number of DEGs next to the bar. Pfam, Protein Family Database; GO, Gene Ontology; PHI Pathogen–Host Interaction; TCDB, Transporter Classification Database; SignalP, presence of secretion signal peptides, CAZy Carbohydrate-Active enZyme; fPox, fungal peroxidases. (b) Enrichment of functional categories across all time points in both tissues. Pairwise comparisons were performed between 14, 24, or 48 hpi compared to 6 hpi, for each maturation stage. The dot size represents their significance (log of the inverted P_{adj} value) obtained in Fisher tests. (c) The magnitude of *M. laxa* response in terms of number of DEGs (P_{adj} <0.05) that have GO terms for some relevant terms in both stages along time. Each color represents one different GO term. (d) Pfam enrichments of *M. laxa* genes that were overexpressed in 14, 24, and/or 48 hpi compared to 6 hpi, for each stage, obtained in DESeq2 (P_{adj} <0.05) (Supplementary Table S4). The color scale of the heat maps represents the log of the inverted P_{adj} value. The number of DEGs in each Pfam are also shown.

number of *M. laxa* upregulated DEGs in immature tissue increased progressively until 24 hpi and then decreased slightly at 48 hpi, whereas in mature tissue, the upregulated DEGs increased along with infection time. Notably, these gene expression patterns resembled the transcriptional response of the host for each developmental stage (Figure 4.3b). In both stages, *M. laxa* induced a high number of DEGs related to oxidative–reduction processes and transmembrane transport, although genes involved in protein translation and proteolysis were only abundantly expressed in mature tissue. However, genes involved in response to oxidative stress were mainly expressed in immature at 48 hpi, together with the enrichment of fungal peroxidases at this time point (Figure 4.5b).

Lastly, the enrichments of Pfam domains (P_{adj} <0.05) were also carried out using the *M. laxa* upregulated DEGs (Figure 4.5d and Supplementary Table S4 at `https://www.nature.com/articles/s41438-020-00387-w#Sec19`). In agreement with previous results,

Pfam categories were mainly enriched at 24 hpi in immature fruit, with the exception of proteins containing the fungal pathogenesis-related CFEM domain (PF05730), which were uniquely enriched earlier at 14 hpi. In addition, Pfam domains related to fungal membrane transport (PF07690 and PF00083) were largely prominent in immature fruit, especially at 24 hpi, where up to 53 genes were induced. Less significantly enriched, fungal glycosyl hydrolases, dehydrogenases (DH), and catalases were found at 48 hpi in immature tissues.

The number of enriched Pfam domains among *M. laxa* upregulated DEGs in mature fruit, such as those related to transcription and translation (e.g., PF03144 and PF00587), increased throughout disease progression (Figure 4.5d). However, other relevant domains, such as some related to proteolysis activity (e.g., PF09286 Pro-kumamolisin domain), uniquely peaked at 14 hpi. Notably, upregulated DEGs annotated as ribosomal proteins and transcriptional factors (PF01248 and PF00400) involved in growth and cell cycle control were prevalent throughout infection of mature fruit. Later, infection time points exhibited enrichments of protein domains belonging to membrane transport (e.g., mitochondrial carrier protein) and redox functions (e.g., an oxidoreductase).

4.5.6 Highly induced *M. laxa* genes during inoculation provide possible targets for disease control

To identify potential target genes for the control of *M. laxa*, a closer examination was conducted of the most highly *M. laxa* upregulated DEGs (i.e., largest Log_2FC) from all time points and tissue comparisons (Table 4.1 and Supplementary Table S4 at `https://www.nature.com/articles/s41438-020-00387-w#Sec19`). The top five *M. laxa*-induced DEGs in immature and mature fruit were unique between the tissue types, reinforcing the evidence that the pathogen displays a different behavior according to the developmental stage of the host. Strongly induced DEGs at 14 hpi unique to early infections of immature fruit included fungal phosphate transporters, phospholipases, and oxidoreductases. A member of the glycosidase hydrolase family 31 (*Monilinia_056600*) was highly expressed at 24 hpi in immature fruit, alongside a transmembrane fructose transporter (*Monilinia_074660*) and histidine phosphatase (*Monilinia_002270*). The

highest induced DEGs in immature fruit were detected at 48 hpi and corresponded to an oxidoreductase gene (*Monilinia_ 010850)*, a homolog of the alcohol oxidase (*OAX1*) from `https://www.nature.com/articles/s41438-020-00387-w#Sec19`, and the same transmembrane fructose transporter (`https://www.nature.com/articles/s41438-020-00387-w#Sec19`) already found at 24 hpi. Interestingly, *M. laxa* DEGs with fungal peroxidase annotations, a catalase (*Monilinia_ 039930*) and a haloperoxidase (*Monilinia_ 049900*), were only detected at 48 hpi in immature fruit. In mature fruit, a single protease gene (*Monilinia_ 077490*) was the highest upregulated *M. laxa* DEG at all time points. Two polygalacturonases (glycoside hydrolase family 28) were among the largest induced DEGs during infections of mature fruit; *Monilinia_ 000560* was highly upregulated at 14 hpi, whereas *Monilinia_ 041700* was highly expressed at 24 and 48 hpi. Another CAZyme (glycoside hydrolase family 71, *Monilinia_ 037020*) was also highly enriched at 14 and 24 hpi. In mature tissue, transporters and hormonerelated genes were among the highest expressed DEGs. An amino acid transporter (*Monilinia_ 015240*) was significantly expressed at 14 hpi, while a tryptophan 2- monooxygenase (*Monilinia_ 013220*) was induced at 48 hpi, known to be involved in virulence in another pathosystem (Cerboneschi, 2016). Altogether, these results suggest that targeting of specific genes involved in response to oxidative stress, nutrient transport, and carbohydrate catabolism may reduce quiescent infections, while specific proteolytic genes and additional CAZymes may help inhibit or reduce the severity of disease in susceptible fruit.

Table 4.1: Top upregulated genes of *M. laxa*

Accession	**Log_2FC**	**Selected functional annotations**
Immature - 14 HPI		
Monilinia_ 058830	5.90	TCDB: 2.A.1.9.2 (Inorganic phosphate transporter) | PHI: *PHO84* (*Cryptococcus neoformans*, reduced virulence)
Monilinia_ 028560	5.37	PFAM: PF04185.14 (Phosphoesterase family) | PHI: *plcC* (*Mycobacterium tuberculosis*, unaffected pathogenicity) | SignalP: 0.811
Monilinia_ 060140	3.51	SignalP: 0.686
Monilinia_ 079910	3.12	PFAM: PF01633.20 (Choline/ethanolamine kinase)

Accession	Log_2FC	Selected functional annotations
Monilinia_009770	2.99	PFAM: PF00264.20 (Common central domain of tyrosinase) | SignalP: 0.667
Immature - 24 HPI		
Monilinia_056600	8.45	CAZy: GH31 | PHI: *Gls2* (*Magnaporthe oryza*e, reduced virulence)
Monilinia_074660	8.09	TCDB: 2.A.1.1.69 (Sugar/H+ symporter) | PHI: *FRT1* (*Botrytis cinerea*, unaffected pathogenicity)
Monilinia_002270	7.72	PFAM: PF00300.22 (Histidine phosphatase superfamily (branch 1) | PHI: *FGSG_02549* (*Fusarium graminearum*, reduced virulence) | SignalP: 0.897
Monilinia_033100	7.68	TCDB: 2.A.1.1.119 (Putative uncharacterized protein *An14g04280*) | PHI: *MoST1* (*Magnaporthe oryzae*, unaffected pathogenicity)
Monilinia_016250	7.42	TCDB: 2.A.1.7.11 (Glucose/galactose transporter) | PHI: *PD0681* (*Xylella fastidiosa*, increased virulence) | SignalP: 0.632
Immature—48 HPI		
Monilinia_010850	9.53	GO: GO:0055114 (oxidation-reduction process) | PFAM: PF00732.19 (GMC oxidoreductase) CAZy: AA3-3 | PHI: *AOX1* (*Passalora fulva*, reduced virulence)
Monilinia_074660	8.77	TCDB: 2.A.1.1.69 (Sugar/H+ symporter) | PHI: *FRT1* (*Botrytis cinerea*, unaffected pathogenicity)
Monilinia_022560	7.92	SignalP: 0.844
Monilinia_039930	7.91	fPox: Catalase | PHI: *CAT1* (*Candida albicans*, reduced virulence)
Monilinia_034450	7.79	CAZy: GH3 | PHI: Avenacinase (*Gaeumannomyces graminis*, loss of pathogenicity) SignalP: 0.718
Mature—14 HPI		
Monilinia_077490	9.43	GO: GO:0006508 (proteolysis) | PFAM: PF01828.17 (Peptidase A4 family) | SignalP: 0.64
Monilinia_037020	6.77	CAZy: GH71 | SignalP: 0.886

Accession	Log_2FC	Selected functional annotations
Monilinia_015240	6.54	TCDB: 2.A.3.4.3 (GABA-specific permease) | PHI: *bcaP* (*Staphylococcus aureus*, unaffected pathogenicity / reduced virulence)
Monilinia_000560	6.10	CAZy: GH28 | PHI: *BcPG2* (*Botrytis cinerea*, reduced virulence) | SignalP: 0.837
Monilinia_050850	5.68	GO: GO:0006508 (proteolysis) | PFAM: PF09286.11 (Prokumamolisin, activation domain) SignalP: 0.84
Mature—24 HPI		
Monilinia_077490	8.90	GO: GO:0006508 (proteolysis) | PFAM: PF01828.17 (Peptidase A4 family) | SignalP: 0.64
Monilinia_006190	7.37	PFAM: PF00107.26 (Zinc-binding dehydrogenase)
Monilinia_041700	7.18	CAZy: GH28 | PHI: *PGX1* (*Cochliobolus carbonum*, unaffected pathogenicity) SignalP: 0.913
Monilinia_041730	6.89	TCDB: 2.A.1.14.38 (Uncharacterized transporter YIL166C) | PHI: *GzMyb019* (*Fusarium graminearum*, unaffected pathogenicity)
Monilinia_073540	6.74	CAZy: AA7 | PHI: *ZEB1* (*Fusarium graminearum*, unaffected pathogenicity) | SignalP: 0.778
Mature—48 HPI		
Monilinia_077490	9.25	GO: GO:0006508 (proteolysis) | PFAM: PF01828.17 (Peptidase A4 family) | SignalP: 0.64
Monilinia_041700	7.99	CAZy: GH28 | PHI: *PGX1* (*Cochliobolus carbonum*, unaffected pathogenicity) SignalP: 0.913
Monilinia_068440	7.64	None
Monilinia_013220	7.46	GO: GO:0055114 (oxidation-reduction process) | PFAM: PF00743.19 (Flavin-binding monooxygenase-like) | PHI: *iaaM* (Pseudomonas savastanoi, reduced virulence)
Monilinia_041730	7.42	TCDB: 2.A.1.14.38 (Uncharacterized transporter YIL166C) | PHI: *GzMyb019* (*Fusarium graminearum*, unaffected pathogenicity)

Represented genes are the five most upregulated genes, obtained in the pairwise comparisons generated by DESeq2. Values correspond to the expression (log_2FC) of each time point (14, 24, and 48 hpi) compared to 6 hpi of both immature and mature fruit. The accession number of genes and selected functional annotations for each gene are also shown. TCDB Transporter Classification Database; PHI Pathogen-Host Interactions; Pfam Protein Family database; SignalP Presence of secretion signal peptides; CAZy Carbohydrate-Active enzyme; GO Gene Ontology; fPox fungal peroxidases.

4.6 Discussion

The first line of plant defense that *M. laxa* has to overcome is the constitutive physical (e.g., cuticle and plant cell wall) and chemical barriers (e.g., preformed antifungal compounds) present in the fruit surface. The developmental process from immature to mature fruit is characterized by physical and chemical changes in fruit firmness, leading to softening at the onset of ripening (Brummell et al., 2004). In fact, the flesh firmness of immature fruit was higher than the mature fruit (Supplementary Table S1). *Monilinia laxa* appeared to produce more CWDE (e.g., CAZymes) in immature fruit, which suggests that the pathogen could be trying harder to overcome the host cell walls in these tissues. Nevertheless, the immature tissue had no visible disease symptoms. Other alterations occurring during fruit development include changes in plant cuticle, sugar accumulation, volatile compounds, and secondary metabolites synthesis, which have been reviewed as promoting susceptibility to pathogens in ripening fruit. Hence, higher soluble solids content and lower titratable acidity on mature fruit (Supplementary Table S1 at `https://www.nature.com/articles/s41438-020-00387-w#Sec19`) could favor pathogen colonization.

Plant–pathogen interactions take place when pathogen-associated molecular patterns (PAMP) are recognized by the plant's pattern recognition receptors (Zipfel, 2014), which ultimately triggers a defense response known as PAMP-triggered immunity (PTI, Pandey et al. (2016). The chitin elicitor receptor kinase 1 (*CERK1*, Kombrink et al. (2011)) (*Prupe.3G213100.1*) was upregulated in the mature tissue at 14 hpi. Also, the expression levels of the transcriptional activator *PTI5* (*Prupe.4G055500.1*) were up to 2.5-fold and 5-fold higher in mature fruit when compared to immature fruit, at 24 and 48 hpi, respectively. PTI responses can be suppressed by effector proteins secreted by the pathogen, which in turn, will elicit effector-triggered immunity (ETI, Jones and Dangl (2006)). In our pathosystem, proteins with the CFEM domain (Pfam PF05730) and signal peptides were enriched in the early infection stage (14 hpi) on immature tissue. Among the annotated genes with the CFEM domain, the *Monilinia_077410* is a homolog of *BcCFEM1* from *B. cinerea*, an effector shared by many *Botrytis* spp. (Valero-Jiménez et al., 2019)

and described to be important for its virulence (Zhu, 2017). These results suggest that *M. laxa* may secrete some type of effector proteins in immature fruit.

Once the host–pathogen interaction began, both pathogen and host triggered their own transcriptional reprograming. In mature tissue, both nectarine and *M. laxa* abruptly changed their gene expression profile at 14 hpi, coinciding with the ability of the pathogen to grow and macerate the fruit tissues within 14 h. From 14 hpi onwards, the pathogen started to penetrate and switched toward an aggressive necrotrophic phase, which was retained at later infection times. Functions related to transmembrane transport, oxidation-reduction process, and translation were among the most abundant activities in mature fruit, denoting the growth and spread of the pathogen. In contrast, the number of nectarine and *M. laxa* DEGs in immature fruit remained somewhat steady through infection time, even when fungal biomass peaked at 24 hpi. Overall, these findings suggest that inoculated mature nectarines displayed an earlier and broader response to *M. laxa* than immature ones, likely due to the faster pathogen growth and virulence mechanisms activation in these tissues.

Both PTI and ETI are able to induce the host hormone signaling transduction pathway (Pandey et al., 2016), which was found to be enriched, starting at 6 hpi in both tissues. Jasmonic acid and ET are known to be involved in defense responses against necrotrophs, such as mediating the host's responses against them (McDowell and Dangl, 2000), but ET is also required for fruit ripening and senescence processes, which are conducive to disease susceptibility (Blanco-Ulate et al., 2013; Pandey et al., 2016; van der Ent and Pieterse, 2012). Jasmonic acid can also mediate the disease resistance of fruit by increasing the fruit antioxidant capacity (Zhu and Tian, 2012), but some fungi are able to hijack the JA signaling pathway to cause disease (Zhang et al., 2017). Although the early steps of JA biosynthesis were highly induced upon *M. laxa* inoculation, downregulation of receptor genes was observed in mature fruit inoculated with *M. laxa* when compared to controls. These findings suggest that *M. laxa* could be somehow blocking the JA signaling pathway, although the mechanisms involved are unknown.

Ethylene biosynthesis increases during ripening of climacteric fruit (Oetiker and Yang,

1995), such as nectarines. In our study, the control immature fruit (System 1, associated with fruit development) produced basal ethylene levels, whereas ethylene production in control mature fruit (System 2, involved in ripening) increased through time after harvest. In inoculated immature fruit, there was a significant peak of ET production as compared to the control at 24 hpi. This discrete induction of ET can be part of the fruit defense responses against *M. laxa*. Alternatively, the pathogen could be inducing fruit ethylene biosynthesis in immature fruit to accelerate ripening, in an attempt to promote fruit physicochemical changes that are conducive to disease (Blanco-Ulate et al., 2013). Along this line, *ACS2* and *ACO1*, involved in System 2 ET production (Tadiello, 2016), were overexpressed in inoculated immature tissues. Previous studies have reported on a similar modulation of ET biosynthesis by the pathogen (Baró-Montel, 2019). However, after 24 hpi, ethylene levels in inoculated immature fruit fell to control levels, and the fruit remained resistant. This may be in part due to the upregulation of the ethylene signaling inhibitors *EBF1/2*, which could mitigate the ethylene-induced ripening processes that contribute to susceptibility. In contrast, in inoculated mature fruit, ET production and signal transduction were lower at 6 hpi in inoculated fruit but grater from 24 hpi onward, following the autocatalytic System 2 ethylene biosynthesis. Overall, the results indicate the ability of *M. laxa* to differentially alter ET production to promote susceptibility and, in turn, the ability for immature fruit, but not mature fruit, to mitigate the consequences of this induction (van der Ent and Pieterse, 2012).

The above observations indicate that although *M. laxa* was deploying some strategies to infect the immature tissues, it was not able to overcome either the surface or the active defense responses deployed by the immature fruit. *Monilinia laxa* remained on the immature tissue, increasing its biomass and multiplying on the surface, until 14 hpi when it ceased to grow. It is known that Monilinia spp. can remain quiescent on fruit surfaces (Luo et al., 2005) and that they can employ appressoria as resting structures on immature nectarines (Lee and Bostock, 2006). After 14 hpi, *M. laxa* biomass and reads started to decrease, switching its transcriptional machinery by employing different sets of genes in order to deploy different strategies to survive on the fruit's surface. Some results point out

that *M. laxa* could either be starting a quiescence period or moving toward an autolysis process, breaking cells to feed on its remains. Another possibility is that the remaining *M. laxa* cells on immature fruit were being attacked by the host defenses. This is supported by the expression of *M. laxa* genes associated with response to oxidative stress at late time points, such as catalases, previously reported in detoxification during infection of tomato leaves by *B. cinerea* (Schouten, 2002). Thus, it is likely that immature fruit was generating reactive oxygen species (ROS) during the interaction through an oxidative burst (Torres et al., 2006) to kill the pathogen.

Monilinia laxa could also be producing ROS for its development and as a pathogenicity mechanism to damage the host tissue. Particularly, the NADPH oxidase (Nox) complex is involved in both fungal ROS production and its use in sclerotia development and virulence (Kim et al., 2011; Li et al., 2016). Some genes encoding the Nox regulator R (NoxR) (e.g., *Monilinia_061250* and *Monilinia_079620*) were found to be upregulated at 24 hpi in both mature and immature tissue. At later stages, a highly induced alcohol oxidase expressed in immature tissue at 48 hpi could be another ROS producer, previously described as an alternative ROS production system. Lin et al. (2019) demonstrated that *AOX1* was involved in pathogenicity and oxygen stress responses in B. cinerea. Concomitantly, nectarine counteracted the pathogen oxidative burst by expressing genes of antioxidant metabolism compounds such as glutathione and redox-related amino acids (Cys and Met).

Plant secondary metabolites such as terpenoids have been described to protect the fruit under biotic and abiotic stresses (Bartwal et al., 2013), although their role can be tissue-dependent. Overall, the enrichment of genes involved in secondary metabolite biosynthesis was higher in resistant immature than susceptible mature tissue, which suggests that either the host was producing terpenoids in the resistant immature tissue to prevent the attack or that *M. laxa* was inhibiting its biosynthesis on mature tissue. *Monilinia laxa* could also be able to degrade and transform terpenoids as described for *B. cinerea* (Collado et al., 2007). The phenylpropanoid metabolism is also triggered in response to brown rot. In both immature and mature fruit, from 14 hpi to 48 hpi, phenylpropanoid-

related pathways were highly induced. While on the immature tissue, these pathways could be involved in reinforcing the cell wall through lignin production (Veloso and van Kan, 2018), the role in the mature fruit could be more focused on the detoxification of fungal ROS production (Lin et al., 2019). Nevertheless, these hypotheses need to be further tested.

On mature nectarines, *M. laxa* deployed other virulence factors in addition to ROS production and scavenging. The pathogen expressed upregulated DEGs related to proteolytic activity, containing domains such as the Pro-kumamolisin domain (PF09286). The list of genes summarized in Table 4.1 could be putative pathogen target genes as they were expressed only when *M. laxa* infected the mature tissues, as none of the top five upregulated genes in mature tissue was found in the immature fruit. For instance, the highest expressed protease (*Monilinia_077490*) at in all time points is a homolog of a nonaspartyl protease (ACP1) found during pathogenesis in *Sclerotinia sclerotiorum* (Poussereau et al., 2001). Cell wall-degrading enzymes are commonly produced by necrotrophic fungi as virulence factors and their secretion by Monilinia spp. on culture media has been previously reported (Garcia-Benitez et al., 2019). A rhamnogalacturonan hydrolase (glycoside hydrolase family 28, *Monilinia_041700*), which was highly expressed at both 24 and 48 hpi, was already described as a putative virulence factor in *M. laxa* infecting peaches (Baró-Montel et al., 2019).

Current information regarding the strategies utilized by either Monilinia spp. or stone fruit or during their interaction is mainly focused on specific metabolic pathways or actions developed by one of the two players. As a novel feature of the present research, we demonstrated the synchronized responses from nectarine and *M. laxa*, by utilizing a resistant immature and susceptible mature fruit throughout a course of infection. Future research studies should be focused on delving into the host defense system for the ongoing development of nectarine cultivars with increased resistance to brown rot, as well as conducting in-depth fungal studies to alter the ability of *M. laxa* to cause disease.

References

Badenes, M. L. and Byrne, D. H., editors (2012). *Fruit Breeding*. Springer.

Baró-Montel, N. (2018). Developing a methodology for identifying brown rot resistance in stone fruit. *Eur. J. Plant Pathol.*, 154.

Baró-Montel, N. (2019). Double-sided battle: the role of ethylene during Monilinia spp. infection in peach at different phenological stages. *Plant Physiol. Biochem.*, 144.

Baró-Montel, N., Vall-llaura, N., Usall, J., Teixidó, N., Naranjo-Ortíz, M. A., Gabaldón, T., and Torres, R. (2019). Pectin methyl esterases and rhamnogalacturonan hydrolases: weapons for successful Monilinia laxa infection in stone fruit? *Plant Pathology*, 68(7):1381–1393.

Bartwal, A., Mall, R., Lohani, P., Guru, S. K., and Arora, S. (2013). Role of secondary metabolites and brassinosteroids in plant defense against environmental stresses. *J. Plant Growth Regul.*, 32.

Blanco-Ulate, B., Vincenti, E., Powell, A. L. T., and Cantu, D. (2013). Tomato transcriptome and mutant analyses suggest a role for plant stress hormones in the interaction between fruit and Botrytis cinerea. *Frontiers in Plant Science*, 4:142.

Bolger, A. M., Lohse, M., and Usadel, B. (2014). Trimmomatic: a flexible trimmer for Illumina sequence data. *Bioinformatics*, 30(15):2114–2120.

Brummell, D. A., Dal Cin, V., Crisosto, C. H., and Labavitch, J. M. (2004). Cell wall metabolism during maturation, ripening and senescence of peach fruit. *J. Exp. Bot.*, 55.

Cerboneschi, M. (2016). Indole-3-acetic acid in plant–pathogen interactions: a key molecule for in planta bacterial virulence and fitness. *Res. Microbiol.*, 167.

Collado, I. G., Sánchez, A. J. M., and Hanson, J. R. (2007). Fungal terpene metabolites: biosynthetic relationships and the control of the phytopathogenic fungus Botrytis cinerea. *Nat. Prod. Rep.*, 24.

De Miccolis Angelini, R. M., Abate, D., Rotolo, C., Gerin, D., Pollastro, S., and Faretra, F. (2018). De novo assembly and comparative transcriptome analysis of Monilinia fructicola, Monilinia laxa and Monilinia fructigena, the causal agents of brown rot on stone fruits. *BMC Genomics*, 19(1):436.

Garcia-Benitez, C., Melgarejo, P., Cal, A., and Fontaniella, B. (2016). Microscopic analyses of latent and visible Monilinia fructicola infections in nectarines. *PLoS ONE*, 11.

Garcia-Benitez, C., Melgarejo, P., Sandin-España, P., Sevilla-Morán, B., and Cal, A. (2019). Degrading enzymes and phytotoxins in Monilinia spp. *Eur. J. Plant Pathol.*, 154.

Gununu, P. R., Munhuweyi, K., Obianom, P. C., and Sivakumar, D. (2019). Assessment of eleven South African peach cultivars for susceptibility to brown rot and blue mould. *Sci. Hortic.*, 254.

Jones, J. D. G. and Dangl, J. L. (2006). The plant immune system. *Nature*, 444.

Kim, H. j. i. n., Chen, C., Kabbage, M., and Dickman, M. B. (2011). Identification and characterization of Sclerotinia sclerotiorum NADPH oxidases. *Appl. Environ. Microbiol.*, 77.

Kombrink, A., Sánchez-Vallet, A., and Thomma, B. P. H. J. (2011). The role of chitin detection in plant-pathogen interactions. *Microbes Infect.*, 13.

Langmead, B. and Salzberg, S. L. (2012). Fast gapped-read alignment with Bowtie 2. *Nature Methods*, 9(4):357–359.

Lee, M. . H. and Bostock, R. M. (2006). Induction, regulation, and role in pathogenesis of appressoria in Monilinia fructicola. *Phytopathology*, 96.

Lee, M. H. and Bostock, R. M. (2007a). Fruit exocarp phenols in relation to quiescence and development of Monilinia fructicola infections in Prunus spp.: a role for cellular redox? *Phytopathology*, 97.

Lee, M.-H. and Bostock, R. M. (2007b). Fruit Exocarp Phenols in Relation to Quiescence and Development of Monilinia fructicola Infections in Prunus spp.: A Role for Cellular Redox? *Phytopathology*, 97(3):269–277.

Li, H., Zhang, Z., He, C., Qin, G., and Tian, S. (2016). Comparative proteomics reveals the potential targets of BcNoxR, a putative regulatory subunit of NADPH oxidase of Botrytis cinerea. *Mol. Plant-Microbe Interact.*, 29.

Lin, Z., Wu, J., Jamieson, P. A., and Zhang, C. (2019). Alternative Oxidase Is Involved in the Pathogenicity, Development, and Oxygen Stress Response of Botrytis cinerea. *Phytopathology®*, 109(10):1679–1688.

Love, M. I., Huber, W., and Anders, S. (2014). Moderated estimation of fold change and dispersion for RNA-seq data with DESeq2. *Genome Biology*, 15(12):550.

Luo, Y., Michailides, T. J., Morgan, D. P., Krueger, W. H., and Buchner, R. P. (2005). Inoculum dynamics, fruit infection, and development of brown rot in prune orchards in California. *Phytopathology*, 95.

Ma, Z., Yoshimura, M. A., Holtz, B. A., and Michailides, T. J. (2005). Characterization and PCR-based detection of benzimidazole-resistant isolates of Monilinia laxa in California. *Pest Manag. Sci.*, 61.

Mari, M. (2019). Stone Fruits. In Palou, L. and Smilanick, J. L., editors, *Postharvest Pathology of Fresh Horticultural Produce*, chapter Stone Frui. CRC Press.

Mari, M., Casalini, L., Baraldi, E., Bertolini, P., and Pratella, G. C. (2003). Susceptibility of apricot and peach fruit to Monilinia laxa during phenological stages. *Postharvest Biol. Technol.*, 30.

Martini, C. and Mari, M. (2014). Chapter 7 - Monilinia fructicola, Monilinia laxa (Monilinia Rot, Brown Rot). In Bautista-Baños, S. B. T. P. D., editor, *Postharvest Decay Control Strategies*, pages 233–265. Academic Press, San Diego.

McDowell, J. M. and Dangl, J. L. (2000). Signal transduction in the plant immune response. *Trends Biochem. Sci.*, 25.

Naranjo-Ortíz, M. A. (2018). Genome sequence of the brown rot fungal pathogen Monilinia laxa. *BMC Res. Notes*, 11.

Oetiker, J. H. and Yang, S. F. (1995). The role of ethylene in fruit ripening. *Acta Hortic.*, 398.

Pandey, D., Rajendran, S. R. C. K., Gaur, M., Sajeesh, P. K., and Kumar, A. (2016). Plant Defense Signaling and Responses Against Necrotrophic Fungal Pathogens. *Journal of Plant Growth Regulation*, 35(4):1159–1174.

Petersen, T. N., Brunak, S., Heijne, G., and Nielsen, H. (2011). SignalP 4.0: discriminating signal peptides from transmembrane regions. *Nat. Methods*, 8.

Poussereau, N., Creton, S., Billon-Grand, G., Rascle, C., and Fevre, M. (2001). Regulation of acp1, encoding a non-aspartyl acid protease expressed during pathogenesis of Sclerotinia sclerotiorum. *Microbiology*, 147.

RosBreed (2020). Peach Brown Rot.

Rungjindamai, N., Jeffries, P., and Xu, X.-M. (2014). Epidemiology and management of brown rot on stone fruit caused by Monilinia laxa. *European Journal of Plant Pathology*, 140(1):1–17.

Schouten, A. (2002). Functional analysis of an extracellular catalase of Botrytis cinerea. *Mol. Plant Pathol.*, 3.

Tadiello, A. (2016). On the role of ethylene, auxin and a GOLVEN-like peptide hormone in the regulation of peach ripening. *BMC Plant Biol.*, 16.

Torres, M. A., Jones, J. D. G., and Dangl, J. L. (2006). Reactive oxygen species signaling in response to pathogens. *Plant Physiol.*, 141.

Usall, J., Casals, C., Sisquella, M., Palou, L., and Cal, A. (2015). Alternative technologies to control postharvest diseases of stone fruits. *Stewart Postharvest Rev.*, 11.

Valero-Jiménez, C. A., Veloso, J., Staats, M., and van Kan, J. A. L. (2019). Comparative genomics of plant pathogenic Botrytis species with distinct host specificity. *BMC Genomics*, 20(1):203.

van der Ent, S. and Pieterse, C. M. J. (2012). Ethylene: Multi-Tasker in Plant-Attacker Interactions. In *Annual Plant Reviews Volume 44*, volume 44, pages 343–377. Wiley-Blackwell, Oxford, UK.

Veloso, J. and van Kan, J. A. L. (2018). Many Shades of Grey in Botrytis-Host Plant Interactions. *Trends in Plant Science*, 23(7):613–622.

Verde, I. (2013). The high-quality draft genome of peach (Prunus persica) identifies unique patterns of genetic diversity, domestication and genome evolution. *Nat. Genet.*, 45.

Verde, I. (2017). The Peach v2.0 release: high-resolution linkage mapping and deep resequencing improve chromosome-scale assembly and contiguity. *BMC Genomics*, 18.

Villarino, M., Sandín-España, P., Melgarejo, P., and Cal, A. (2011). High chlorogenic and neochlorogenic acid levels in immature peaches reduce Monilinia laxa infection by interfering with fungal melanin biosynthesis. *J. Agric. Food Chem.*, 59.

Zhang, L., Zhang, F., Melotto, M., Yao, J., and He, S. Y. (2017). Jasmonate signaling and manipulation by pathogens and insects. *J. Exp. Bot.*, 68.

Zhu, W. (2017). BcCFEM1, a CFEM domain-containing protein with putative GPI-anchored site, is involved in pathogenicity, conidial production, and stress tolerance in Botrytis cinerea. *Front. Microbiol.*, 8.

Zhu, Z. and Tian, S. (2012). Resistant responses of tomato fruit treated with exogenous methyl jasmonate to Botrytis cinerea infection. *Sci. Hortic.*, 142.

Zipfel, C. (2014). Plant pattern-recognition receptors. *Trends Immunol.*, 35.